December 2020

Performance-based Seismic Design of Multi-Story Light-frame Wood Buildings using Adaptive Displacement-based Design Procedure

Bikal Shakya
Clemson University, bshakya@g.clemson.edu

PERFORMANCE-BASED SEISMIC DESIGN OF MULTI-STORY LIGHT-FRAME WOOD BUILDINGS USING ADAPTIVE DISPLACEMENT-BASED DESIGN PROCEDURE

A Thesis
Presented to
the Graduate School of
Clemson University

In Partial Fulfillment
of the Requirements for the Degree
Master of Science
Civil Engineering

---

by
Bikal Shakya
December 2020

Accepted by:
Dr. Weichiang Pang, Committee Chair
Dr. Laura Redmond
Dr. Brandon Ross

.

ABSTRACT

Light-frame wood construction is one of the most common types of construction in the North America, particularly for low-rise residential dwellings and apartment buildings. Light-frame wood buildings were found to perform well during recent earthquakes. However, past earthquake events also revealed a common deficiency in many light-frame wood buildings, namely soft first-story damage, and, in some extreme cases, pancake collapse. Many buildings have a soft first-story because of an open-space floor plan used for retail or parking with minimal partition walls while the upper stories are apartment units. Typically, partition walls are considered as non-structural elements, however, they add strength to the overall lateral load resisting system. When both the structural elements (prescribed by engineers) and non-structural elements (partition walls sheathed with gypsums) are considered, vertical irregularities in strength and stiffness often occur in buildings with open floor plan in the first story. The current force-based design procedure, namely the Equivalent Lateral Force (ELF) procedure, does not explicitly consider the contribution of non-structural elements. This research (1) studied soft-story deficiency in light-frame wood buildings due to unintended stiffness and strength contributions from non-structural elements and (2) developed a strategy through the use of an adaptive displacement-based design (ADD) method in which the demand (required story shears) of the as-designed building is revised continually as the design progresses from one story to another. Nonlinear time history and incremental dynamic analyses were performed for the as-designed buildings using both ELF and ADD methods. The seismic performance in terms of (1) collapse probability at the Risk-targeted Maximum Considered Earthquake

(MCE_R) level, and (2) peak median story drift ratios at various hazard levels were used to evaluate the overall performance of a soft-story building designed using both the ELF and the ADD procedure. It was observed that for a building designed using the ELF procedure, the collapse probability increased on the inclusion of non-structural elements in the model, signaling the detrimental effects of non-structural elements due to the inability of the ELF procedure to quantify the contribution of these elements. In contrast, the ADD procedure took into account the contribution of these elements and was able to provide a structural design for which the collapse probability actually decreased on the inclusion of non-structural elements.

In addition, a parametric study was carried out to compare the differences in MCE_R collapse probabilities obtained using a 3D building model with biaxial ground motions and an equivalent 2D building model with uniaxial ground motion. The result of this parametric study was a factor that can be used to relate the MCE_R collapse probabilities between the 3D and 2D models, referred to as the 3D factor. The study confirmed that if the collapse results from both directions were used in calculating the overall collapse probability for a 2D building model, the 3D factor is 1.2 whether the building is designed for equal strengths or unequal strengths in its two lateral directions.

DEDICATION

To all the lives lost and all of us still reeling through

the COVID-19 pandemic

ACKNOWLEDGMENTS

I would like to thank my advisor, Dr. Weichiang Pang for his continued support and guidance throughout the time I worked as a graduate research assistant. Without his support, this thesis by any means would not have been possible. I would like to thank my committee members Dr. Laura Redmond and Dr. Brandon Ross for their inputs and participation. I would like to thank the Glenn Department of Civil Engineering for supporting me financially throughout my time at Clemson. And I would also like to express my gratitude for all the courses I took, not just from the committee members but also to other structures faculty members Dr. Thomas E. Cousins and Dr. Mohannad Z. Naser for assistance in and out of the class.

I am grateful to Philip Line for providing me the wall test data as well as for the collaboration, time and, insights he provided.

I would also like to extend my gratitude towards all of my colleagues in the department, including Ershad Ziaei, Michael Stoner, Bibek Bhardwaj, Amir Safiey and Sereen Majdalaweyh for all the help they provided at different times during this study.

I would also like to thank Palmetto Cluster at Clemson University which made this research possible and offer my sincerest appreciation to the team there for continued assistance.

And finally, I am grateful for the immense backdrop of support from my family and friends before and throughout my time in grad school.

TABLE OF CONTENTS

TABLE OF CONTENTS (CONTINUED)

PAGE

TABLE OF CONTENTS (CONTINUED)

PAGE

LIST OF TABLES

TABLE **PAGE**

LIST OF TABLES (CONTINUED)

TABLE **PAGE**

LIST OF TABLES (CONTINUED)

TABLE **PAGE**

LIST OF FIGURES

FIGURE **PAGE**

LIST OF FIGURES (CONTINUED)

FIGURE **PAGE**

LIST OF FIGURES (CONTINUED)

FIGURE **PAGE**

LIST OF FIGURES (CONTINUED)

FIGURE **PAGE**

LIST OF FIGURES (CONTINUED)

FIGURE **PAGE**

LIST OF FIGURES (CONTINUED)

FIGURE **PAGE**

LIST OF FIGURES (CONTINUED)

FIGURE **PAGE**

LIST OF ABBREVIATIONS

ADD	*Adaptive Displacement-based Design*
ASCE	*American Society of Civil Engineers*
ASD	*Allowable Strength Design*
ATC	*Applied Technology Council*
AWC	*American Wood Council*
DBD	*Displacement-based Design*
DBE	*Design Basis Earthquake*
DDA	*Direct Displacement-based Assessment*
DDD	*Direct Displacement-based Design*
ELF	*Equivalent Lateral Fore*
FBD	*Force-based Design*
FEMA	*Federal Emergency Management Agency*
IBC	*International Building Code*
IDA	*Incremental Dynamic Analysis*
LRFD	*Load and Resistance Factor Design*
MCE	*Maximum Considered Earthquake*
MSTEW	*Modified Stewart*
NDS	*National Design Specifications*
NLTHA	*Non-Linear Time History Analysis*
NS	*Non-Structural Elements*
PBD	*Performance-based Design*
RESST	*Residual Strength*
SDPWS	*Special Design Provisions for Wind and Seismic*

CHAPTER ONE

1. INTRODUCTION

1.1. Motivation

Light-frame wood construction is often the go-to framing option for low-rise to mid-rise residential and commercial buildings. Low material cost, minimal environmental impact, and its forgiving nature during construction have made wood in general and light-frame construction the most common type of construction in the North America.

Earthquake hazard often is a major concern for design professionals, particularly on the West Coast. Buildings in earthquake-prone regions must be designed to maintain structural integrity and occupant safety. Extensive economic losses and even fatalities during seismic events often occurred in buildings with one or more structural deficiencies. Recent earthquakes (e.g. Loma Prieta 1989 and Northridge 1994) revealed that a common defect was observed in many of these light-frame wood constructions. It was observed that structural damage often concentrated on the first story in old multi-story residential wood-frame buildings with open floor plans for retail or parking space while the upper stories with many partition walls were largely unaffected. For instance, the first story of the Northridge Meadows apartment complex collapsed (shown in Figure 1-1 a) during the 1994 Northridge earthquake killing 16 people in their sleep with only minor damages to the upper stories. Such a defect is referred to as a "soft-story" effect.

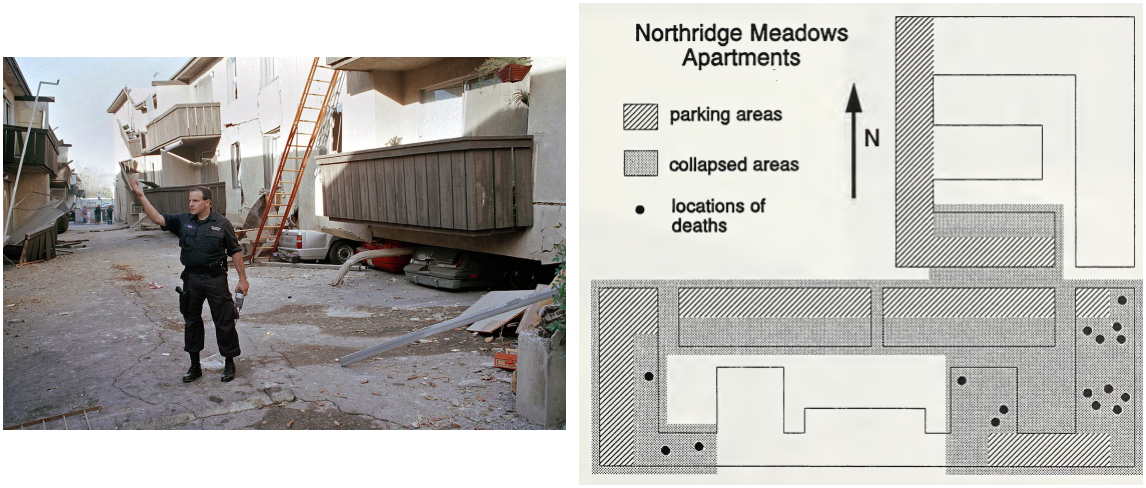

a) b)

Figure 1-1 a) Pancake collapse of the Northridge Meadows Apartment complex, 1994 (AP Photo/Chuck Jackson, 2014) and b) the floor plan at first story (Todd, et al., 1994, p. 23)

The primary lateral force-resisting system (LFRS) in these structures is the shearwall-and-horizontal diaphragm systems. However, a building also consists of other materials used for finishing the structure like gypsum on the interior for fire resistance, stucco on the building exterior. These elements hereafter referred to as non-structural elements, are never taken into account during design, partly because the strength of these non-structural elements is highly variable. In addition, these non-structural elements might not be retained throughout the life of the building due to future remodeling and other repurposing of the building. On closer inspection of the floor plan at the first story (Figure 1-1 b), it can be observed that there is a correlation between the open parking areas and the collapsed areas. Non-structural elements are minimally provided to accommodate such open spaces which is in contrast to the provision of ample non-structural elements on the upper stories. Hence, it can be inferred that the damage in the first story of the multi-story apartment could be due to the stark difference in the number of non-structural elements

and their unaccounted contribution among the stories. In addition, this might have also been aggravated because of the over-designed LFRS in the upper stories. And admittedly, given that these buildings were designed and built prior to the introduction of modern seismic codes, these buildings could be more vulnerable than newer construction built in accordance to modern seismic codes.

On the other hand, considering the intensity of these earthquakes, these wood buildings are very resilient to structural collapse and life safety. For instance, in the 1994 Northridge Earthquake, 22 of the total 58 fatalities were related to structural collapse (Todd, et al., 1994). On the other hand, half of approx. $44B in property losses were related to the damage to the structures and as many as 125,000 individuals were displaced from their homes at least temporarily, showing that wood structures are not as resilient to economic losses due to damage. In the light of this, a slew of alternative seismic design philosophies has been developed over the years to limit the damages and losses incurred and enhance the seismic performance of the building. This collectively represents the philosophy of performance-based design. Oftentimes, damage to the structural as well as non-structural elements is a function of the inter-story drift produced between the stories during an earthquake. A performance-based design approach that uses inter-story drifts as the key parameter to achieve its objectives is referred to as displacement-based design and is the focus of this thesis.

In addition, numerical modeling and simulation of light-frame wood structures are not as simple as those of concrete or steel structures. In engineered light-frame wood buildings, while the structural members are defined by engineers, the actual load paths

when considering the contribution of non-structural elements are not as easily identifiable as those of steel and concrete structures. However, with the advent of and ease of access to computing resources, more and more numerical packages are being developed that allow for the two-dimensional (2D) as well as three-dimensional (3D) analyses of light-frame wood buildings. Among these two, 2D analysis is simpler, easier to perform, and hence, more common. But 3D analysis is also becoming just as simple and easy to perform because of software packages. Therefore, in addition to the aforementioned displacement-based design of the light-frame wood building, another study has also been conducted that explores the relationship between 2D and 3D analyses in the context of light-frame wood structures.

1.2. Research Tasks

The main objectives of this research were:

- To quantify the seismic performance of a building with soft-story deficiency due to (1) unintended and unaccounted contribution from non-structural elements, and (2) overdesigned structural elements in upper stories
- To develop an Adaptive Displacement-based Design (ADD) procedure to address the possibility of unintended soft-story defect when designing light-frame wood buildings using the current force-based Equivalent Lateral Force (ELF) procedure in building code
- To evaluate, compare and calibrate the design parameters (target drift limit and resistance factor) for the ADD procedure to achieve the same collapse risk as that of the ELF procedure

- To investigate the relationship between the collapse probabilities obtained from 2D and 3D numerical models

1.3. Organization

Chapter 2 presents literature review of the state-of-the-art (1) performance-based design and displacement-based design, and (2) finite element modeling of light-frame wood buildings. Additionally, it includes a brief overview of the FEMA P695 methodology for the performance evaluation of buildings as well as the assumptions and techniques derived in this study from the ATC116 project.

Chapter 3 briefly reviews the code-based seismic design methodology, introduces the example building(s) used throughout this study, designs them using the force-based design method (ELF), and finally, evaluates the performance of the as-designed buildings.

Chapter 4 first sets up the structural and non-structural performance criteria. It then discusses and elaborates on the displacement-based design procedure adopted in this study. It introduces some key concepts associated with the procedure as well as suggests some modifications that were found essential. Using this procedure, it then calibrates the performance criteria against the ELF design. And finally, it also briefly discusses a design assessment technique based on this procedure.

Chapter 5 first presents the reasoning behind and the steps involved in this new procedure. Using this procedure, it then redesigns the example building first with no consideration of non-structural elements and then with consideration of non-structural elements. It then evaluates the performance of each of these buildings and compares against that of the ELF-designed building from Chapter 3.

Chapter 6 involves a study independent from that in the previous chapters and uses its own set of models to develop an understanding of the relationship between 2D and 3D analysis results.

Finally, Chapter 7 concludes with the summary and key findings of this thesis. It also presents some recommendations for future studies.

2. LITERATURE REVIEW

This chapter delineates some relevant concepts pertaining to seismic design, finite element modeling approach and software used, a methodology adopted by the Federal Emergency Management Agency (FEMA) to assess seismic performance, and a relevant Applied Technology Council (ATC) project and its underlying assumptions used in this thesis. Most of the important performance parameters have also been defined in this chapter and the reader is advised to go through this chapter prior to proceeding onto the following chapters or read hand-in-hand with the following chapters.

2.1. Prescriptive Design and Performance-based Design

Most building codes offer two paths for compliance: prescriptive or performance. A prescriptive code requires that each component is designed to a certain standard. On the other hand, a performance-based code requires that the building as a whole perform to a certain standard and at least perform just as well as the prescriptive one (Ekotrope, 2020). Current building codes are prescriptive in nature with the intent to provide life safety when a design level event occurs. On the other hand, the performance-based design is founded on the premise that structural systems must meet specific performance objectives at specific hazard levels. The current design codes prescribe the seismic demand in terms of strength and story drift or displacement is a secondary consideration. Many Performance-Based Design (PBD) procedures proposed integrate drift as a principal design parameter from the very start. In addition to these, PBD allows the stakeholders to select the desired performance objective, beyond the minimum code requirement, that meets their needs.

2.1.1. Displacement-based Design of Light-frame Wood Structures

The concept of Displacement-based design (DBD) was originally presented by Priestly (1998) for reinforced concrete structures; the fundamental philosophy being that the structures be designed to achieve a specified performance level (defined in terms of drift limits) under a given level of seismic hazard. This was then later adopted by Folz and Filiatrault firstly to design a wooden shearwall (2002) and later to design a two-story wood-frame building (2006). The method was referred to as Direct-DBD (or D-DBD) method (Loss, Tannert, & Tesfamariam, 2018). The procedure modeled the global behavior of the shearwall system and the two-story building as a single-degree-of-freedom (SDOF) system with equivalent mass and viscous damping properties representative of the original system. This method relied on pushover analysis of the complete system to gain knowledge about the global monotonic load-displacement behavior as well as the variation of damping with deformation. The need for a pushover analysis which requires additional knowledge about finite element packages and the possible inaccessibility of these packages to everyone can be taken as a drawback to the method.

Other than this method, as noted by Loss (2018), the two notable methods available in the literature are N2-DBD in Annex B of Eurocode 8 (EC8) and Modal-DBD. The N2 method uses a similar approach to that by Folz and Filiatrault (2006). The method requires the transformation of the building into a single-degree-of-freedom system whose characteristics are to be determined using nonlinear static (NLS) analyses of the whole building structure. Hence, the N2 method also presents the same drawbacks as the D-DBD

method. Also, the N2 method is not as well tested as the D-DBD method and is only applicable to certain building systems and materials.

On the other hand, the modal-DBD by Pang and Rosowsky (2009) requires neither the global pushover performance nor the variation of damping ratio with deformation. The method was mainly formulated with the multi-story light-frame wood buildings in mind and considers the inter-story drift as the primary seismic design parameter. This research uses the method by Pang and Rosowsky (2009) as the foundation and makes improvements to the original procedure. Chapter 4 firstly elaborates on the key concepts of modal-DBD method by Pang and Rosowsky (2009) and then, Chapter 5 builds upon these to propose a new adaptive design procedure which is the primary focus of this thesis.

2.2. Finite Element Models of Light-frame Wood Buildings

Numerical models for Light-frame Wood buildings used in this study were built in MATLAB-based program Timber3D (Pang, Ziaei, & Filiatrault, 2012). Timber3D package was developed as part of the NEES-Soft project and is an extension of the 2D model developed for collapse analysis of light-frame wood structures (Pang & Shirazi, 2012). Timber3D uses a co-rotational formulation and large displacement theory to simulate the in-plane and out-of-plane motions of the diaphragms and shearwalls when subjected to gravity and seismic loading (Ghehnavieh, 2017). Timber3D can be used in three levels namely, connection level, assembly level, and building level. A hysteresis model can be fitted to test data of a connection at the connection level. This fitted model can then be used as an input to a shearwall or diaphragm assembly at the assembly level to simulate the overall behavior of that assembly. And finally, each of these fitted models from the

connection and assembly level is used as inputs at the building level to simulate the overall behavior of the whole building. Figure 2-1 illustrates each of these levels and the graphical user interface (GUI) available within the Timber3D package for each level.

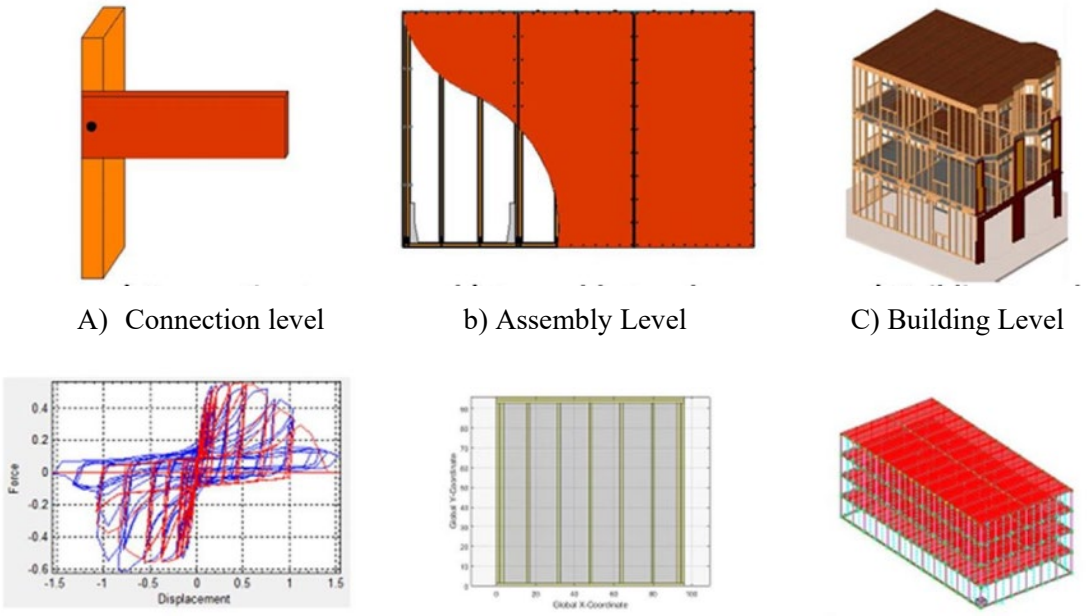

Figure 2-1 Modeling of light-frame wood building and GUI at a) connection level (guiMSTEWfit) b) assembly level (guiMCASHEW2) and c) building level (guiTimber3D) (Ghehnavieh, 2017)

Since the overall performance of a building is of primary concern, this study only uses Timber3D at the building level and guiTimber3D. Figure 2-2 shows a schematic illustration of a three-dimensional, one-story Timber3D model. The framing elements like vertical wood studs, sill plates, and those used within the diaphragm are all modeled using 3D 12-degrees-of-freedom, two-node frame elements that can account for geometric nonlinearity. Stud-to-diaphragm, sill plate-to-diaphragm, hold-downs, and anchoring bots

are modeled using 3D, 6-DOF, two-node Frame-to-Frame (F2F) link elements. More details on the approaches used to model the shearwalls and diaphragms are discussed in the next few sections.

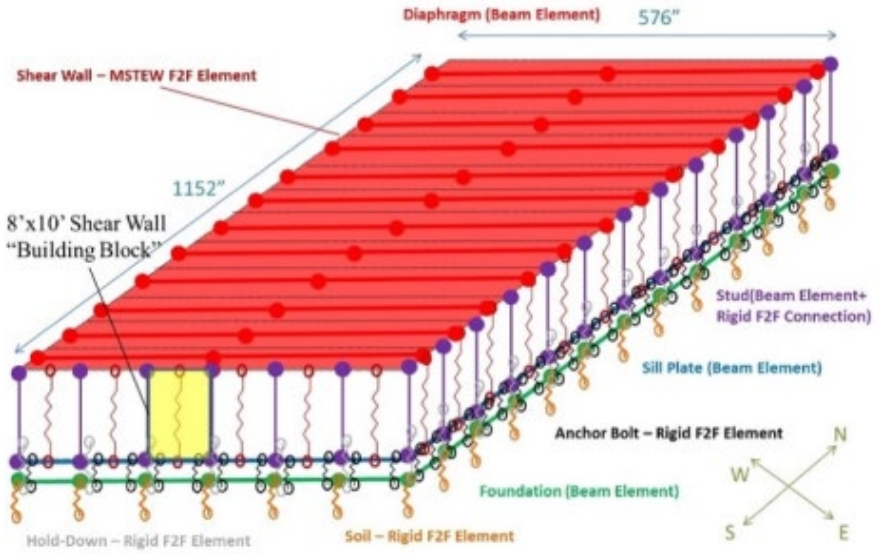

Figure 2-2 Schematic Illustration of a 3D, 1-story building (ATC, 2017)

2.2.1. Shearwall modeling

Rather than modeling shearwall down to each and every member and nailing connection (as in the assembly level), typical wall building blocks as shown in Figure 2-3 can be used. This building block comprises four nodes with two vertical end studs and two horizontal plates modeled by elastic frame elements. These building blocks incorporate a F2F link element activated only in the wall in-plane direction to simulate the nonlinear lateral in-plane cyclic behavior of walls. The lateral in-plane response of a wall can be modeled using two approaches, the first being the Modified Steward (MSTEW) model, commonly known as the CUREE (Consortium of Universities for Research in Earthquake

Engineering) model (Folz & Filiatrault, 2001) and the other being the relatively new Residual Strength (RESST) model which was derived from the MSTEW/CUREE model.

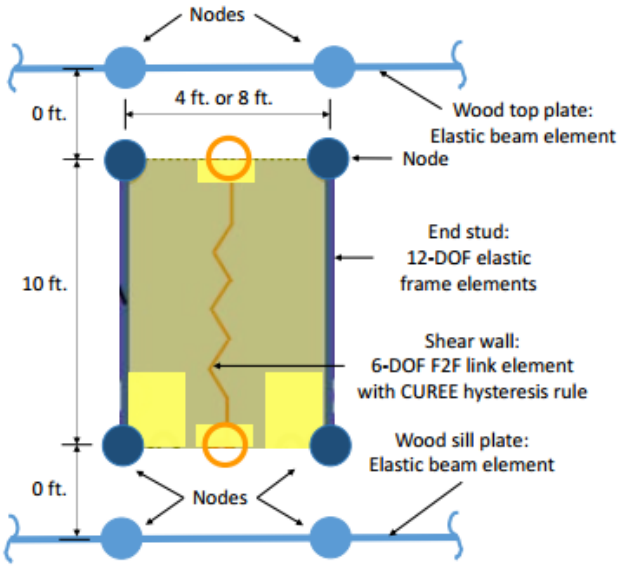

Figure 2-3 Typical Shearwall Building Block (ATC, 2017)

The MSTEW model was developed by Folz and Filiatrault (2001) based on the initial hysteretic model proposed by Stewart (1987) for modeling the cyclic response of shearwalls. MSTEW model uses 10-parameters to capture the non-linear cyclic response of shearwalls as shown in Figure 2-4. The MSTEW model is equivalent to the SAWS material model used in OpenSees (Folz & Filiatrault, 2001).

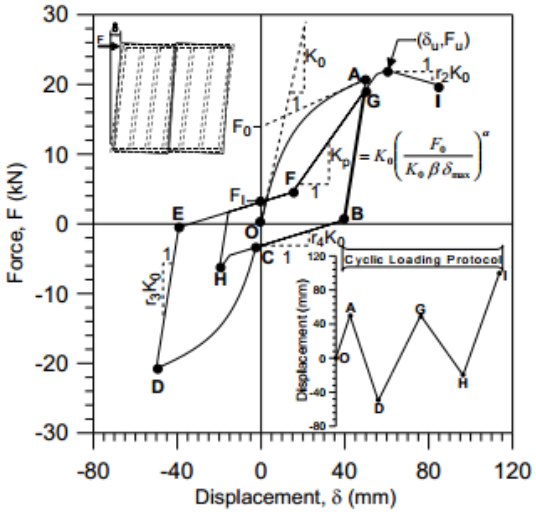

K_0: Initial Stiffness

r_1: Asymptotic stiffness ratio under monotonic loading

r_2: Post-capping strength ratio under monotonic loading

r_3: Unloading stiffness ratio

r_4: Reloading pinched stiffness ratio

F_0: Force intercept of the asymptotic stiffness at ultimate strength

F_1: Zero-displacement load intercept

Δ: Displacement at ultimate load

α: Hysteretic parameter for stiffness degradation

β: Hysteretic parameter for stiffness degradation

Figure 2-4 MSTEW model and its ten parameters (Folz & Filiatrault, 2001)

On the other hand, the RESST model is an enhancement upon the MSTEW model and has only been recently introduced in the ATC116 (2017) project discussed later in this chapter other than this study. RESST model uses 12-parameters instead of 10 and tries to capture the post-peak residual strength of shearwalls and provide for a realistic lateral displacement capacity of building archetypes. RESST model replaces the linearly descending post-capping strength and stiffness of the MSTEW model by an S-shaped curve anchored at displacement D_x and converging to predetermined post-capping residual strength at large displacements (ATC, 2017). Figure 2-5 illustrates the RESST model and its 12-parameters.

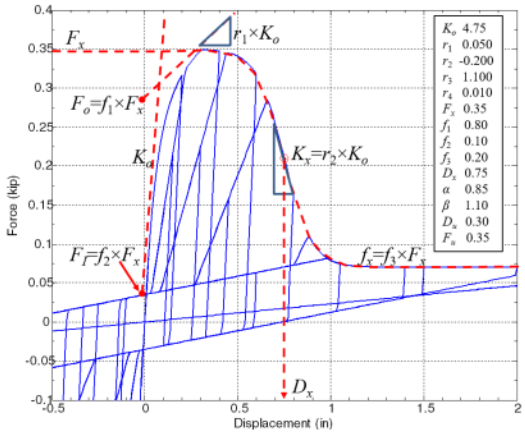

K_0: Initial Stiffness

r_1: Asymptotic stiffness ratio under monotonic loading

r_2: Post-capping strength ratio under monotonic loading

r_3: Unloading stiffness ratio

r_4: Reloading pinched stiffness ratio

F_x: Peak Strength

F1: Ratio of force intercept to ultimate strength

F2: Ratio of force intercept at zero-displacement

F3: Ratio of post-capping residual strength to ultimate strength

D_x: Displacement anchor for the S-shaped post-capping descending curve

α: Hysteretic parameter for stiffness degradation

β: Hysteretic parameter for stiffness degradation

Figure 2-5 RESST model and its 12-parameters (ATC, 2017)

The wall building block along with its adopted hysteretic model can represent walls with various sheathing materials. If the wall is sheathed on both sides with similar or dissimilar materials, the hysteresis models need to be appropriately combined. According to the FEMA P807 Seismic Evaluation and Retrofit of Multi-unit Wood Frame Buildings with Weak First Stories (FEMA, 2012),

a) if similar sheathing materials are used on both sides of the wall, the walls are directly additive and

b) if dissimilar sheathing materials are used on the two sides of the wall, they are combined such that 100% of the stronger material and 50% of the other materials are used.

2.2.2. Diaphragm modeling

Diaphragms can be modeled in Timber3D using two techniques. If rigid diaphragms are required, 2-node, 12-DOF frame elements, as used for other framing members, can be used. The length, width, and depth of these elements would be the same as that of the diaphragm segment under consideration. And to ensure the rigid behavior, section modifiers would be set to large values. These elements would be connected to each other using F2F elements that can either represent rigid or pin-connections. This modeling approach in Timber3D is illustrated in Figure 2-6.

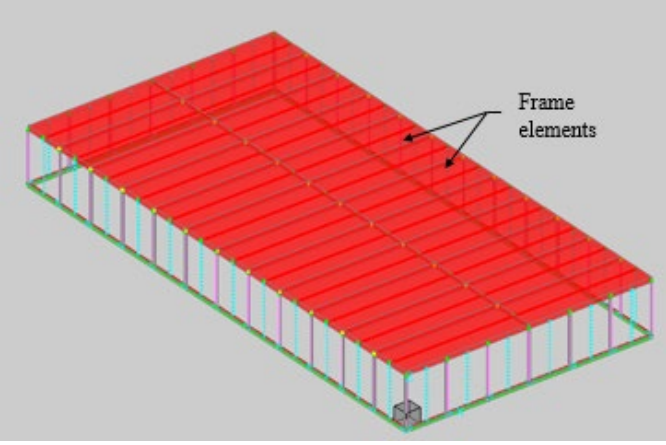

Figure 2-6 Diaphragm modeled as frame elements in Timber3D

The other technique is to make up a grid of pinned, highly rigid framing elements with an equivalent shear beam used within each grid block, shown in Figure 2-7, to represent the in-plane stiffness (G_a) of the diaphragm. This method is appropriate when there is a need to explicitly model the stiffness of the diaphragm. The equivalent shear beam is connected to the boundary members that make up the grid, through rigid link elements, and minimal flexural deflection in the out-of-plane direction is allowed for this shear beam by assigning a large stiffness modifier. This means the primary deflection in

the diaphragm is in the in-plane direction. The stiffness of these shear beams is manipulated by assigning a modification factor obtained as follows:

$I_{zmod} = \frac{12I_z}{bd^3}$ where $I_z = \frac{A_{sy}GG_aL^2B}{12E\left(A_{sy}G - G_aB\right)}$ derived from $\frac{12EI_z}{L^3\left(1+\varphi_y\right)} = \frac{G_aB}{L}$ $where\ \varphi_y = \frac{12EI_z}{GA_{sy}L^2}$

Here, $G = \frac{E}{2(1+\nu)}, A_{sy} = \frac{2}{3}bd$

For instance, if $G_a = \frac{8kip/in}{ft}, L = 96in, B = 96in, E = 1400\ ksi, \nu = 0.3, b = 8in, d = 8in$

$$\rightarrow I_z = \frac{A_{sy}GG_aL^2B}{12E\left(A_{sy}G - G_aB\right)} = 436in^4 \qquad \rightarrow I_{zmod} = \frac{12I_z}{bd^3} = 1.28$$

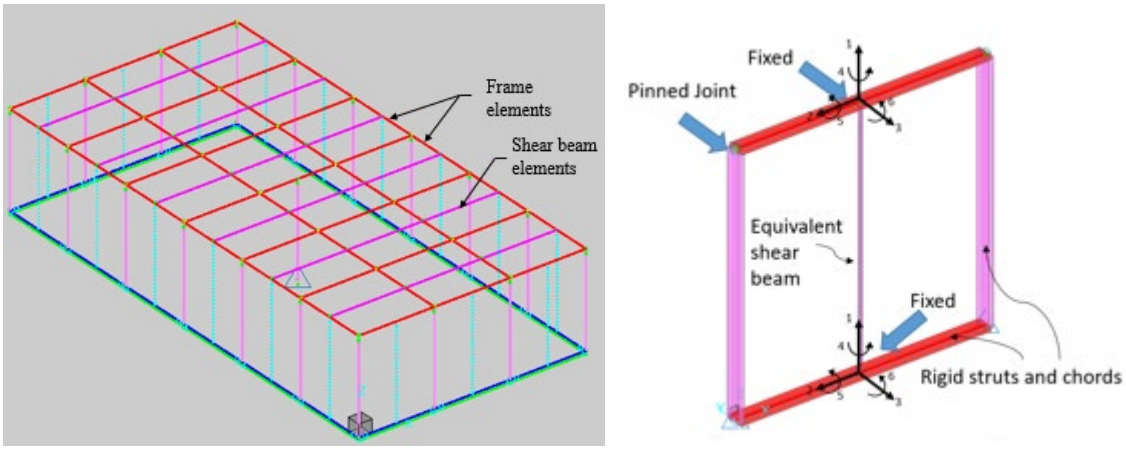

a) b)

Figure 2-7 Diaphragm building block a) in model and b) in isolation

2.3. FEMA P-695 Procedure for Performance Evaluation

FEMA P695 document titled 'Quantification of Building Seismic Performance Factors' was prepared by Applied Technology Council under Federal Emergency Management Agency with a goal in mind to "develop a procedure to establish consistent and rational building system performance and response parameters (R, C_d, Ω_o) for the linear design methods traditionally used in current building codes" (FEMA, 2009). The seismic

performance factors are used to estimate strength and deformation demands on systems designed using linear methods but are well within the nonlinear range and are very critical in the determination of seismic loading and the seismic design of structures.

An alternative application for this procedure is the evaluation of traditional as well as new structural systems. The metrics that the procedure utilizes can also be used only in a sense to assess and quantify the nonlinear behavior and seismic performance of a structural system. The methodology and the performance measures are applicable on their own and have been discussed below:

2.3.1. Nonlinear Static (Pushover) Analyses

Pushover analyses are conducted under the factored gravity load combination of **1.05 DL + 0.25 LL** and static lateral forces as per the FEMA P695 guidelines and following the nonlinear static procedure of ASCE/SEI 41 Section 3.3.3. And the distribution of lateral force along the height of the building should be in proportion to the fundamental mode shape of the archetype model.

An idealized pushover curve as shown in Figure 2-8 can be obtained from the pushover analysis. The peak strength V_{max}, effective yield displacement $\delta_{y,eff}$ and ultimate displacement δ_u are defined as shown in Figure 2-8. Then, the overstrength factor Ω and the period-based ductility μ_T can be computed as follows:

$$\Omega = \frac{V_{max}}{V} = \frac{V_{max}}{C_s W} \qquad \text{and} \qquad \mu_T = \frac{\delta_u}{\delta_{y,eff}}$$

Where C_s is the seismic coefficient defined in ASCE7-16 and W is the total effective weight of the building.

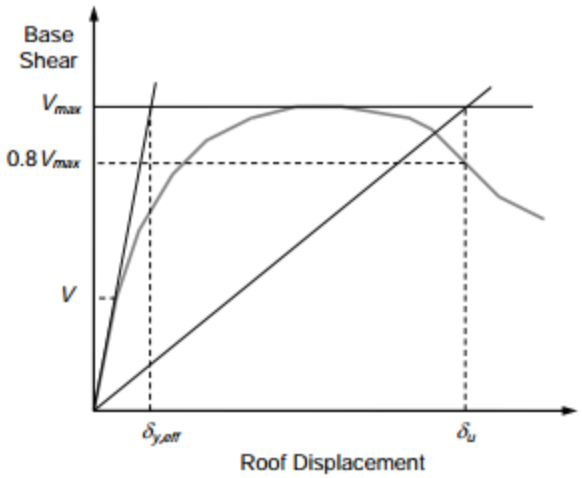

Figure 2-8 Idealized nonlinear static pushover curve (FEMA, 2009)

2.3.2. Nonlinear Dynamic (Response History) Analyses

Nonlinear dynamic analyses are also to be conducted under the factored gravity load combination of **1.05 DL + 0.25 LL** and input ground motions from the Far-Field record set in Table 2-1 as per the FEMA P695 guidelines. The nonlinear dynamic analyses are performed to determine the median collapse intensity (S_{CT}), collapse margin ratio CMR and the collapse probability for MCE level (PCOL|MCE). But prior to delving into these, it would be wise to first discuss the far-field record set, ground motion scaling, the concept of incremental dynamic analyses, spectral shape factor, and more.

2.3.2.1. Far-Field Record Set

The Far-Field record set consists of twenty-two ground motion pair records from the Pacific Earthquake Engineering Research (PEER) ground motions database (PEER Center, n.d.). Table 2-1 shows all 22 of these earthquakes along with the year and recording station. Figure 2-9 shows the response spectra for each of these earthquakes along with the median of the set.

Table 2-1 Far-Field Record set

ID No.	*Name*	*Year*	*Recording Station*	*Normalization factor*
1	Northridge	1994	Beverly hills – Mulhol	0.65
2	Northridge	1994	Canyon Country-WLC	0.83
3	Duzce, Turkey	1999	Bolu	0.63
4	Hector Mine	1999	Hector	1.09
5	Imperial Valley	1979	Delta	1.31
6	Imperial Valley	1979	El Centro Arrary #11	1.01
7	Kobe, Japan	1995	Nishi-Akashi	1.03
8	Kobe, Japan	1995	Shin-Osaka	1.10
9	Kocaeli, Turkey	1999	Duzce	0.69
10	Kocaeli, Turkey	1999	Arcelik	1.36
11	Landers	1992	Yermi Fire Station	0.99
12	Landers	1992	Coolwater	1.15
13	Loma Prieta	1989	Capitola	1.09
14	Loma Prieta	1989	Gilroy Array #3	0.88
15	Manjil, Iran	1990	Abbar	0.79
16	Superstition Hills	1987	El Centro Imp. Co.	0.87
17	Superstition hills	1987	Poe Road (temp)	1.17
18	Cape Mendocino	1992	Rio Dell Overpass	0.82
19	Chi-Chi, Taiwan	1999	CHY101	0.41
20	Chi-Chi, Taiwan	19999	TCU045	0.96
21	San Fernando	1971	LA – Hollywood Stor	2.10
22	Friuli, Italy	1976	Tolmezzo	1.44

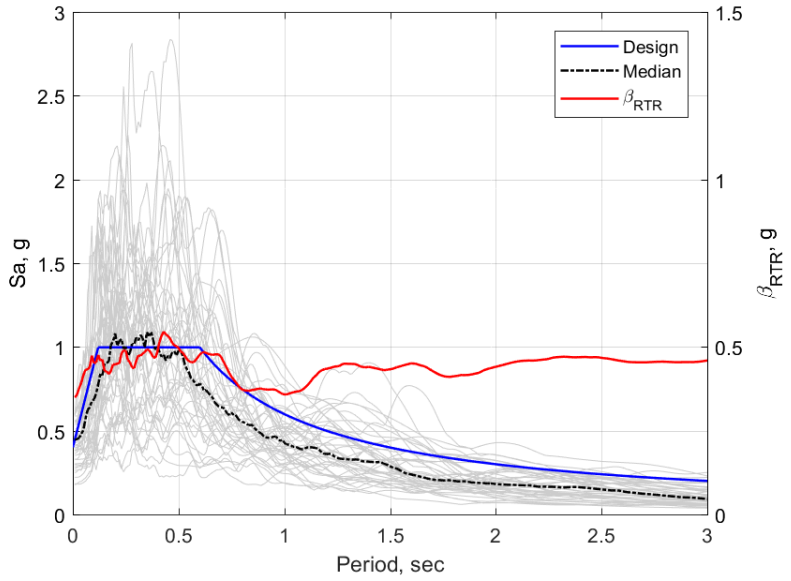

Figure 2-9 Response Spectra for FF Record set with median and standard deviation of natural log (β) plotted against period

2.3.2.2. Scaling of Ground Motions

Unscaled ground motions are not strong enough to collapse a typical archetype building, hence, scaling of the ground motions is required. The scaling process consists of normalization and scaling.

To remove the unwarranted variability between the records due to inherent differences in magnitude, distance-to-source, site conditions, etc., individual records in a given set are normalized by factor defined as: NM_j = median (PGV_{median})/PGV_j, PGV_{median} being the median PGV for the record set. The normalization factor is unique to each ground motion and was included in Table 2-1. These values can also be looked up in FEMA P695 Table A-4D.

After normalization, the ground motion records set is collectively scaled such that the median response spectrum matches the desired level of seismic intensity at a given time

period. Figure 2-10 shows the median of the FF record set matched to different MCE levels at the period of 1 second and each of these median spectra lines is said to be "anchored" to that MCE level. Table A-3 in FEMA P695 provides the anchoring factor for different periods and Seismic Design Categories.

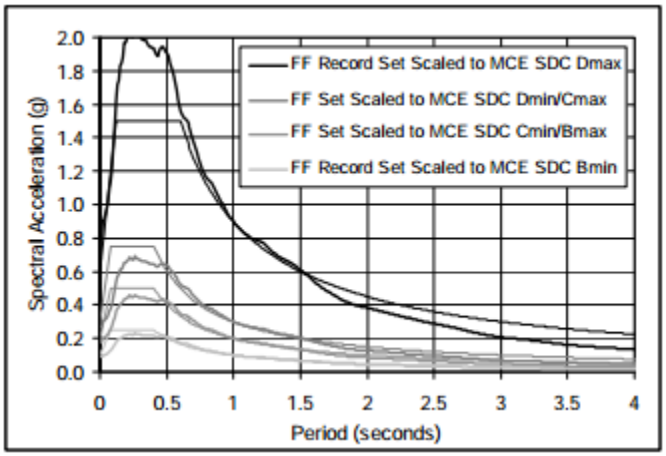

Figure 2-10 Median Spectra of FF record set anchored to MCE level for Seismic Design Categories B, C and D (FEMA, 2009, pp. A-13)

2.3.2.3. Incremental Dynamic Analysis (IDAs)

Also known as a dynamic pushover, incremental dynamic analysis involves a series of nonlinear dynamic analyses performed on the same structure for an increasing level of Intensity Measure (IM) while keeping a record of a Damage Measure (DM) (Vamvatsikos & Cornell, 2002). Commonly used IMs are peak ground acceleration, peak ground velocity, and 5%-damped Spectral Acceleration. And commonly used DMs are peak roof drifts, peak inter-story drifts, maximum base shear, etc. An IDA curve is a plot of DM along the X-axis to IM along the Y-axis. A set of example IDA curves is shown in Figure 2-11.

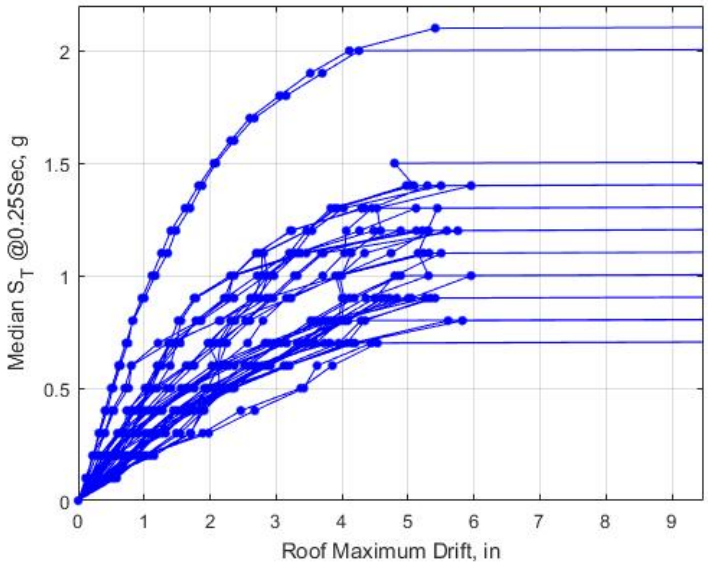

Figure 2-11 IDA curves example

In the light of the FEMA P695 study, all 44 ground motions (2 from each pair) are scaled collectively to varying seismic intensity levels until at least 50% of the ground motion records cause the archetype model to collapse. This intensity that causes 50% collapse is the median collapse capacity (S_{CT}). And the ratio of the median collapse intensity to the MCE demand (S_{MT}) is called the Collapse Margin Ratio (CMR).

$$CMR = {}^{S_{CT}}/_{S_{MT}}$$

For this study, seismic hazard representative of Southern California region is assumed. The design short-period spectral acceleration S_{MT} is equal to 1.5g.

2.3.2.4. Spectral Shape factor and Adjusted Collapse Margin Ratio (ACMR)

Each response spectra for a ground motion has a unique spectral shape (and frequency content), which is very different from that of the design response spectrum. If the peak of a spectrum is near the fundamental period of the building, collapse tends to

happen for much lesser collapse intensity. Because of this highly variable shape between the records and the design response spectrum and its significant impact on the seismic performance, FEMA P695 introduces the spectral shape factor (SSF) as a function of period-based ductility, seismic design category, and time period of the building.

$$SSF = \exp(\beta_1(\bar{\varepsilon_0}(T) - \bar{\varepsilon}(T)_{records})$$

Where $\beta = 0.14\ (\mu_T - 1)^{0.42}$

$\bar{\varepsilon}(T)_{records}$ = 1.0 for SDC B/C, 1.5 for SDC D and 1.2 for SDC E

$\bar{\varepsilon}(T)_{records} = 0.6(1.5 - T), \quad \bar{\varepsilon}(T)_{records} = 0.6\ if\ T \leq 0.5\ and\ 0\ if\ T \geq 1.5$

This SSF factor is then multiplied to obtain the Adjusted Collapse Margin Ratio (ACMR) to take into account the variability between the spectral shape between the ground motion records.

$$ACMR = SSF \times CMR$$

ACMR is the primary parameter of interest in the FEMA P695 procedure used to quantify the seismic performance factors previously discussed.

2.3.2.5. Adjustment of CMR if using three-dimensional analysis

In the case of a two-dimensional analysis, a ground motion is applied to the structure model one at a time. However, in the case of three-dimensional analysis, a ground motion pair (one in each orthogonal direction) is applied to the structure one at a time. Studies show that median collapse intensity from the three-dimensional analysis is on average 20% less than the median collapse intensity from two-dimensional analysis (FEMA, 2009, pp. 6-14). Hence, to achieve parity and to remove the conservative bias in three-dimensional analysis, FEMA P695 introduces a 3D factor of 1.2. This shall be

multiplied to the median collapse intensity from IDA in addition to SSF to obtain ACMR i.e.

$$ACMR = 1.2 \times SSF \times CMR \quad \text{in case of 3D analysis}$$

It is to be noted that Chapter 6 in this thesis carries out a study to verify this factor. The preceding chapters however use the 3D factor of 1.2 just as it is. The SSF factor and the 3D factor are shown graphically in Figure 2-12.

2.3.2.6. System Collapse Uncertainty

Uncertainty in the collapse capacity of a system could be from many sources. Primarily, those are due to record-to-record uncertainty, design requirements uncertainty, test data uncertainty, and modeling uncertainty. Each of these is combined to obtain the overall system uncertainty as follows (FEMA, 2009, pp. 7-9):

$$\beta_{TOT} = \sqrt{{\beta_{RTR}}^2 + {\beta_{DR}}^2 + {\beta_{TD}}^2 + {\beta_{MDL}}^2}$$

Where β_{RTR}, β_{DR}, β_{TD} and β_{MDL} are record-to-record uncertainty, design requirement uncertainty, test data-related uncertainty and modeling related uncertainty.

2.3.2.7. Collapse Fragility and Collapse Probability

It can be observed in Figure 2-11 that the 44 ground motions can lead to different collapse intensities. These collapse intensities can be fitted to a probability distribution function (PDF) or a cumulative distribution function (CDF) to relate a ground motion intensity to the probability of collapse. FEMA P695 uses a lognormal distribution which is defined by two parameters, median collapse intensity (S_{CT}) and the logarithmic standard

deviation (β). And finally, based on this distribution, the probability of collapse at the MCE level for the building can be determined. This is graphically shown in Figure 2-12 below.

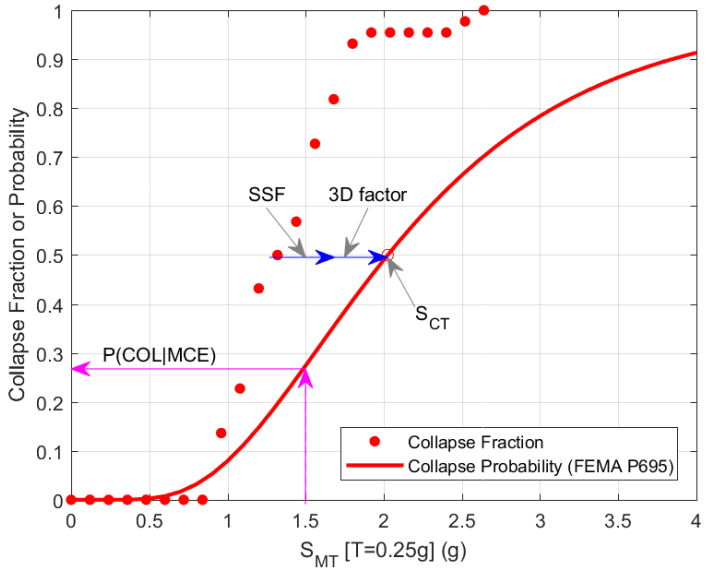

Figure 2-12 Fragility curves showing SCT, SSF, 1.2 3D factor and collapse probability at MCE level

2.4. ATC-116 Project: Objectives and Assumptions

Low rise buildings with short period make up the bulk of the building stock in the United States. Numerical modeling shows that these short-period buildings tend to have a much higher risk of collapse compared to long-period buildings. However, damage reports from recent major earthquakes do not support these results. Hence, the ATC-116 Project entitled "Developing Solutions to the Issue to Short-Period Building Performance Paradox" was initiated to study this discrepancy between the damage reports from earthquakes and the numerical modeling results. The studies conducted in this thesis are by no means related to the ATC-116 project. However, the assumptions made in this project, the simplified modeling and analysis approach used as well as the naming

conventions for wall types and terminologies proposed were deemed useful for the studies conducted in this thesis. Following are some major assumptions derived from the ATC-116 project used in this thesis:

- Damping tends to alleviate seismic performance, hence to avoid such an effect, damping for all of the numerical models has been set to zero.
- The period-based ductility μ_T depends on the ultimate displacement δ_u of the building which was previously shown to correspond to 80% post-peak strength. But the use of 80% post-peak strength is arbitrary and an argument can be made that the ultimate displacement can be taken the same as the collapse displacement capacity (i.e. displacement at which the building actually collapses), which highly varies with each building model. However, μ_T for a typical light-frame wood building is usually greater than 8 resulting in SSF of 1.33.
- FEMA P695 methodology requires that the ground motions be scaled to the desired intensity level at the fundamental period of the structure. However, every building has its own period and the shape of response spectra for individual earthquakes can vary significantly from that of the design response spectra meaning that scaling ground motions according to these individual periods could lead to differently scaled ground motions for different buildings even though they are all supposedly being scaled to the same intensity level. Hence, for uniformity across all models, ATC-116 uses a period of 0.25 sec as a representative time period for all of the buildings in this short-period range, the range within which all of the models in this

thesis are supposed to be. This means an anchoring factor of 1.93 can be taken as a constant for a site with short-period design spectral acceleration at MCE_R = 1.5g.

- The Spectral Shape Factor (SSF) as already discussed depends on period-based ductility μ_T, seismic design category and time period of the building. Given the previous two assumptions and the fact that seismic design category D has been used for all the models, SSF can be calculated as equal to 1.33. This value, hence, is considered a constant for all of the models.
- System uncertainty parameter β as previously discussed is a function of multiple sources of uncertainty including modeling-related variability among others. Even though the value of the β parameter varies with each model, uncertainty is difficult to quantify and because of this, calculation of the β parameter for each model is a cumbersome process. To simplify the calculation of collapse probability, the ATC-116 project uses a constant β parameter equal to 0.5 across all of its models.

3. FORCE-BASED DESIGN (FBD) AND ANALYSES

This chapter presents the fundamentals of seismic design in the light of current seismic design codes and light-frame wood buildings. In addition, this chapter introduces the example building as well as the shearwall types that are used throughout this study for design and analyses. The subsequent section then details the design process as well as the seismic performance evaluation of the designed buildings.

3.1. Current Seismic Design provisions

Seismic building codes require that structures be designed to resist specific equivalent static lateral forces, which are a function of the dynamic properties of the structure and the seismicity of its location (Chopra, 2001). Seismic hazard level is normally quantified in the form of a response spectrum wherein the earthquake-induced acceleration is plotted as a function of the fundamental natural period of the structure. Specified formulae in the current building codes are then used to determine the base shear and the distribution of lateral forces over the height of the building. This static analysis provides the design demands (for instance, shears and moments) for the structural components to design for. Further, the designed components are to be checked for excessive deformations and if it meets the relevant serviceability criteria.

Figure 3-1 shows the general design acceleration response spectrum in Chapter 11 of the ASCE 7-16 standard. The plot is a function of design spectral acceleration parameters S_{DS} and S_{D1} which are in turn dependent on the seismicity of the region. S_{DS}

and S_{D1} can be calculated from the mapped spectral acceleration parameters using the accompanying equations in the standard.

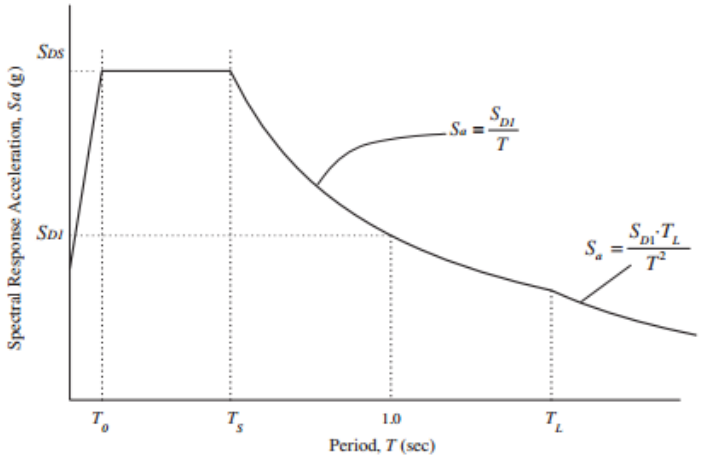

Figure 3-1 General Response Spectrum (Minimum Design Loads for Buildings and Other Structures (ASCE/SEI 7-16), 2016, p. 84)

Figure 3-2 shows an array of response spectra applicable to a structure located in the Southern California region for different hazard levels and are based on ASCE7-16. Interpolation (and extrapolation) equations in ASCE 41 were used to generate the response spectra for seismic hazard levels other than the DBE and MCE level. These hazard levels have been used in the subsequent chapters for the performance-based design.

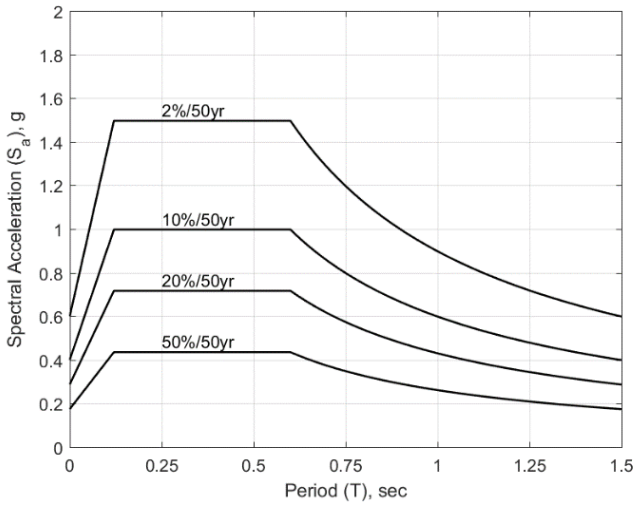

Figure 3-2 Design Response Spectrum

3.1.1. Equivalent Lateral Force (ELF) procedure

The ELF procedure as outlined in ASCE7-16 Chapter 12 is used to determine the base shear as well as the vertical distribution of lateral forces along the height of the building. The seismic base shear is determined from the following equation:

$$V = C_s W$$

where C_s is the seismic design coefficient and W is the total seismic weight of the structure in question.

The seismic design coefficient is obtained as:

$$C_s = {S_{DS}}\Big/{\left(\frac{R}{I}\right)}$$

where S_{DS} is the short-period (0.2 sec) design spectral acceleration parameter

R is the response modification factor and

I is the importance factor (taken as 1 for a Risk Category II building)

Table 3-1 shows the factors pertaining to light-frame wood construction.

Table 3-1 Design Coefficients and Factors for Light-frame Wood Systems

Seismic Force-resisting System	*Response Modification Factor R*	*Overstrength Factor Ω_0*	*Deflection Amplification Factor C_d*
Light-frame wood walls sheathed with wood structural panels rated for shear resistance	6.5	3	4

The base shear can then be distributed among the stories using the following equations:

$$F_x = C_{vx}V \text{ and } C_{vx} = \frac{w_x {h_x}^k}{\sum_{i=1}^{n} w_i {h_i}^k}$$

where C_{vx} = vertical distribution factor

V = total lateral base shear

W_i or W_x = weight at the level i or x

H_i and h_x = height from the base to level i and x

K = exponent related to fundamental period (k = 1 for period 0.5 sec or less, k = 2 for period 2.5 sec or more and determined by linear interpolation for periods in between)

The design story shear is the summation of the lateral forces on all the stories above as:

$$V_x = \sum_{i=x}^{n} F_i$$

This story shear is then distributed among the structural components to determine the design forces for each. For light-frame wood construction, this story shear is distributed

to the structural shearwalls in that story according to either rigid or flexible diaphragm assumption.

3.1.2. Design of Light-frame wood shearwalls

The design shear resistance must be provided to meet and exceed the shear demand in each shear wall. The shear resistance is the nominal shear capacity of the wall times the strength reduction factor of 0.8 for LRFD design (or ½ for ASD design); the nominal shear capacity can be obtained from the tabulated unit shear capacities for various wall types in SDPWS Tables 4.3 A through D times the wall length. The consideration must also be made for the adequacy of the framing members, the anchoring devices used and the effect of any perforations in the walls. Finally, the deflection of the shearwall is checked against the allowable story drift limit in ASCE 7-16 (for instance, 2.5% for Risk Category-II buildings).

3.2. Example Building (and its variants)

The example building used in this study is a Type-III or Type-V construction, light-frame wood building primarily intended for residential purposes and also partially for commercial use. It is intended that the building qualifies as a Risk Category II building. It has four stories, each story 10 feet in height. The intent is that the building be in the short-period range wherein the seismic response is the most intense. The general floor plan for the building, including the structural and non-structural shearwalls is shown in Figure 3-3 and hereafter referred to as Floor Plan A. To simplify analysis and design, a rectangular plan is used and the wall lengths are limited to 4 feet increments. The floor plan is symmetrical in both directions to eliminate any possible torsion (which is not the focus of

the study). Also, the floor plan has been thought through such that the building could be designed for the same strength in both directions. However, since the building has a rectangular floor plan, it is anticipated that the contribution from the non-structural components are not equal in the two lateral directions.

Figure 3-4 shows a variant of the same floor plan and same layout for structural shearwalls but much more open with lesser nonstructural partition walls. This floor plan, hereafter referred to as Floor Plan B, is intended for commercial use (for instance, a retail space).

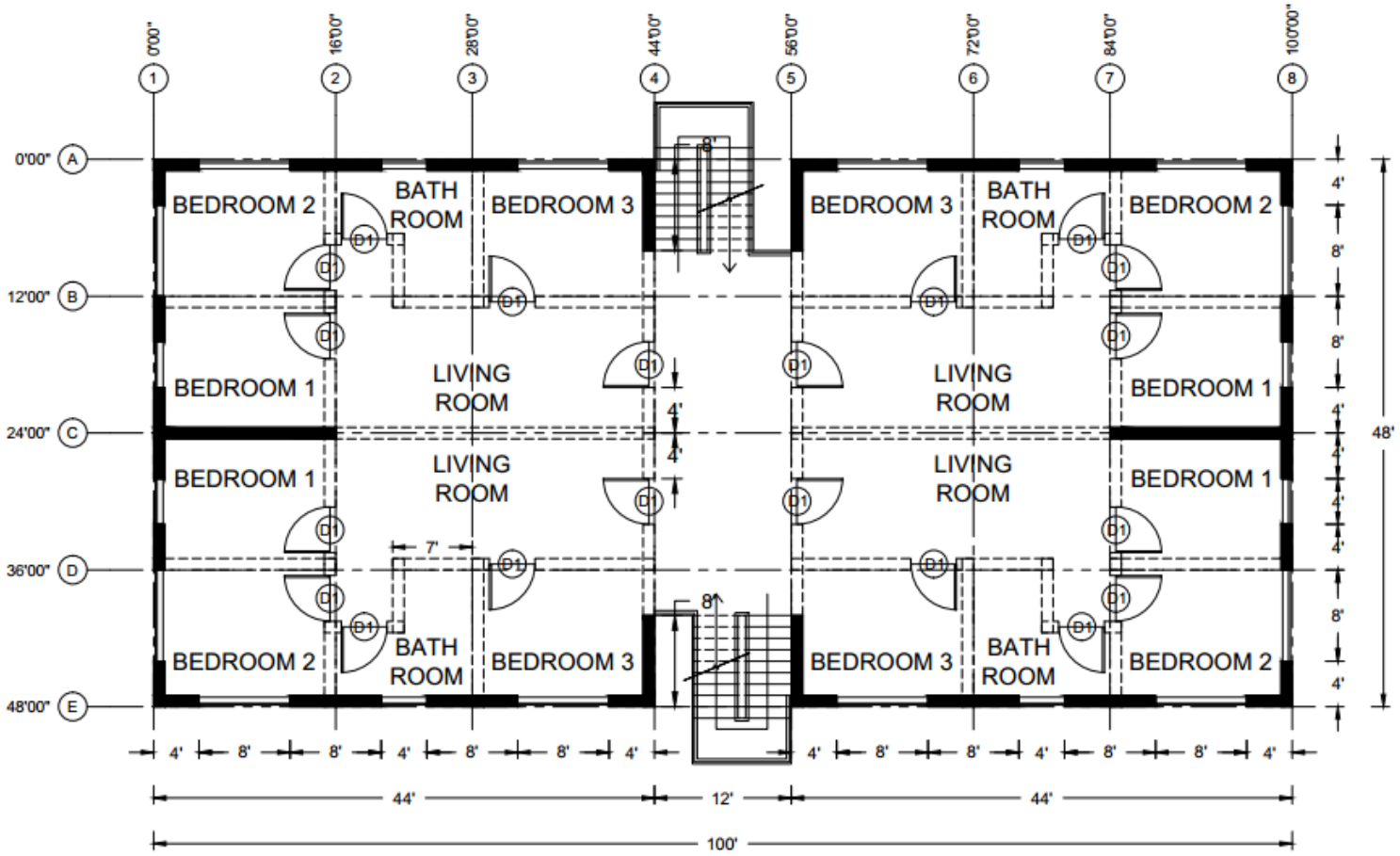

Figure 3-3 Floor Plan A

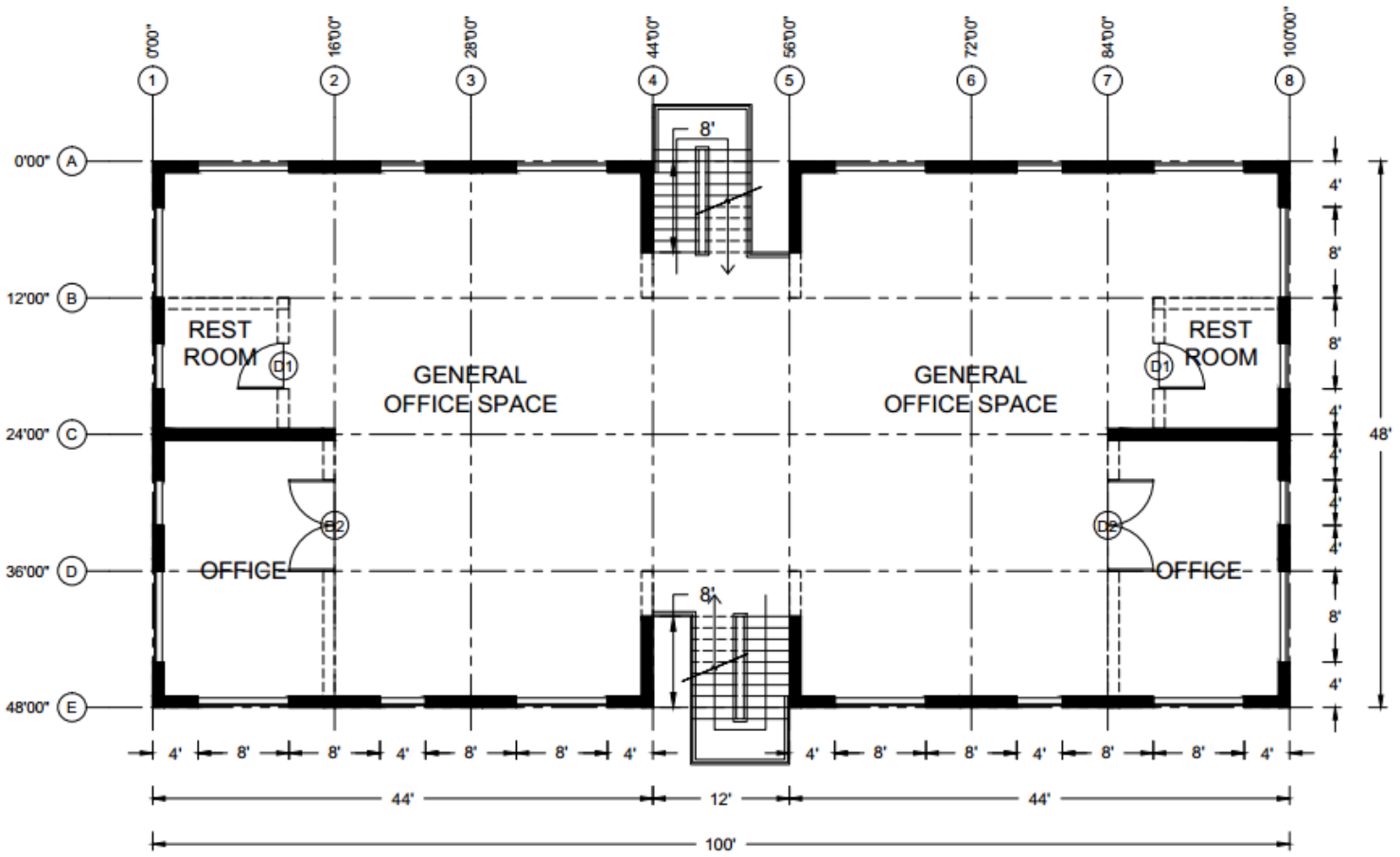

Figure 3-4 Floor Plan B

This study uses three different building designs using a combination of floor plans A and B. Table 3-2 enlists each of these buildings along with their description. It is to be noted that the building configuration is similar to the COM3B building used in the ATC116 study.

Table 3-2 Example building variants

Building	*Description*
V1	Floor plan A on all the floors
V2	Floor plan B on the first story and Floor plan A on all the upper stories; same structural design as V1
V3	Same floor plans as V2; same structural design on the 1st story as V1 and V2 but upper stories structurally designed about 20% stronger than the 1st story

The V1 building has the same floor plans for all four stories with four apartment units on each floor. Since the floor plans are identical in each story, the contribution of non-structural walls in each floor is the same.

The V2 building is identical to the V1 building, except the ground floor (first floor) is replaced by Floor Plan B (Figure 3-4). The first floor has an open floor plan, which is assumed to be the office space and reception floor of the apartment. The purpose of building V2 is to explore a scenario which could result in a soft story due to reduced contribution from non-structural elements in the first floor compared to upper floors.

The V3 building is identical in floor plans to the V2 building. However, the upper stories are designed to be 20% stronger than the first story. The purpose of building V3 is to explore the design limit of vertical structural irregularity in ASCE7-16 Chapter 12 Table

12.3-2 (as shown in Figure 3-5), which allows for a story to have lateral strength which is less than 80% of the lateral strength in the story above.

Type	Description	Reference Section	Seismic Design Category Application
5a.	**Discontinuity in Lateral Strength–Weak Story Irregularity:** Discontinuity in lateral strength–weak story irregularity is defined to exist where the story lateral strength is less than 80% of that in the story above. The story lateral strength is the total lateral strength of all seismic-resisting elements sharing the story shear for the direction under consideration.	12.3.3.1 Table 12.6-1	E and F D, E, and F
5b.	**Discontinuity in Lateral Strength–Extreme Weak Story Irregularity:** Discontinuity in lateral strength–extreme weak story irregularity is defined to exist where the story lateral strength is less than 65% of that in the story above. The story strength is the total strength of all seismic-resisting elements sharing the story shear for the direction under consideration.	12.3.3.1 12.3.3.2 Table 12.6-1	D, E, and F B and C D, E, and F

Figure 3-5 Vertical Structural Irregularities (ASCE, Minimum Design Loads for Buildings and Other Structures (ASCE/SEI 7-16), 2016)

Also, the foundations are all integral with the ground level slab on grade and adequate anchorage devices such as hold-downs or full height tied-down rod systems are used to provide overturning resistance for the four-story building.

3.2.1. Design Criteria

The building is designed to satisfy the requirements of ASCE7-16 and the provisions of 2018 NDS and 2015 SDPWS. Table 3-3 shows the gravity loads and Table 3-4 shows the seismic design criteria for the three example buildings. These loads were derived from those used in the ATC116 study.

Table 3-3 Gravity loads

Floor Dead Load (psf)	*Floor Live Load (psf)*	*Roof Dead Load (psf)*	*Roof Live Load (psf)*	*Wall Dead Load (psf)*
40	50	27	20	16

Table 3-4 Seismic Design Criteria

Seismic Design Level	*Seismic Design Category*	*MCE Ground Motion*				*Design Criteria*	
		S_S	**S_1**	**F_a**	**S_{MS}**	**S_{DS}**	**C_s**
High	SDC D_{max}	1.5	0.6	1.0	1.5	1.0	0.154

To obtain the effective seismic weight of the building, a load combination of **1.05D+0.25LL** as recommended in FEMA P695 Chapter 6 (for numerical model development) has been used. Table 3-5 shows the calculated the story weights, the total building weight and the relative mass ratio (normalized by the mass of the first story). Detailed calculations are provided in Appendix A.

Table 3-5 Example Building Story Weights

Story	*Effective Story Weights W_I, kips*	*Mass ratio (β_m)*
4	186	0.6
3	311	1.0
2	311	1.0
1	311	1.0

3.3. Database for Shearwalls Used

All of the buildings were modeled in Timber3D using the approach explained in Chapter 2 and use only the RESST model for numerical simulation. For this study, the shearwall options for design were limited to three shown in Table 3-6. Two of these walls were tested as part of a test program to determine the seismic equivalency parameters for shearwall configurations defined in the 2005 Wind and Seismic standard and 2006 IBC (Line, Waltz, & Skaggs, 2008). These walls used framing of nominal 2x4 Douglas-fir spaced at 24" on center (o.c.). The third wall was part of a separate test program with high unit shear capacity walls with 2-inch edge nail spacing and representative multi-story details in mind (Line, Hohbach, & Waltz, 2019). This wall used framing members consisting of nominal 2x6 studs at 16" o.c. and representative top and bottom plate extension beyond the sheathed width of the wall framing. Each of these walls are listed in the table below with pertinent details. The walls are hereafter referred to as 'OSB-Low', 'OSB-Med' and 'OSB-High' and this naming convention for the walls has been retained from the ATC116 study. On the other hand, no new tests were done for non-structural wall types and the backbone properties of non-structural walls are adopted from the ATC116 study, and are also been enlisted in Table 3-6.

Table 3-6 Walltypes used in this Study

Name	*Description*	*Nominal Strength (plf)*
OSB-Low	7/16-inch OSB sheathing on Douglas-Fir framing, single row of 8d common nails at 6 inches o.c along all panel edges	520
OSB-Med	7/16-inch OSB sheathing on Douglas-fir framing, single row of 8d common nails at 3 inches o.c. along all panel edges	980
OSB-High	19/32-inch OSB sheathing on Douglas-for framing, single row of 10 common nails at 2 inches o.c along all panel edges	1740
OSB-Nonstructural	Same as OSB-Low but with minimum nailing	Not applicable
Gypsum Wall Board	½-inch gypsum wallboard on unblocked studs at 16 inches o.c., 5d cooler nails at 7 inches o.c. along all panel edges	Not applicable
Stucco	Stucco construction	Not applicable

3.3.1. Shearwall Backbones and RESST Parameters

The RESST model explained in Chapter 2 was fitted to each of the structural walltypes and the fitted backbones against the test backbones are shown in Figure 3-6 through Figure 3-8 (these are different than ones used in ATC116). The RESST parameters for structural wall elements are provided in Table 3-7 and those for non-structural elements in Table 3-8 besides also being shown in the corresponding plots.

Table 3-7 RESST model parameters for 8’ wide by 10’ high structural walls

	K_0	r_1	r_2	r_3	r_4	F_x	f_1	f_2	f_3	D_x	α	β
OSB-Low	26.92	0.04	-0.11	1.01	0.01	6.46	0.68	0.13	0.30	4.25	0.86	1.15
OSB-Med	28.20	0.05	-0.12	1.01	0.02	12.05	0.64	0.19	0.30	5.63	0.86	1.30
OSB-High	29.40	0.04	-0.18	1.01	0.01	21.70	0.80	0.13	0.30	7.40	0.86	1.15

Table 3-8 RESST model parameters for 8’ wide by 10’ high non-structural elements

	K_0	r_1	r_2	r_3	r_4	F_x	f_1	f_2	f_3	D_x	α	β
OSB-NS	12.00	0.08	-0.03	1.01	0.01	5.24	0.59	0.13	0.30	6.50	0.75	1.05
GWB	2.50	0.46	-0.12	1.45	0.01	2.26	0.56	0.09	0.30	3.10	0.38	1.09
Stucco	25.00	0.13	-0.03	1.45	0.01	9.04	0.44	0.09	0.30	4.70	0.38	1.09

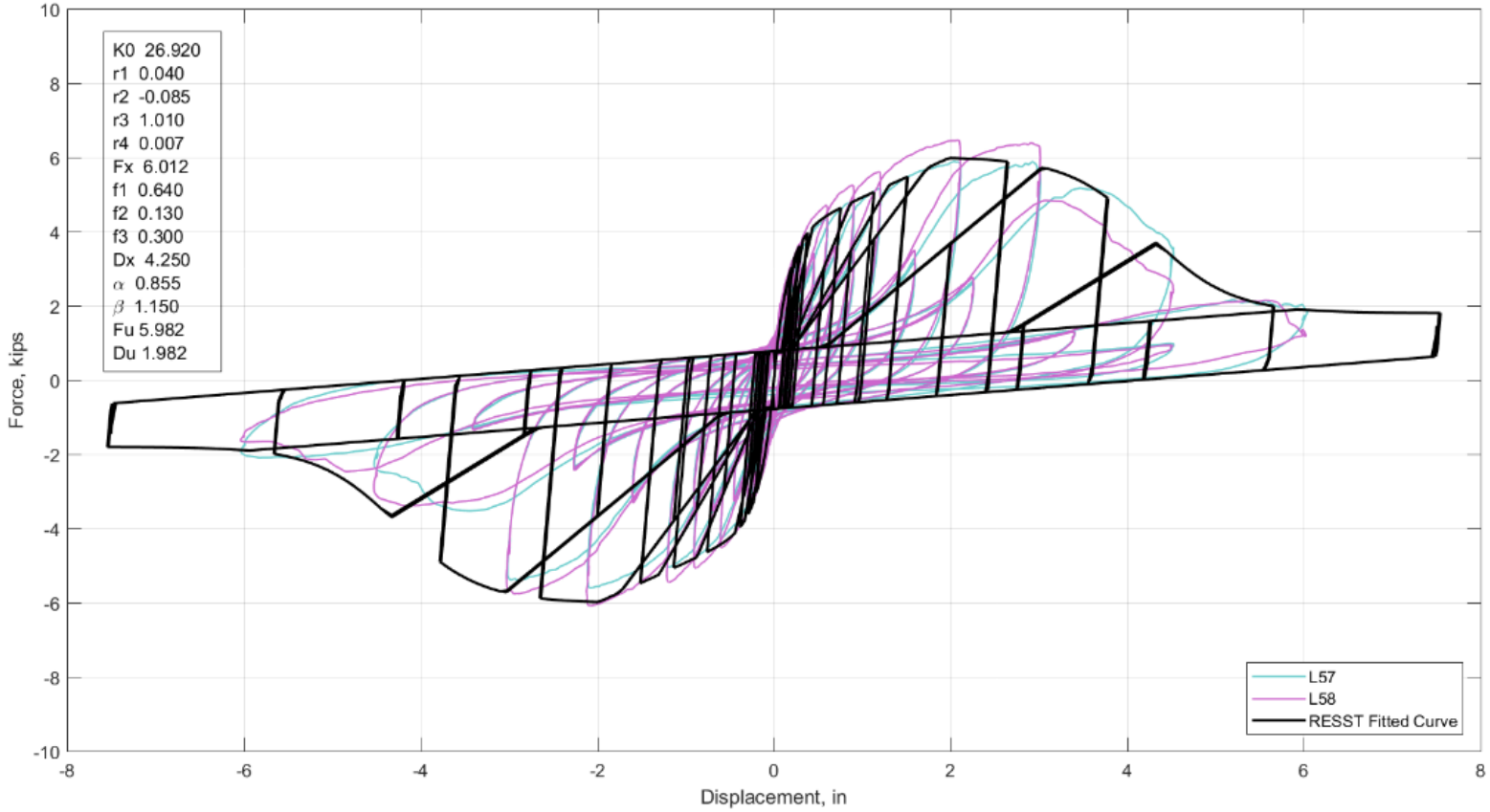

Figure 3-6 RESST model for OSB-Low

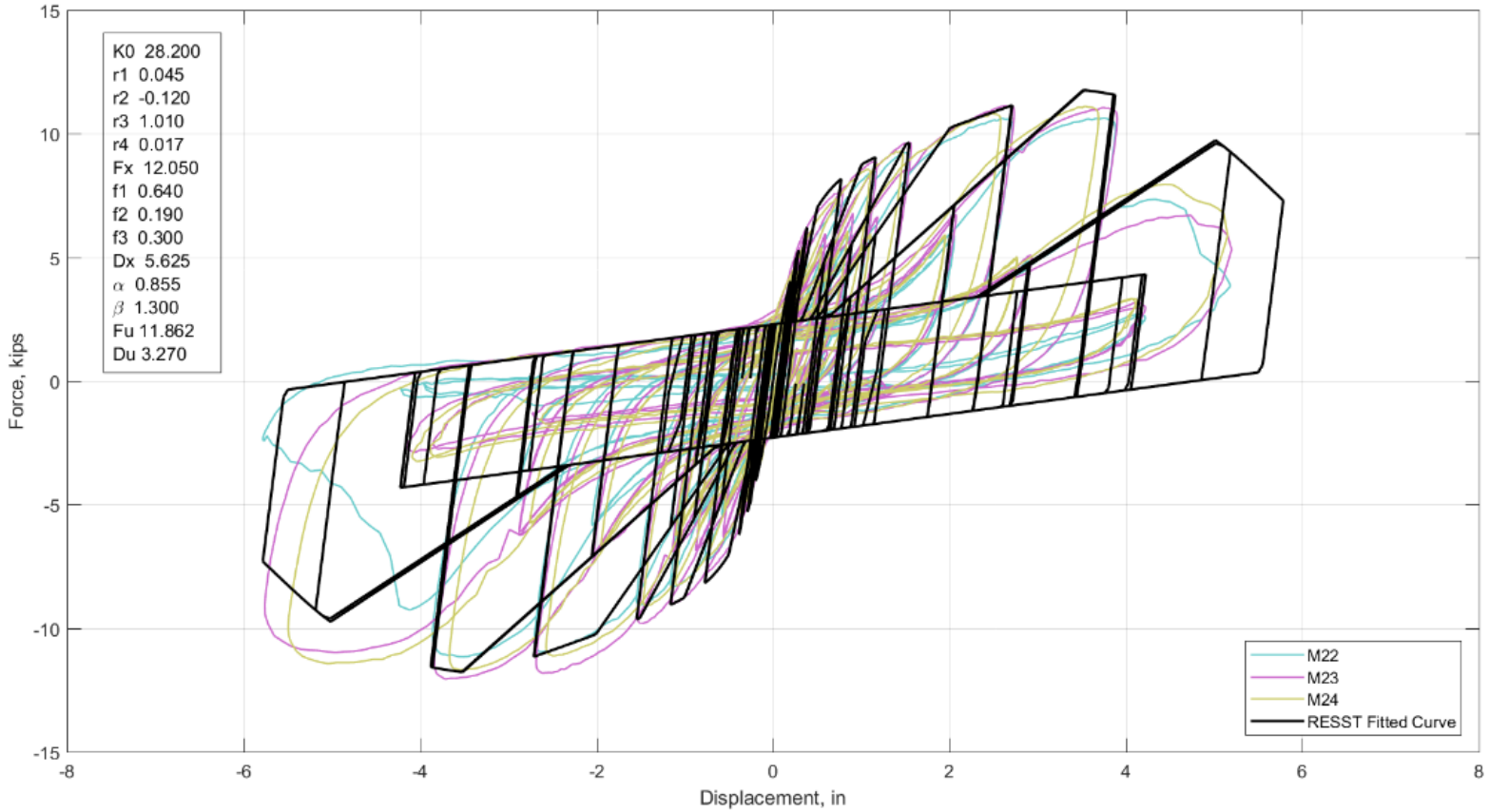

Figure 3-7 RESST model for OSB-Med

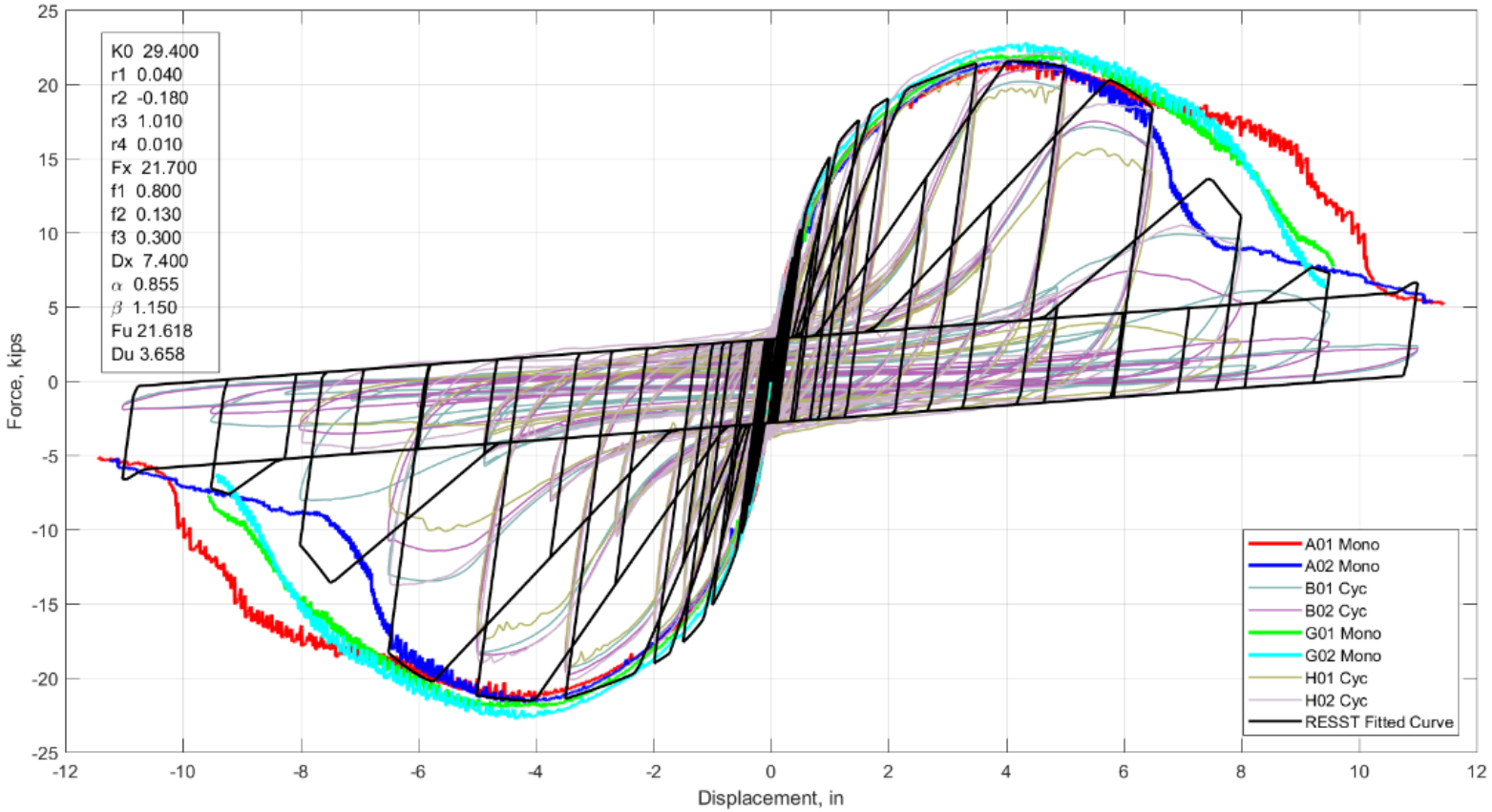

Figure 3-8 RESST model for OSB-High

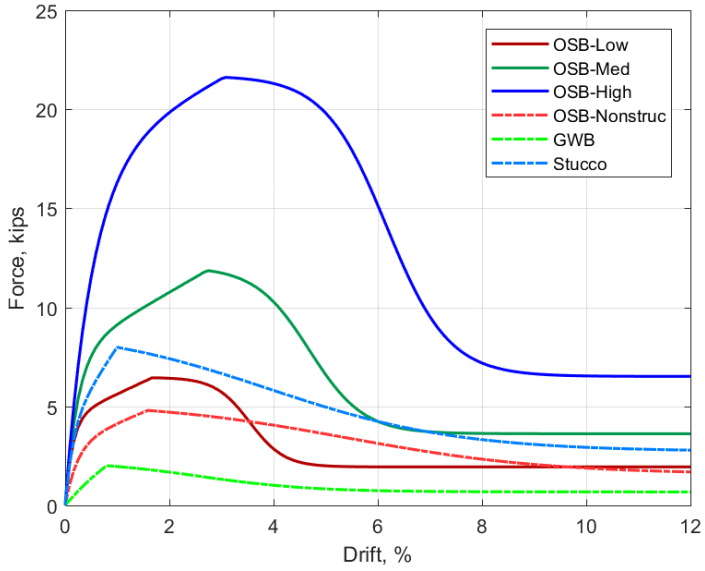

Figure 3-9 Backbones curves for all six wall elements

3.4. Seismic Design per ASCE7-16

3.4.1. Equivalent Lateral Force (ELF) Calculation

Using the relation for the approximate fundamental period from ASCE7-16,

$$T_a = C_t h_n^x = 0.02 \times 40^{0.75} = 0.32 \text{ sec}$$

Using S_{DS} = 1.0g, R = 6.5 and I = 1.0,

$$C_S = {S_{DS}}/{\left(\frac{R}{I}\right)} = {1}/{\left(\frac{6.5}{1}\right)} = 0.154$$

Table 3-9 Equivalent Lateral Force and Story Shear Calculation

Story i	$\beta_{m,i}$	m_i *kips/g*	h_i *in*		C_{vxi}	*Cumulative* C_{vxi}	V_{xi} *kips*
(1)	**(2)**	**(3)**	**(4)**	**(5) = (2)*(4)**	**(6)**	**(7)**	**(8)**
4	0.60	186.60	480.00	288.00	0.29	0.29	49.21
3	1.00	311.00	360.00	360.00	0.36	0.64	110.73
2	1.00	311.00	240.00	240.00	0.24	0.88	151.74
1	1.00	311.00	120.00	120.00	0.12	1.00	172.25
		1119.60		**1008.00**			

It is to be noted that these forces are the same for all three buildings.

3.4.2. Diaphragm Design

Floor diaphragm were designed to resist and further distribute the calculated equivalent lateral forces. The diaphragm was designed as a flexible diaphragm. Detailed calculations are provided in the Appendix B. The same diaphragm design was decided upon for all of the floors to simplify modeling.

Final Design: 15/32" STR I, nominal 2x members, blocked with 10d nails @ 4" spacing

With the in-plane stiffness G_a of 15 kips/in, the flexural deflection for 44' span at mid-span was found to be about 0.94 inches.

3.4.3. Shearwall Design

For shearwall design, it has been assumed that the diaphragm for the building is rigid i.e. the distribution of story shear forces from the diaphragm to shearwalls is directly proportional to the stiffnesses of the shearwalls resisting the motion in the direction. This

assumption shall be checked for using the clause 12.3.1 in ASCE7-16. Also, the walls were designed such that there is little to no overstrength and the provided lateral strength is not much larger than the story shear. This was done only for research purposes and by no means, suggests that this is a better practice. However, to accommodate this, the total wall lengths would have to be varied in contrast to the popular practice in construction of providing the same wall lengths on all the floors since there are only three walltypes to choose from (and six if double sheathing is considered). Shearwall lengths have been limited to a 4-ft increment as would be in the numerical model. Table 3-10 and Table 3-11 show the exterior and interior wall units (each 4-ft long), wall types and the provided capacity against the demand along short and long direction of the building. It is to be noted that buildings V1 and V2 would share this same design. Because of the use of double sheathing on the exterior walls along short direction and only single sheathing on the exterior along long direction and same number of doubly-sheathed interior walls, the designs in both directions have exactly the same lateral strength.

Building V3 has been designed that such that the first story design (total capacity of structural walls) is same as that for V1 & V2, however, with a much stronger upper stories as was previously noted. Similar strength against demand calculation for building V3 are shown in Table 3-12 and Table 3-13.

Table 3-10 Provided Strength against Demand Calculation (short direction)

	Exterior Walls				*Interior Walls*				*Combined*			
Story	**#Sh.**	**Wall Units**	**Type**	**Capacity kips**	**#Sh.**	**Wall Units**	**Type**	**Capacity kips**	**Capacity kips**	**Capacity (normalized)**	**Demand kips**	**C/D**
4	2	4	Med	25.09	2	4	Med	25.09	50.18	0.27	49.21	1.02
3	2	12	Med	75.26	2	6	Med	37.63	112.90	0.61	110.73	1.02
2	2	12	High	133.63	2	6	Low	19.97	153.60	0.84	151.74	1.01
1	2	12	High	133.63	2	8	Med	50.18	183.81	1.00	172.25	1.07

Table 3-11 Provided Strength against Demand Calculation (long direction)

	Exterior Walls				*Interior Walls*				*Combined*			
Story	**#Sh.**	**Wall Units**	**Type**	**Capacity kips**	**#Sh.**	**Wall Units**	**Type**	**Capacity kips**	**Capacity kips**	**Capacity (normalized)**	**Demand kips**	**C/D**
4	1	8	Med	25.09	2	4	Med	25.09	50.18	0.27	49.21	1.02
3	1	24	Med	75.26	2	6	Med	37.63	112.90	0.61	110.73	1.02
2	1	24	High	133.63	2	6	Low	19.97	153.60	0.84	151.74	1.01
1	1	24	High	133.63	2	8	High	50.18	183.81	1.00	172.25	1.07

Table 3-12 Provided Strength against Demand Calculation (short direction) for V3

	Exterior Walls				*Interior Walls*				*Combined*			
Story	**#Sh.**	**Wall Units**	**Type**	**Capacity kips**	**#Sh.**	**Wall Units**	**Type**	**Capacity kips**	**Capacity kips**	**Capacity (normalized)**	**Demand kips**	**C/D**
4	2	4	Med	133.63	2	4	Med	89.09	222.72	1.21	49.21	4.53
3	2	12	Med	133.63	2	6	Med	89.09	222.72	1.21	110.73	2.01
2	2	12	High	133.63	2	6	Low	89.09	222.72	1.21	151.74	1.47
1	2	12	High	133.63	2	8	Med	50.18	183.81	1.00	172.25	1.07

Table 3-13 Provided Strength against Demand Calculation (long direction) for V3

	Exterior Walls				*Interior Walls*				*Combined*			
Story	**#Sh.**	**Wall Units**	**Type**	**Capacity kips**	**#Sh.**	**Wall Units**	**Type**	**Capacity kips**	**Capacity kips**	**Capacity (normalized)**	**Demand kips**	**C/D**
4	1	8	Med	133.63	2	4	Med	89.09	222.72	1.21	49.21	4.53
3	1	24	Med	133.63	2	6	Med	89.09	222.72	1.21	110.73	2.01
2	1	24	High	133.63	2	6	Low	89.09	222.72	1.21	151.74	1.47
1	1	24	High	133.63	2	8	High	50.18	183.81	1.00	172.25	1.07

3.4.3.1. Check for Shearwall Deflection

Detailed calculations for shearwall design and deflection calculation are provided in Appendix C. The shearwall deflection was checked for the 1st story, 4 feet long wall at the corner of the building along Wall Line A. It was found that the shearwall deflection at the top was about 1.04 inches. ASCE7-16 Table 12.12-1 provides an allowable story drift of 2.5% for a Risk Category II light-frame wood construction. For a drift limit of 2.5%, the drift limit would be 0.025x120 = 3 inches, which is well above the calculated deflection. Hence, the design meets the current code provisions.

3.4.3.2. Check for Flexible Diaphragm

According to clause 12.3.1.3 in ASCE7-16, if the deflection at the mid-span of a diaphragm is greater than twice the average drift of the diaphragm induced by the deflection of the shearwalls, the diaphragm is permitted to taken as flexible. Numerically,

$$\frac{\delta_{MDD}}{\Delta_{ADVE}} > 2$$

where δ_{MDD} and Δ_{ADVE} are defined as shown in Figure 3-10.

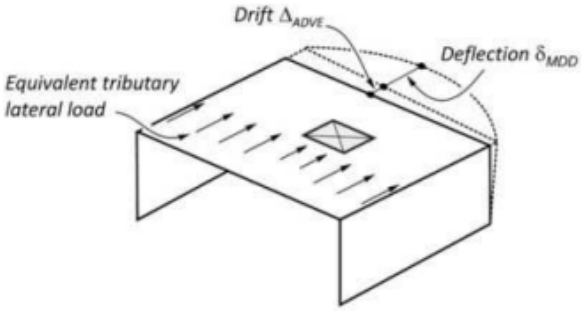

Figure 3-10 Flexible Diaphragm (Minimum Design Loads for Buildings and Other Structures (ASCE/SEI 7-16), 2016, p. 96)

Based on the diaphragm and shearwall deflection calculated previously, it is clear that diaphragm deflection (0.94”) is not greater than twice the average inter-story deflection (taken same as the shearwall deflection of 1.04”). This check does not disprove the rigid diaphragm assumption made earlier and hence; the assumption has been used in this chapter as well as the following chapters. Note that for modeling purpose, the diaphragm shear stiffness of 15 kip/in is used in all numerical models.

Finally, the structural walls were distributed symmetrically across the floor plan as shown for Story 1 in Figure 3-11. All of the other design floor plans for V1 (& V2) and V3 are provided in the Appendix D.

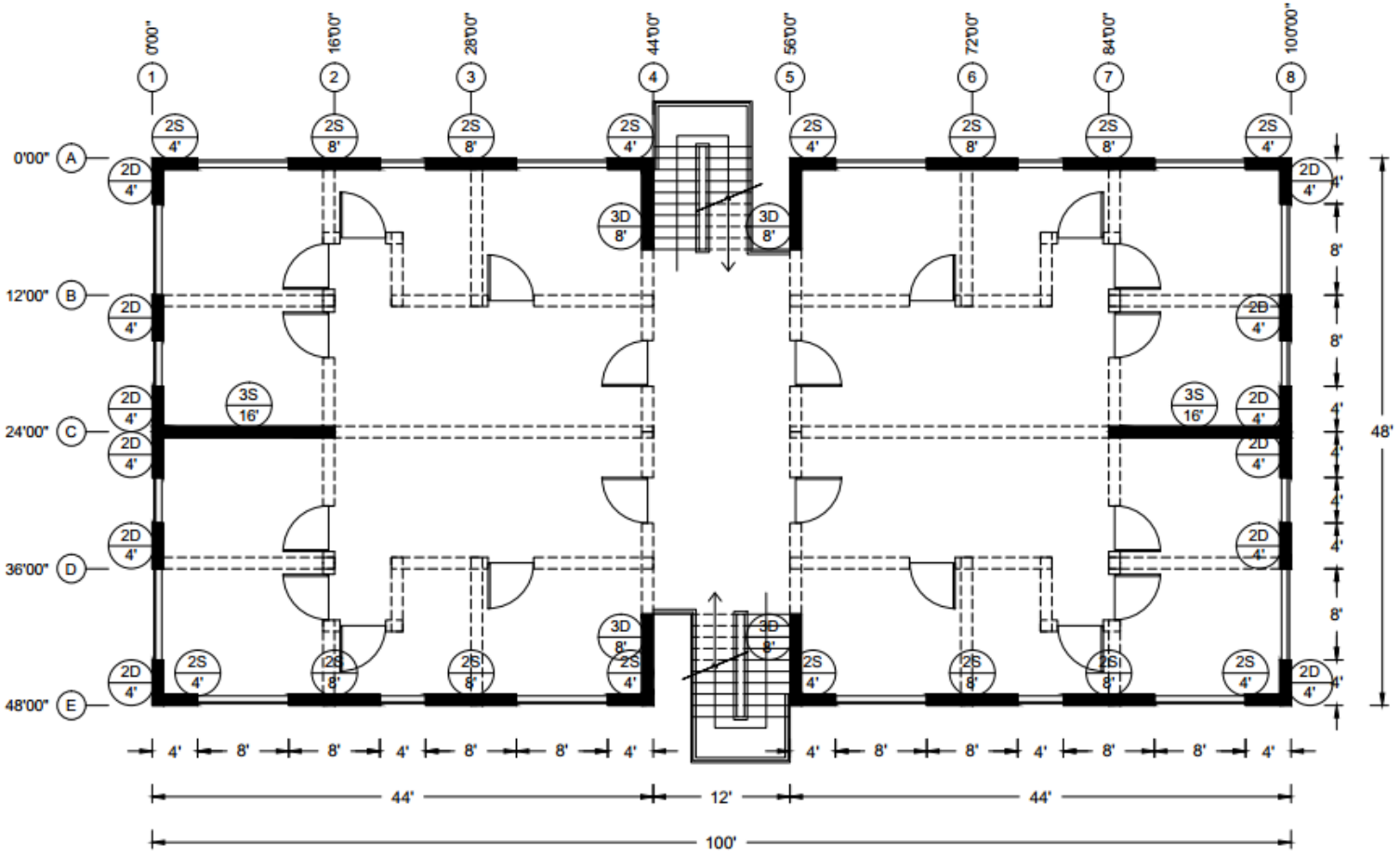

Figure 3-11 Story 1 shearwall design floor plan (same for V1, V2, V3)

3.4.4. Design Story Backbones

Figure 3-12 shows the story backbones for V1 along the width and length of the building and Figure 3-13 shows the shear strength profiles for each of these buildings. Also shown in Figure 3-13 is the combined strength profile inclusive of the non-structural elements. This was obtained by proportionately scaling the design strength (ϕ factor times nominal strength) of structural walls based on the peak backbone force. These profiles were only plotted to get a sense of how the strength among the stories compares against one another. Figure 3-14 through Figure 3-17 show the backbones as well as shear profiles for V2 and V3 buildings. Here on forth, X direction refers to along the short dimension and Y-direction along the long dimension of the building. And also, a simple notation has been introduced and shown in the backbone plots to represent the structural walls in a concise form. This notation shall be used in latter chapters as well.

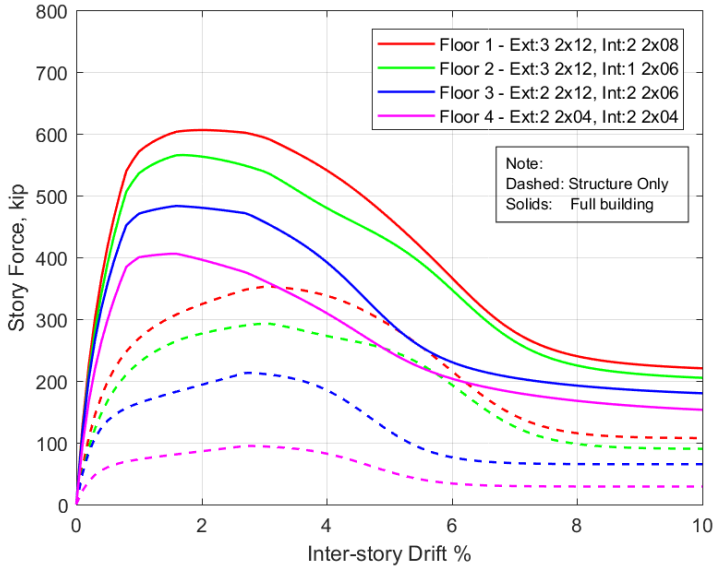

a) Along X-direction

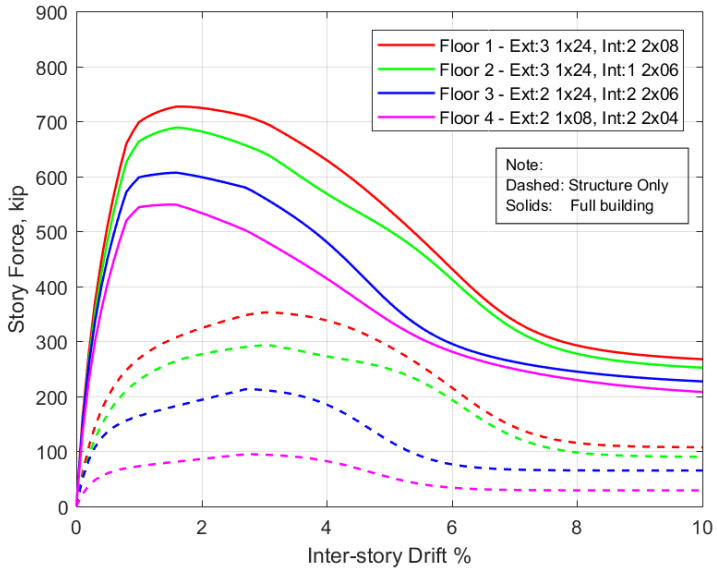

b) Along Y-direction

Figure 3-12 Story backbones for V1

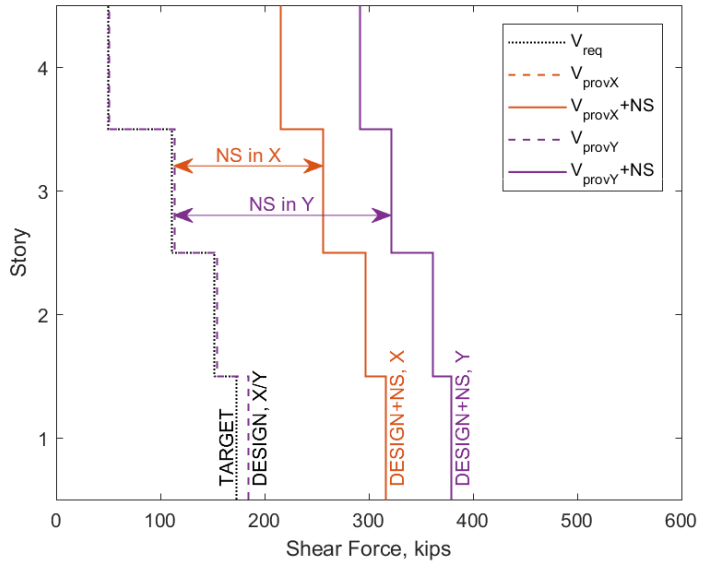

Figure 3-13 Shear strength Profile for V1

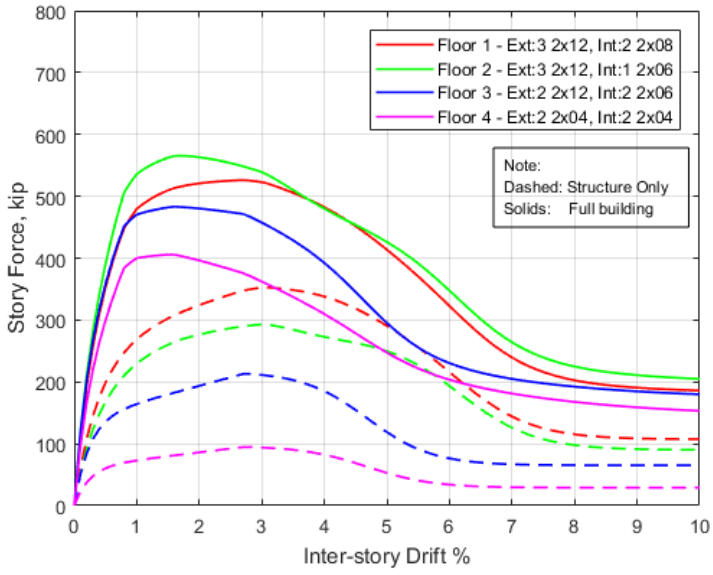

a) Along X-direction

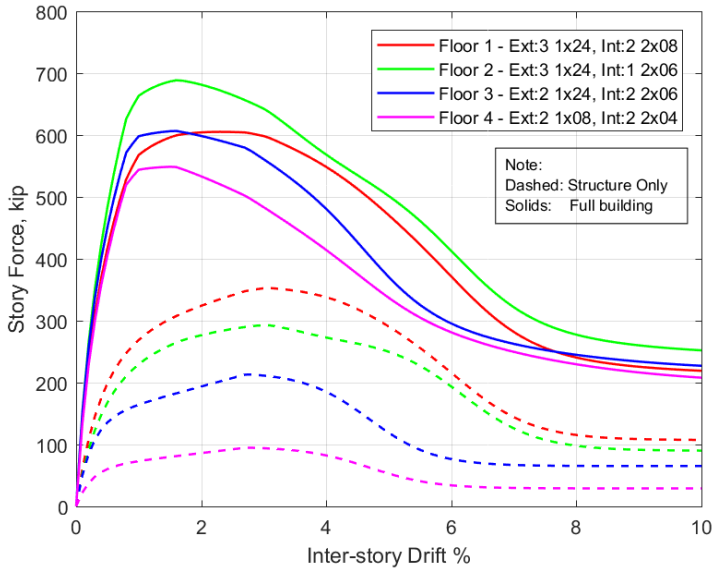

b) Along Y-direction

Figure 3-14 Story backbones for V2

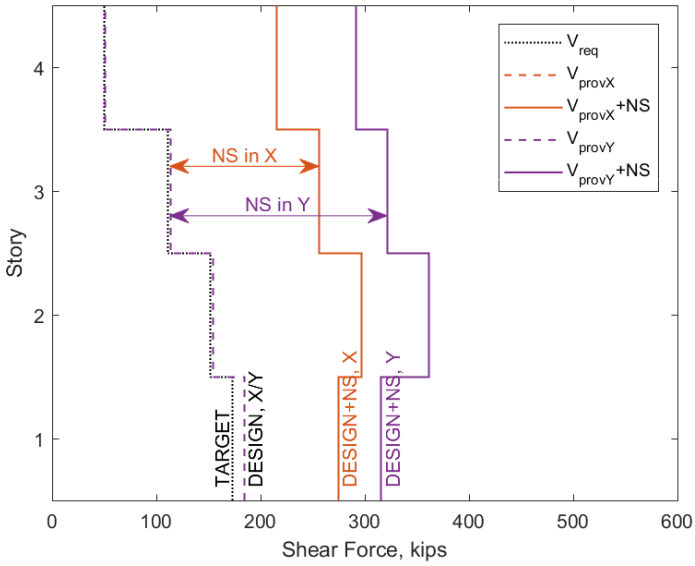

Figure 3-15 Shear strength Profile for V2

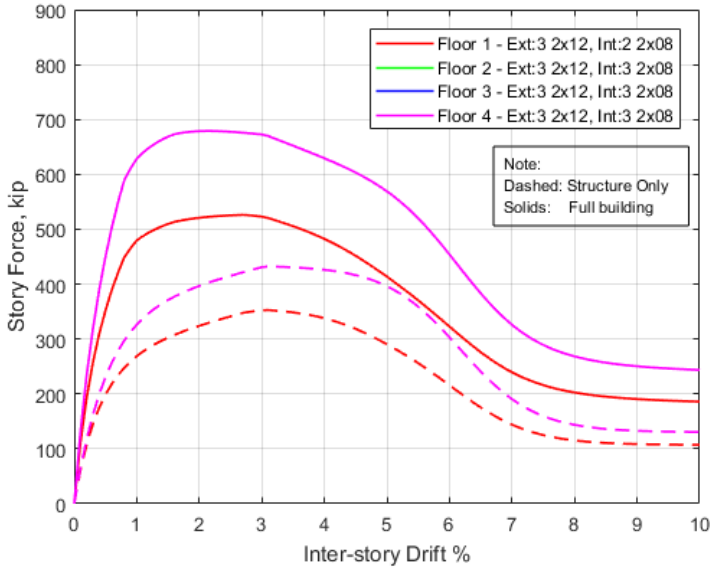

a) Along X-direction

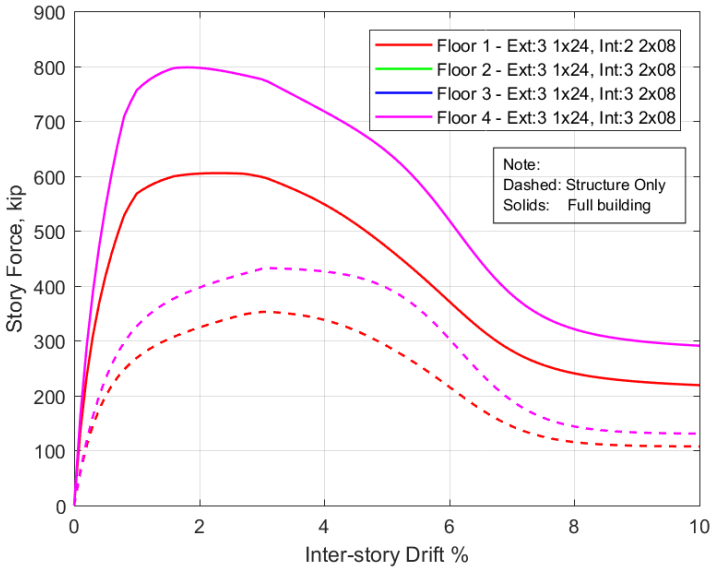

b) Along Y-direction

Figure 3-16 Story backbones for V3

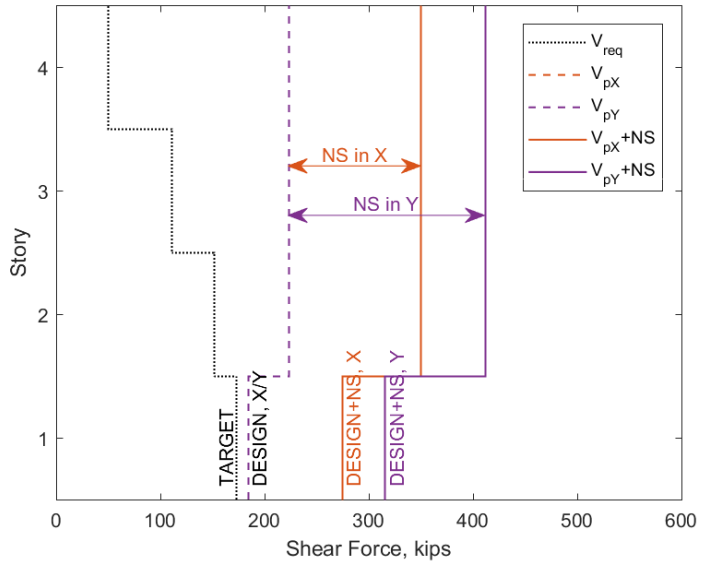

Figure 3-17 Shear strength Profile for V3

3.5. Performance Evaluation

A total of six Timber3D models were built for each of the buildings with and without modeling the non-structural elements. Results for modal analyses and nonlinear static and dynamic analyses are presented in each of the following subsections. To differentiate between structure-only and full building models (i.e. with non-structural elements), the models when referred to as just V1 represents the structure-only V1 model while V1+NS represents the corresponding full building model. Figure 3-18 shows the one of Timber3D models.

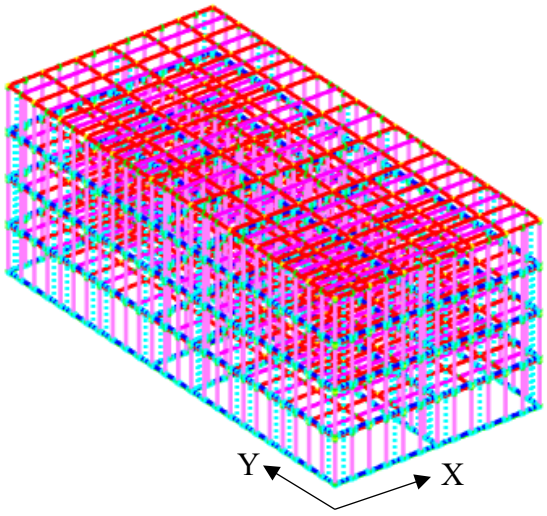

Figure 3-18 3D configuration of an example building in Timber3D

3.5.1. Difference in story backbones between Floor Plan A and Floor Plan B

Using these fitted backbone curves for each of these wall components from Section 3.3 and based off the provided design, the total backbone for a building story can be obtained. The key interest here being difference in backbones between Floor Plan A and Floor Plan B. Figure 3-19 a) shows the first story backbones for Floor Plan A (in V1) and Floor Plan B (in V2) and Figure 3-19 b) shows only the non-structural elements in the floor plan along each direction. On average there is a 40% difference between the two directions if only non-structural elements are considered (i.e. Y direction has 40% more strength from non-structural elements than X direction) and about 16% difference if the total backbone is considered.

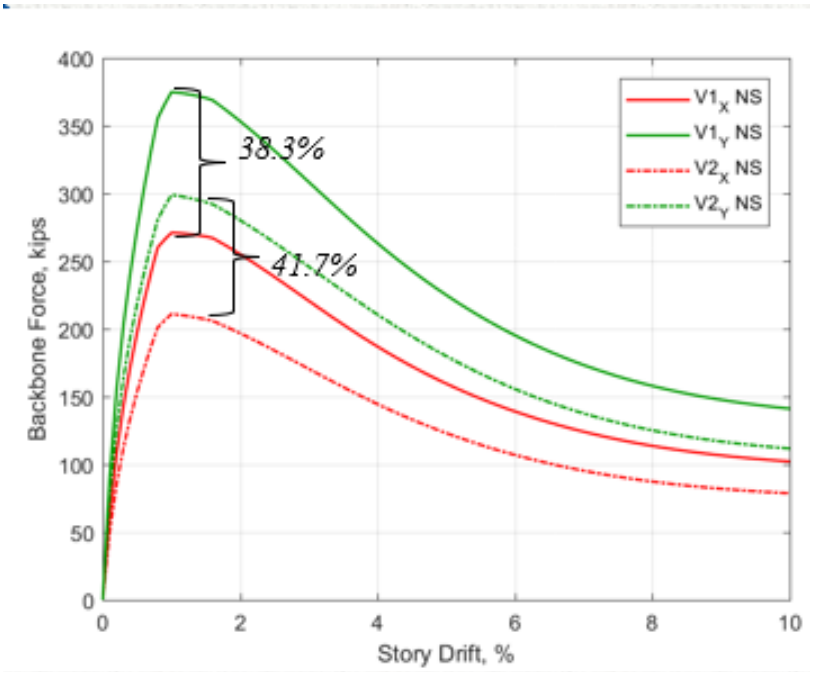

a)

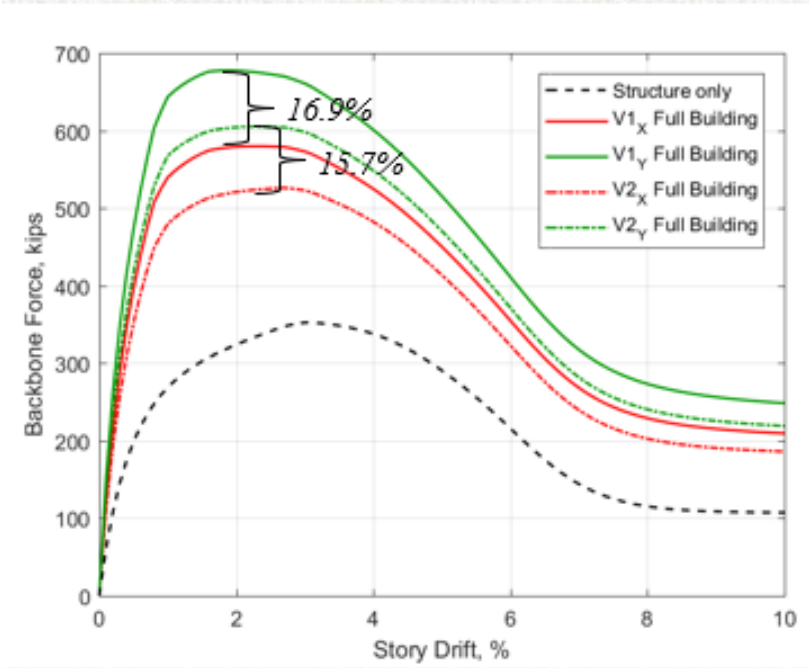

b)

Figure 3-19 First story Backbones showing (a) only non-structural elements and (b) total backbone

3.5.2. Modal Analyses

Modal analyses were conducted on each of the six models. The first three modes shapes for V1 building are shown in Figure 3-20 and the first three periods for the six models in Table 3-14. The first two modes are purely translational in either direction while the third is torsional. Note that the Timber3D models provide other higher modes and periods. However, those are not reported here.

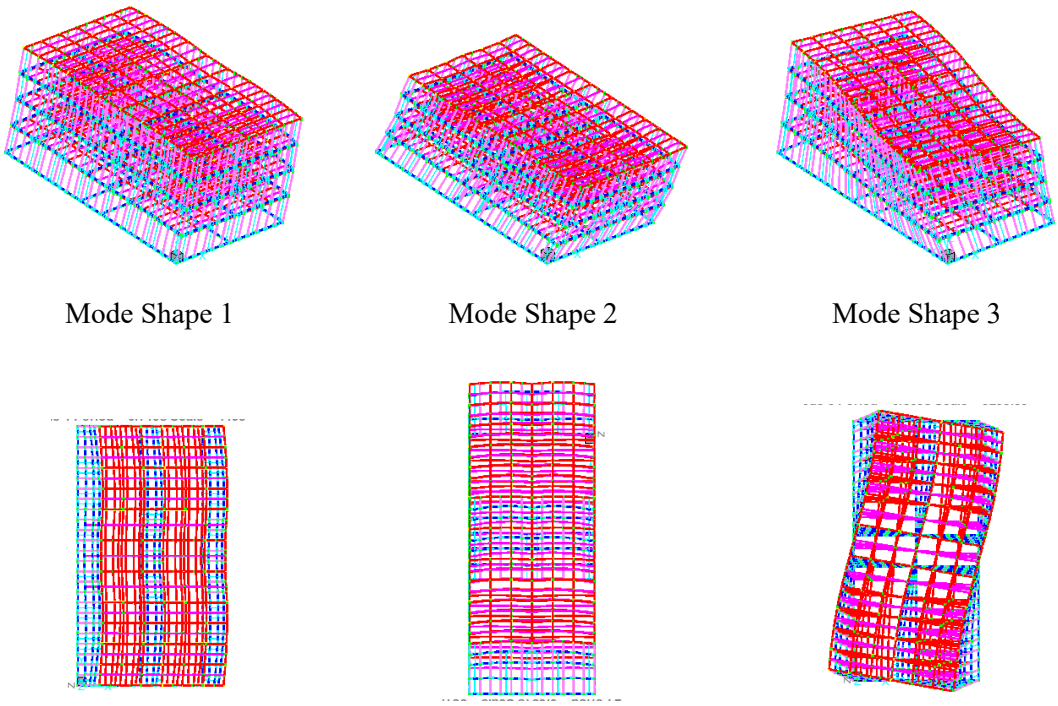

Figure 3-20 First three modes shapes in 3D and in plan

Table 3-14 First three periods (seconds) for models (V1, V2 and V3) with and without NS

Mode	*Structure Only*			*Full building*		
	V1	**V2**	**V3**	**V1+NS**	**V2+NS**	**V3+NS**
1	0.71	0.71	0.67	0.57	0.58	0.57
2	0.68	0.68	0.64	0.51	0.52	0.51
3	0.57	0.57	0.55	0.46	0.46	0.46

3.5.3. Nonlinear Static (Pushover) Analyses

Nonlinear static pushover analyses were conducted along each horizontal direction of each model to determine the overall base shear-roof displacement response and the characteristic parameters defined in Chapter 2. The monotonic push was based on the first-mode distribution of lateral forces. P-Δ effects were included. It was found that the pushover along the two directions are only slightly different hence, Figure 3-21 shows the backbones curves and Table 3-15 tabulates all the relevant parameters for pushover only along the long direction (Y-direction) of the buildings.

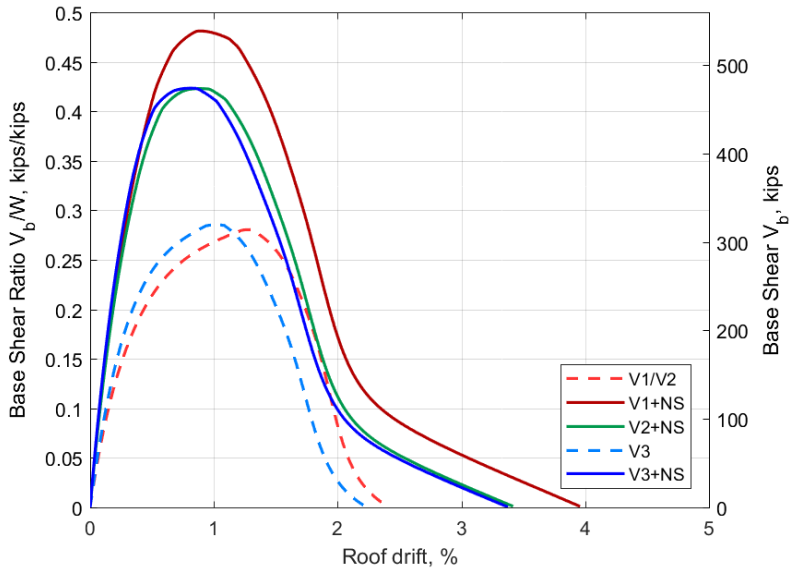

Figure 3-21 Pushover backbones for V1, V2 and V3

Table 3-15 Pushover backbone parameters for V1, V2 and V3

Parameters	*V1*	*V2*	*V3*	*V1+NS*	*V2+NS*	*V3+NS*
V_{max}/W	0.28	0.28	0.285	0.481	0.423	0.423
Ω_0	1.82	1.82	1.854	3.128	2.749	2.752
μ_T	> 8	> 8	> 8	> 8	> 8	> 8

Following observations can be made from the figure and the table:

a. In the case of structure only models, V1 and V2 have same backbone parameters. High overstrength in design in the upper stories for V3 does not amount to a much larger overall overstrength. This is likely due to the unnecessary irregularity (soft story) in V3. Also, it can be pointed out that V3 has a reduced ductility compared to V1 or V2. For the V3 building, since the upper stories are stiffer and stronger

than that of V1 and V2, the inter-story displacements in the upper stories are less than that of V3, thus the smaller overall displacement at peak backbone strength.

b. In the case of full building models, V1+NS has the highest peak strength while V2+NS and V3+NS have comparable peak strength. Also, V2+NS and V3+NS models have similar static collapse displacement capacity (defined as displacement at zero restoring force at post-peak) and ductility while V1+NS has a slightly larger collapse displacement capacity (4% roof drift) and ductility.

c. Non-structural (NS) elements can contribute to an additional 50-70% lateral strength which is substantial when consider the fact that non-structural elements are neglected from design calculations.

It can be inferred from the observations that irregularity such as a soft story can lead to deterioration in strength and performance of a building structure with or without NS elements and also that the contribution from NS to overall lateral strength can be substantial and be undocumented even though they are not considered in design.

3.5.4. Incremental Dynamic Analyses (IDAs)

Three-dimensional IDAs were conducted on each of the models following the FEMA P695 guidelines and ground motions (outlined in Chapter 2) to further explore the observations made in pushover analyses. Figure 3-22 shows the fragility curves and Table 3-16 tabulates the relevant IDA parameters.

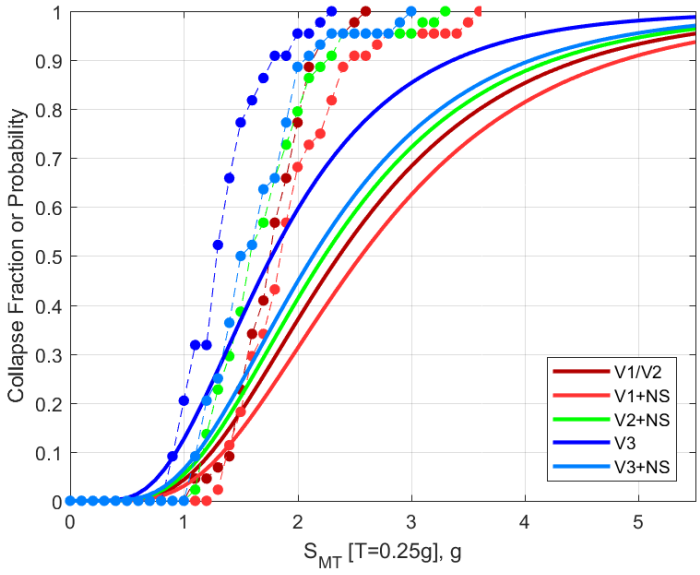

Figure 3-22 Fragility curves for V1, V2 and V3

Table 3-16 IDA parameters for V1, V2 and V3

Parameters	*V1*	*V2*	*V3*	*V1+NS*	*V2+NS*	*V3+NS*
S_{CT} *(g)*	2.84	2.84	2.13	3.07	2.68	2.56
CMR	1.42	1.42	1.07	1.54	1.34	1.28
ACMR	1.89	1.89	1.42	2.05	1.79	1.71
P(COL|MCE)	10.1%	10.1%	24.2%	7.6%	12.2%	14.2%

Following observations can be made from the IDAs:

a. In the case of structure only models, V1 and V2 have same performance. And as anticipated, V3 has a much greater collapse probability because of the soft story introduced in design.

b. Inclusion of NS helps reduce the collapse probabilities in case of V1 and V3. In contrast, NS elements have a negative effect on the performance of V2 because of

the irregularity introduced through a more open first-story floor plan. The strength and stiffness contributions of non-structural elements in the upper stories are larger than in the first story resulting in seismic demand concentration in the first story, thus the higher MCE_R collapse probability in V2+NS compared to V2. Also, the increased irregularity on the addition of NS elements to the already soft V3 decreased the MCE_R collapse probability from 24.2% to 14.2%. This suggests that there could be a tipping point for irregularity beyond which any additional irregularity due to NS elements or overdesign becomes more helpful than harmful. However, this threshold has not explored in this thesis.

The difference in collapse probabilities are not as significant but the trend is clear that NS elements may or may not be good for the seismic performance of the building depending on the plan configuration among stories. Furthermore, vertical irregularities introduced into a building through structural design only or inclusion of NS elements may be detrimental and may lead to increased chance of collapse for certain building configurations. Note that the strengths of upper stories in V3 building are 1.21 times that of the first story. This is below the threshold vertical irregularities of 1.25 that the ASCE7-16 allows for. It is anticipated that a building reaching the threshold would result in worse performance than that observed for V3 building. Further investigation into this issue and provision may be necessary.

For performance-based design in the subsequent chapter, it would be useful to determine the drift at which these buildings tend to collapse. Figure 3-23 superimposes the pushover backbones against the distribution of peak inter-story drift at collapse. Lognormal

distribution is fitted to peak inter-story drifts for each building. For structure only models, the median drifts at collapse are between 4% to 6%. Comparatively, full building collapses between 6% to 7 % median drifts. From Figure 3-23, It can be seen that a relationship could be determined between the displacement at peak load from the pushover curve and the incipient collapse displacement from IDA.

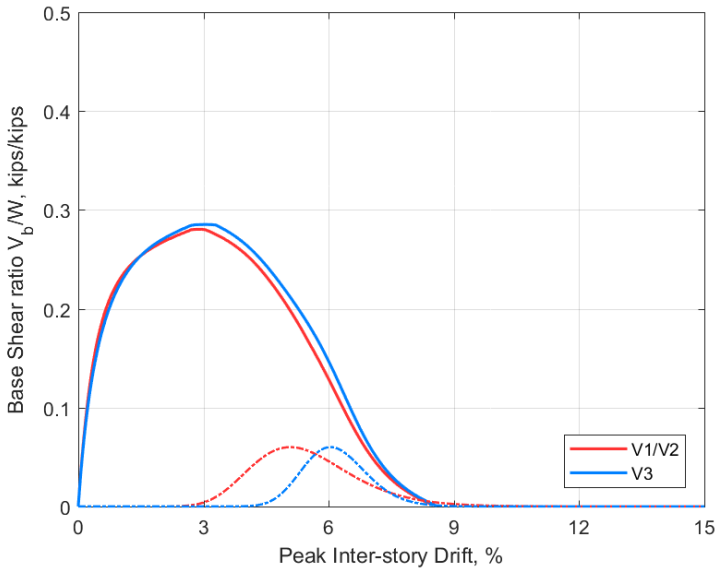

a)

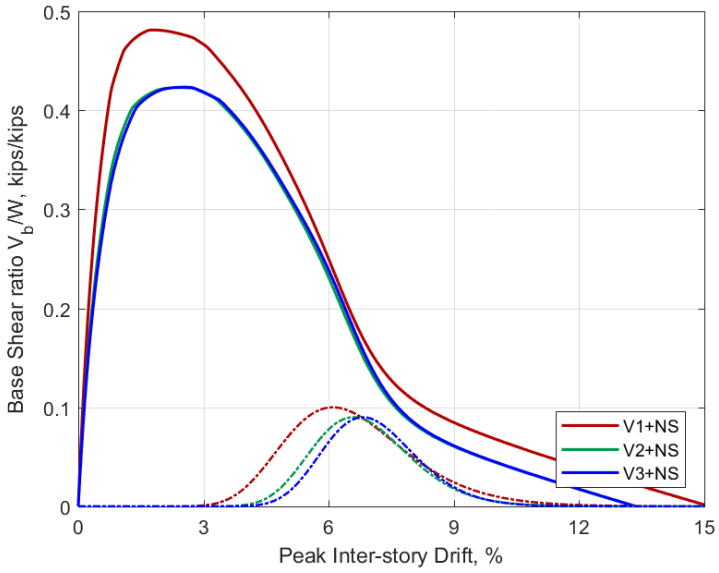

b)

Figure 3-23 Peak-story drift distribution superimposed onto the pushover curves for (a) structure only and (b) full building

4. DIRECT DISPLACEMENT-BASED DESIGN (DDD) PROCEDURE

This chapter elaborates on the key concepts used in the displacement-based design (DDD) procedure proposed by Pang and Rosowsky (2009) and suggests some modifications that were found essential. The chapter also explores building design profiles associated with different drift limits for the same seismic hazard level and, compares and determines the suitable drift limit and the associated design profile that best corresponds to the force-based design ELF procedure implemented in the design codes. Lastly, the chapter talks about a pushover-like assessment procedure based on the formulations from the DDD procedure and suggests some of its applications.

4.1. Design Performance Levels

ASCE/SEI-41, "Seismic Rehabilitation of Existing Buildings" provides guidance for various performance objectives defined in terms of seismic hazard level and drift limit pairs for structural as well as non-structural elements in buildings. The seismic hazard levels are therein referred to as BSE-1N and BSE-2N for new buildings which are each equivalent to DBE and MCE level earthquakes with probabilities of exceedance of 10% and 2% respectively (referred hereafter as 10%/50yr and 2%/50yr). Four performance levels are defined in ASCE 41: Immediate Occupancy (IO), Damage Control (DC), Life Safety (LS) and Collapse Prevention (CP). Figure 4-1 shows the basic performance objectives for new buildings.

Risk Category	Seismic Hazard Level	
	BSE-1N	BSE-2N
I and II	Life Safety Structural Performance Position Retention Nonstructural Performance (3-B)	Collapse Prevention Structural Performance Hazards Reduced Nonstructural Performance[a] (5-D)

Figure 4-1 Basic Performance Objective for New Buildings (Seismic Evaluation and Retrofit of Exsting Building (ASCE/SEI 41-17), 2017, p. 25)

To understand the relationship between each of the performance levels and possible drifts that could be associated with these, The results and damages observed from the full-scale shake table testing of a two-story light-frame wood building, known as the NEESWood benchmark building, were used to establish the drift limits for the various performance levels (Christovasilis, Filiatrault, & Wanitkorkul, 2009). Table 4-1 shows the structural as well as non-structural damages observed at various drifts during the Benchmark test. The building was not tested to collapse and the test was stopped just beyond 2% peak inter-story drift. Based on these damages, the drift limits associated with the performance levels of IO, DC, LS and CP were assigned (Table 4-2). Note that while 4% of peak inter-story drift may not result in pancake collapse of well-built light-frame wood buildings with redundant load paths, 4% drift limit is deemed as an appropriate limit for design purpose.

In the NEESWood benchmark test, seismic intensities corresponding to 50%/50yr, 20%/50yr, 10%/50yr and 2%/50yr were used which produced maximum drifts of about 0.5%, 1.0%, 2.0% and >2.0% enlisted in Table 4-1.

Table 4-1 Damages observed at different drifts

Drift (%)	*Structural Damage*	*Non-structural Damage*
0.5	Minor splitting of sill plates, minor racking of studs	Minor hairline cracking of GWB & stucco
1.0	Partial nail pull-out, propagation of splitting and cracking	Cracking of GWB & stucco at door openings, partial screw pull-out
2.0	Sheathing pull-out at corner, major cracking and splitting	Crushing at wall corners
>2.0	Total splitting of sill plates and studs, failure of anchor bolts	Separation of GWB from ceiling, significant cracking and crushing

Using the observed damages from the Benchmark test, a set of basic performance objectives for design purpose is defined using drift limits observed for different damage mechanisms (Table 4-2). The performance levels of IO and DC are non-safety related, hence, the drifts observed at the onset of damages to non-structural elements are used to specify the design drift limits for IO and DC performance objectives. Hence for IO and DC performance levels, the peak drift responses of full building models are used to assess the adequacy of the design. For safety related performance objectives (i.e. LS and CP) which are related to partial collapse of building components and full building collapse, structure only models are used to check the drift and collapse probability of the as-designed buildings. Since non-structural walls and elements are not regulated, partition walls may be replaced or removed due to remodeling or change in occupancy type over the life of the building, the structure-only models are used to assess the performances at LS and CP levels.

Table 4-2 Basic performance objectives

Seismic Hazard	*Performance Level*	*Drift Limits*
50%/50yr	IO	0.5%
20%/50yr	DC	1.0%
10%/50yr (DBE)	LS	2.0%
2%/50yr (MCE)	CP	4.0%

In this study, the drift limits specified in Table 4-2 are assumed to be the median drifts (i.e. probability of non-exceedance, P_{NE} of 50%). To achieve higher performance, a higher PNE can be prescribed. For instance, for performance levels like Life Safety and Collapse Prevention, a higher non-exceedance probability of 80% may be more appropriate for enhanced safety level (e.g. analogous to higher risk category of the current design code). A methodology to consider different non-exceedance probability for the target drift limit is discussed in (Pang W. , Rosowsky, Pei, & van de Lindt, 2010).

4.2. Inter-story Drift Spectra

A displacement response spectrum $S_d(T)$ can be obtained from the design acceleration spectrum $S_a(T)$ as:

$$S_d(T) = \left(\frac{T}{2\pi}\right)^2 S_a(T) \qquad (Equation\ 4.1)$$

From modal analysis of a structure, the mode shape vectors ϕ_n as well as the modal participation factors Γ_n for each mode n can be determined. As used in modal spectrum analysis, the product of Γ_n, ϕ_n and $S_d(T_n)$ gives an estimate of the absolute displacement profile for the mode n, which can then be combined using square-root-of-sum-of-squares rule (as shown below for story j) to obtain the overall displacement profile for the building.

$$\Delta_j = \sqrt{\sum_n \left[\Gamma_n \phi_{jn} S_d(T_n)\right]^2} \qquad (Equation\ 4.2)$$

Knowing that inter-story drift is a more useful parameter, Pang and Rosowsky (2009) use inter-story mode shape instead, collectively represent the $\Gamma_{n,}(\phi_{jn} - \phi_{(j-1)n})$ term as inter-story drift factor γ_{jn} and rewrite the above equation in terms of drift as:

$$\Delta_j(\bar{T}) = \frac{1}{H_j}\sqrt{\sum_n \left[\gamma_{jn} \times \left(\frac{\bar{T}}{\frac{\alpha_n}{2\pi}}\right)^2 \times S_a\left(\frac{\bar{T}}{\alpha_n}\right)\right]^2} \qquad (Equation\ 4.3)$$

Here, H_j is the height of the story j;

$\gamma_{jn} = \Gamma_n \times (\phi_{jn} - \phi_{j-1,n})$ called inter-story drift factor

And, two new terms $\bar{T}$ and α_n defined as

$\bar{T} = 2\pi\sqrt{\frac{k_1}{m_1}}$ is the characteristic period of the first story; *k* and *m* are the stiffness and mass of the first story

And $\alpha_n = \frac{\bar{T}}{T_n}$ is a factor relating the characteristic period $\bar{T}$ to the natural period of each mode. The natural frequency ω_n for mode *n* is $\frac{\bar{T}/\alpha_n}{2\pi}$.

The purpose for using this characteristic period is to provide a common axis to normalize and consider the contribution of other natural periods in a multi-DOF system.

The inter-story drift spectra (Δ_j) can be used to gauge the individual as well as collective impact of story stiffnesses on the drift profile of the building. The inter-story drift spectra are a function of (1) story stiffness ratios, (2) story weights, and (3) design response spectrum or hazard level. Figure 4-2 (a) shows a set of inter-story spectra lines

for each mode and Figure 4-2 (b) shows a set of combined spectra lines for each story. The influence of higher modes on the overall inter-story drift spectra is discussed in a latter section.

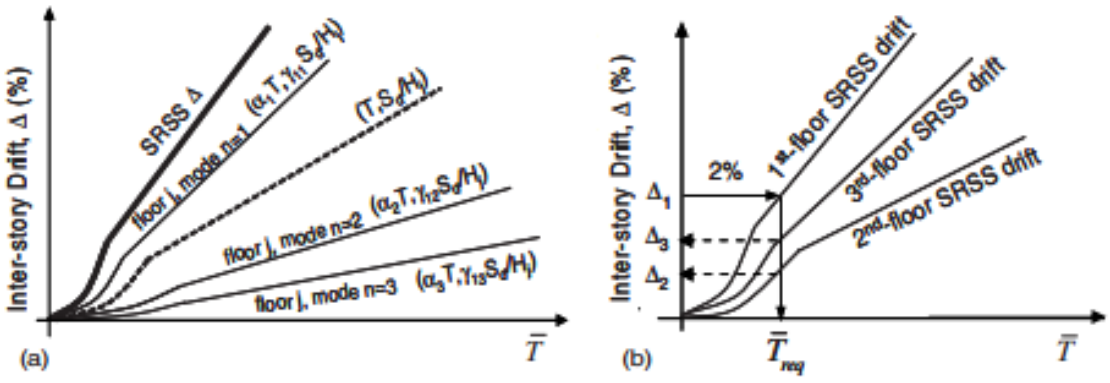

Figure 4-2 Inter-story spectra lines for a) different modes and b) different stories (Pang & Rosowsky, 2009)

To consider the effective mass of each mode, the effective mass participation factor (EMPF) is introduced in Equation 4.3. The reason for this has been discussed in a latter section of this chapter because the assessment tool discussed there can best illustrate the reasoning.

$$\Delta_j(\bar{T}) = \frac{1}{H_j}\sqrt{\sum_n \left[\frac{EMPF_n}{\sum EMPF} \times \gamma_{jn} \times \left(\frac{\bar{T}}{\frac{\alpha_n}{2\pi}}\right)^2 \times S_a\left(\frac{\bar{T}}{\alpha_n}\right)\right]^2} \qquad (Equation\ 4.4)$$

4.3. Design Profile Optimization and Target Story Stiffnesses

To obtain an optimal stiffness profile that yields equal inter-story drifts for all stories, an iterative approach can be used. An optimal solution is achieved when the inter-story drift spectra converge into a single curve (Figure 4-3 (b)). An initial equal stiffness

profile for all stories (i.e. stiffness ratios of unity assigned to all stories (see Figure 4-3 (b)) can be used as a starting point. If $\{k_j\}$ is a vector of stiffness ratios (normalized to the first-story stiffness) and $\{\theta_j\}$ is a vector of inter-story drifts for a given characteristic period such that $\max(\{\theta_j\})$ is equal to the target drift limit θ_{target}, then, modified stiffness ratios can be obtained as shown below:

$$k_j^{\,i+1} = k_j^{\,i} \times \frac{\theta_j^{\,i}}{\theta_{target}}$$ where i is the iteration number

The new estimated stiffness ratios using the above equation are then used as inputs to compute the next set of stiffness ratios. The process is repeated until all the values in $\{\theta_j\}$ have converged to the target drift limit. Figure 4-3 shows the inter-story spectra lines before and after optimization.

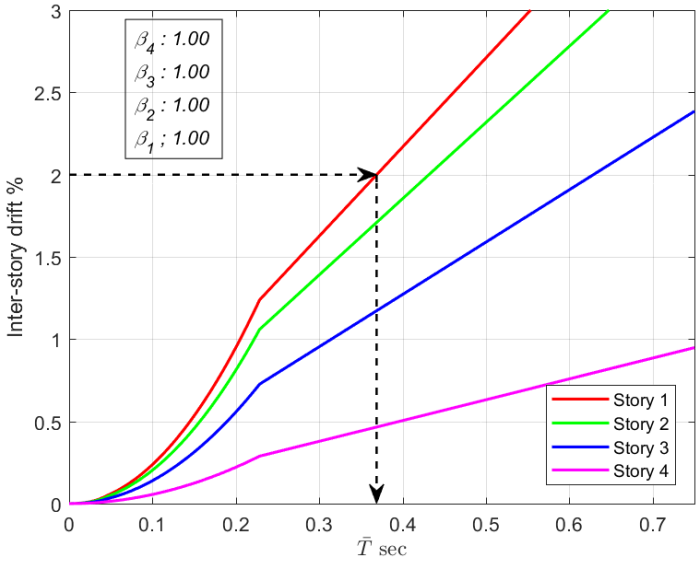

a)

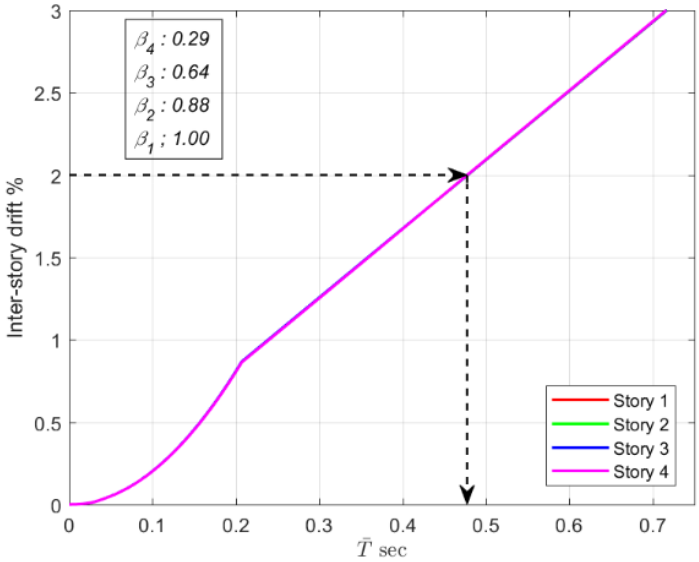

b)

Figure 4-3 Inter-story drift spectra a) before and b) after optimization

Once an optimal set of stiffness ratios are obtained, the required (maximum) characteristic period $\bar{T}_{req}$ can be read from the optimized inter-story drift spectra using the

target drift limit (Figure 4-3 (b)). The characteristic period can then be used to calculate the required stiffness values at each story using the following relation:

$$\left(k_{req}\right)_j = \left(\frac{2\pi}{\bar{T}_{req}}\right)^2 m_1 \beta_{kj}$$

where m and β_{kj} are the first-floor mass and stiffness ratio at story j (relative to first floor). Note that the optimal stiffness ratios are analogous to the vertical distribution factors of the equivalent lateral force (ELF) procedure in the current building code. The main difference between the aforementioned iterative DDD procedure and the ELF procedure are (1) the DDD procedure is a stiffness and displacement (drift) based procedure whereas the ELF procedure is force-based and (2) the DDD procedure can be utilized to obtain a design profile for varying target inter-story drifts while the ELF method does not allow customization of target inter-story drifts..

Table 4-3 and Table 4-4 show the optimized stiffness ratios and values for a suite of drift limits. It can be observed that the optimized ratios are essentially the same for all target drift limits considered. Also, these ratios are exactly the same as the normalized ELF target profile from Chapter 3 also shown in the table, implying that even though the normalized target profile remains the same. As previously discussed, DDD procedure allows one to design for varying drift limits which is an advantage over the ELF procedure.

Table 4-3 Optimized Stiffness ratios for DBE level and various drift limits

Story	*0.5%*	*1.0%*	*1.5%*	*2.0%*	*4.0%*	*ELF*
4	0.29	0.29	0.29	0.29	0.29	0.29
3	0.64	0.64	0.64	0.64	0.64	0.64
2	0.88	0.88	0.88	0.88	0.88	0.88
1	1.00	1.00	1.00	1.00	1.00	1.00

Table 4-4 Optimized Stiffness values (kips/in) for DBE level and various drift limits

Story	*0.5%*	*1.0%*	*1.5%*	*2.0%*	*4.0%*
4	367.4	159.1	70.9	40.0	10.0
3	825.8	357.4	159.0	89.5	22.4
2	1132	489.7	217.8	122.6	30.7
1	1285	556.0	247.3	139.3	34.8

After the required stiffness in each floor has been determined, a suitable wall design can be selected for each story using a database containing the equivalent stiffness for various shearwalls at the target drift. The determination of equivalent stiffness ratio for shearwalls is presented in the next section.

4.4. Equivalent Story Stiffness definition

The original displacement-based design procedure suggested by Priestly (1998) as well as that by Folz and Filiatrault (2002) use secant stiffness and equivalent viscous damping to characterize the substitute structure representative of the original structure. This requires a nonlinear pushover analysis of the complete structure and adds to the

complexity of the procedure. The procedure in Pang & Rosowsky (2009) eliminates the need for the equivalent viscous damping as well as the pushover analysis by introducing a substitute linearization approach in which an equivalent stiffness at a given drift level for a linear elastic model is determined such that the energy stored in the original nonlinear backbone within that drift level is conserved. Figure 4-4 shows a shearwall backbone curve and its equivalent stiffness triangle at the displacement Δ_t both with same area.

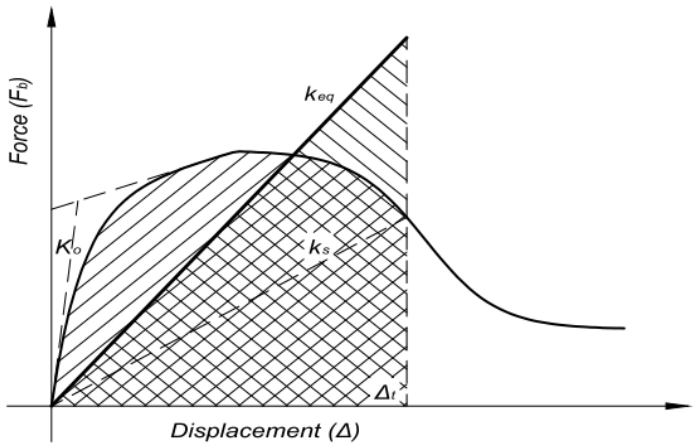

Figure 4-4 Equivalent Stiffness definition

Using this formulation, any backbone can be converted into its equivalent stiffness curves. Figure 4-5 shows the equivalent stiffness backbone curves for the walltypes considered in this study. Table 4-5 tabulates the equivalent stiffness values at discrete displacements.

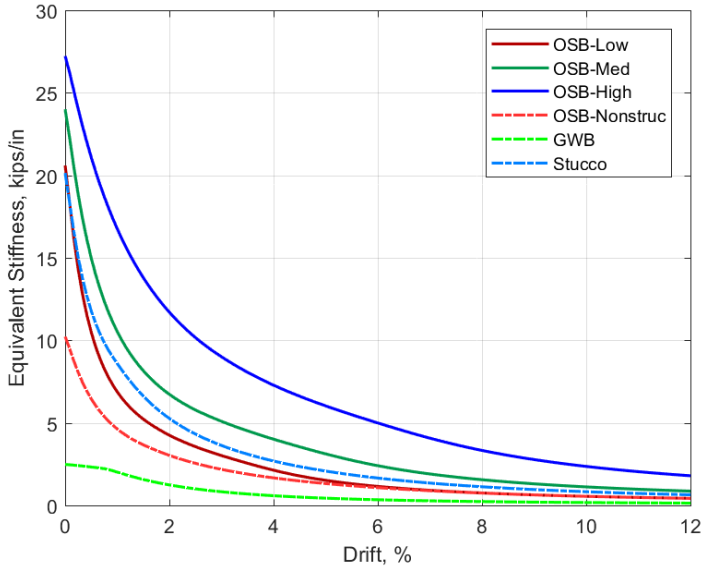

Figure 4-5 Equivalent Stiffness Curves for wall length of 4 feet

Table 4-5 Equivalent Stiffness values (in kips/in/4 ft) at discrete displacements

Drift (%)	*0.0*	*0.5*	*1.0*	*1.5*	*2.0*	*2.5*	*3.0*
OSB-Low	20.6	10.5	6.9	5.2	4.3	3.6	3.0
OSB-Med	24.0	15.0	10.5	8.2	6.7	5.8	5.1
OSB-High	27.2	21.1	16.8	13.8	11.7	10.2	9.0

4.5. Design Example Building using DDD procedure

For the target story stiffness values, different combination of shearwalls can then be chosen based on Table 4-5 such that the total stiffness provided exceeds the target story stiffness at the target drift limit. And it is to be noted that so far, no partial safety factors have been introduced, hence, only the following relation is to be satisfied:

$$k_{required} \leq k_{provided}$$

Designing the example buildings using this DDD procedure alone is possible but this procedure just as it is, cannot limit the issue associated with vertical structural irregularities or influence of non-structural elements as discussed in Chapter 3.

Chapter 5 will address the issue but before that, to evaluate the potential advantage of using DDD procedure over FBD procedure and to get a sense of how the choice of drift limit for a seismic hazard level can influence the design, a set of models were built and studied.

Instead of using models with detailed floor plans such as the three buildings (V1, V2 and V3 presented in Chapter 3), a simple rectangular building plan was utilized in this study. The simple rectangular building model has the same story weights as the detailed models presented in Chapter 3. These simple building models were designed using varying target drift limits and analyzed using IDA to obtain the MCE_R collapse probabilities. These MCE_R collapse probabilities are then compared against that based the ELF model. The primary reason for this comparison is to determine the target drift limit that would yield the same seismic performance (MCE_R collapse probability) as the ELF procedure. This comparison will allow for a better understanding of the influence of drift profile on the performance of structure and aid in choosing the suitable drift limit for design in the subsequent chapter.

In this parametric study, only OSB-High was used (i.e. OSB-Low and OSB-Med were not considered). In addition, the backbone curve of OSB-High was used to convert the required stiffness values obtained in design to their respective strength values to compare against the strength profile in ELF design. Since the equivalent stiffness of OSB-

High at the target drift limit (say 2%) is known from Table 4-5 for a wall unit (4 feet long), a scaling factor representative of the required wall length can be determined. For the scaled wall length, the design strength, which is the nominal strength times the strength reduction factor of 0.8, can be calculated for each story and the representative strength profiles corresponding to any stiffness profile can be obtained.

However, it should be noted that since each of the walls in the shearwall database has a distinct backbone shape (see normalized equivalent stiffness curves in Figure 4-6), using OSB-High alone cannot properly replicate the performance that would have otherwise been achieved when combination of these are used and hence, discrepancies are expected.

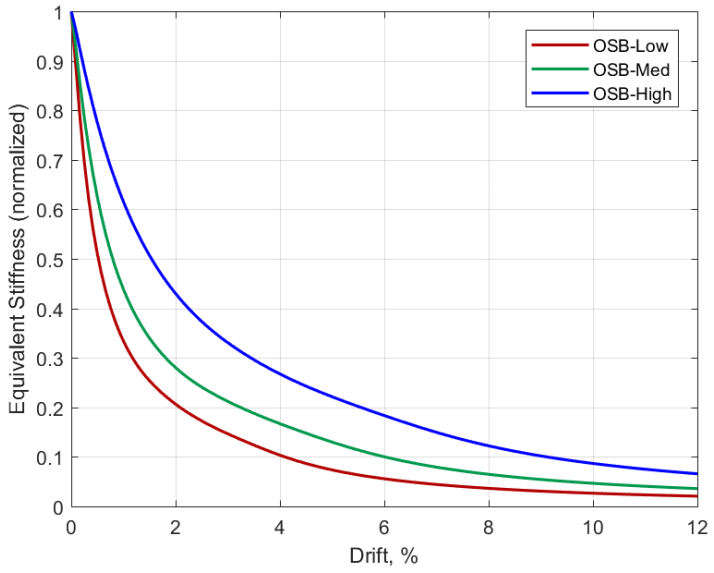

Figure 4-6 Equivalent Stiffness curves normalized by initial stiffness

Table 4-6 and Table 4-7 show the optimized stiffness profiles and the corresponding strength profiles for a multitude of different drift limits given DBE level. Figure 4-7 shows

the strength profiles graphically. To get a strength profile that is almost the same as ELF, drift limits of 1.6% and 1.7% were also considered. It can be observed that the ELF profile is slightly stronger than that for 1.7% and is in between those for 1.6% and 1.7%.

Table 4-6 Optimized stiffness profiles (kips/in) from DDD with their associated drift limits

Story	*1.5%*	*1.6%*	*1.7%*	*2.0%*	*2.5%*
4	70.87	62.32	55.24	39.98	25.59
3	158.97	139.74	123.81	89.51	57.29
2	217.81	191.47	169.64	122.63	78.49
1	247.32	217.42	192.64	139.28	89.14

Table 4-7 Corresponding strength profiles (kips) from DDD

Story	*ELF*	*1.5%*	*1.6%*	*1.7%*	*2.0%*	*2.5%*
4	49.21	57.56	52.42	48.06	38.25	28.16
3	110.73	129.12	117.54	107.71	85.63	63.04
2	151.74	176.92	61.05	147.58	117.32	86.37
1	172.25	200.88	182.87	167.59	133.24	98.09

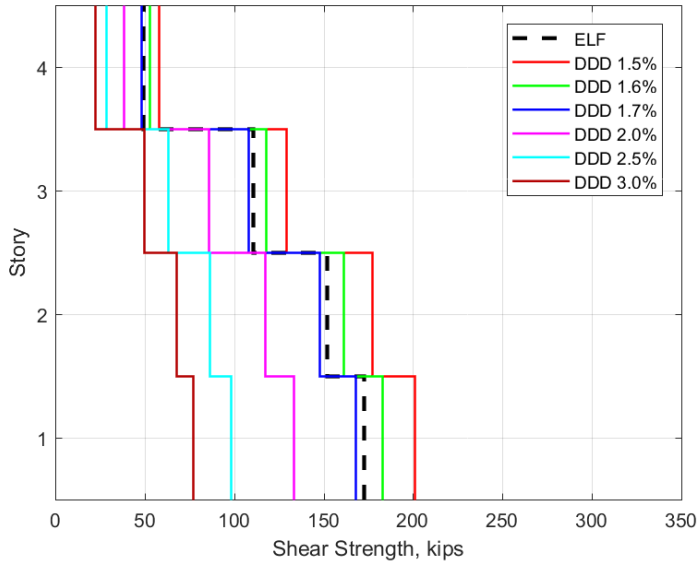

Figure 4-7 Strength profiles from DDD

The next step is to verify the collapse performance of each of these design profiles through IDA. The full Timber3D model for the example building that was studied in Chapter 3 can be used for this series of IDAs as well. However, because of the large number of nodes and relative complexity of the building model, a simplified model with a smaller, rather not complex building plan is more suitable for this parametric study. The simplified model had plan dimensions of 8ft by 16ft, shown in Figure 4-8, with same floor heights and weights as the original example building. Other than that, no damping was used in this model as well and only OSB-High was used in the F2F elements in the numerical model. The backbone for the OSB-High was scaled proportionately to match the strength requirement for each of the stories.

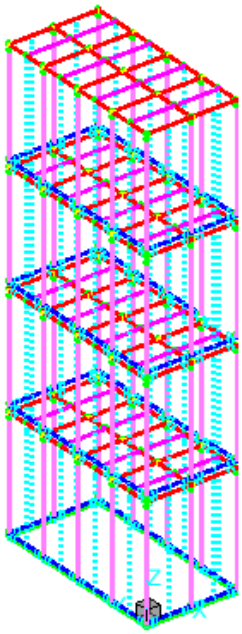

Figure 4-8 Timber3D model for the simplified building

4.5.1. IDA results

Table 4-8 shows the collapse performance measures for each of the building design profiles from DDD procedure compared against the ELF procedure. Figure 4-9 shows the fragility curves based on each of the analyses. It can be observed that the collapse fragility curve of the building designed using ELF procedure is in between those using DDD with drift limits of 1.6% and 1.7%.

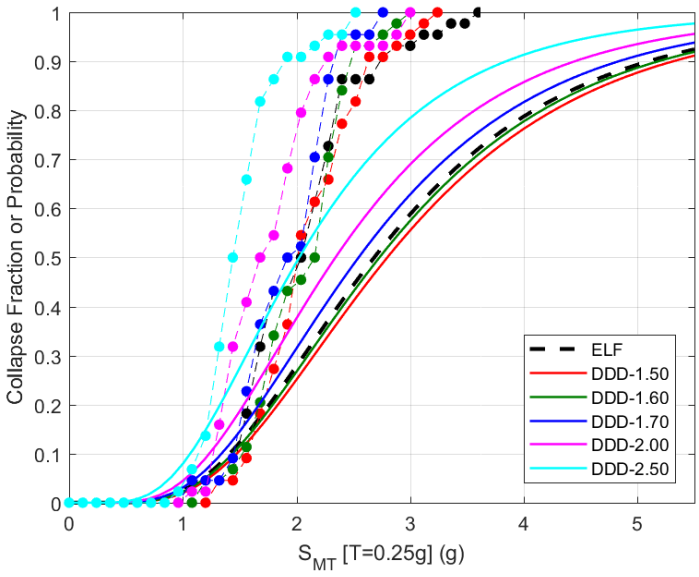

Figure 4-9 Fragility curves for simplified models

Table 4-8 Collapse Performance for designs associated with different drift limits

Parameters	*ELF*	*1.5%*	*1.6%*	*1.7%*	*2.0%*	*2.5%*
SCT (g)	2.68	2.80	2.73	2.55	2.34	2.02
CMR	1.34	1.40	1.37	1.28	1.17	1.01
ACMR	1.79	1.87	1.82	1.70	1.56	1.35
P(COL|MCE)	12.2%	10.6%	11.6%	14.5%	18.6%	27.5%

Even though now we know that a design profile for a drift limit of 1.6-1.7% best resembles the ELF profile for our building, it is uncommon to use a drift limit of 1.6-1.7% in design (and considering the study is only limited to one building with constant story weights, these could be applicable only to this building). And it is to be noted that for a drift limit of 2.5% (previously used as a deflection check in force-based design), the required stiffness values are significantly smaller than what the contemporary force-based

design requires and the overall design profile is just as more susceptible to failure. A possible explanation could be that the DDD procedure discussed so far does not account for a reduction factor ϕ for stiffness as is used in force-based design. A parametric study was carried out to examine the effect of including a resistance factor ϕ in the DDD procedure. Strength profiles similar to those in Figure 4-9 were plotted for ϕ factor equal to 0.8 and 0.9 and are shown in Figure 4-10. Hereafter, ϕ_k will be used as the reduction factor for stiffness to differentiate from the strength reduction factor ϕ for strength in the current force-based procedure following the Load and Resistance Factor Design (LRFD).

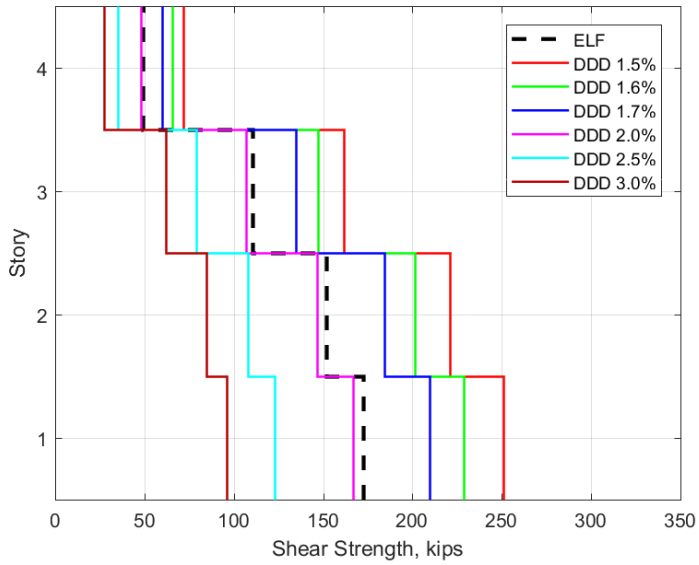

a)

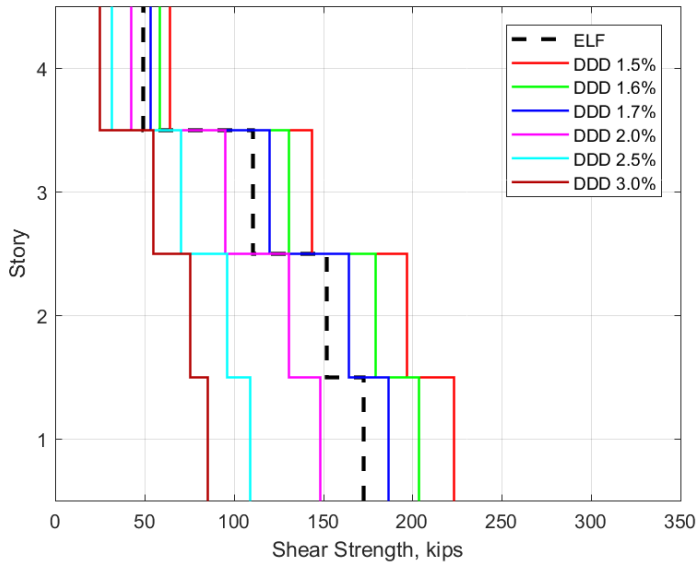

b)

Figure 4-10 Strength profiles for a) ϕ_k = 0.8 and b) ϕ_k = 0.9

For ϕ_k = 0.8, it can be seen that the strength profile for drift limit of 2% is similar to the ELF profile. A drift limit of 2% is more commonly used than the drift limit of 1.6-

1.7%. Also, note that the current force-based design using ELF procedure uses a reduction factor of 0.8. Hence, the use of a reduction factor ϕ_k of 0.8 is consistent with the current practice and for the design examples in Chapter 5, a stiffness reduction factor ϕ_k of 0.8 has been used.

4.6. Displacement-based Design Assessment (DDA) procedure

Before proceeding to the design example in the next chapter, this section discusses and further develops a design assessment procedure also included in Pang and Rosowsky (2009). A structure designed using a displacement-based design approach is expected to satisfy the initially set performance levels under the given seismic hazard level. Pang and Rosowsky (2009) introduced a direct displacement assessment (DDA) procedure that can be used to calculate inter-story drifts and ascertain that the performance level has been met. This procedure uses the initial stiffness values and Equation 4.4 described in the previous sections to estimate an interstory drift profile. This profile is then iteratively used to determine a new set of stiffness values from the design equivalent stiffness curves and a new interstory drift profile. The process is iterated until the drift profile converges. The convergence is checked using the following criterion:

$$\lambda^{(i)} = \frac{(\Delta^T)^{(i)} K^{(i)} \Delta^{(i)}}{(\Delta^T)^{(i)} M^{(i)} \Delta^{(i)}}, \qquad \frac{\left|\lambda^{(i+1)} - \lambda^{(i)}\right|}{\lambda^{(i)}} \leq tolerance$$

Here, *(i)* is the iteration number and Δ and Δ^T are the drift profile and its transpose. A tolerance of 0.05, as was suggested in Pang and Rosowsky (2009), has been used in this study as well. The process has been illustrated along the equivalent stiffness curves and as a drift profile in Figure 4-11 below.

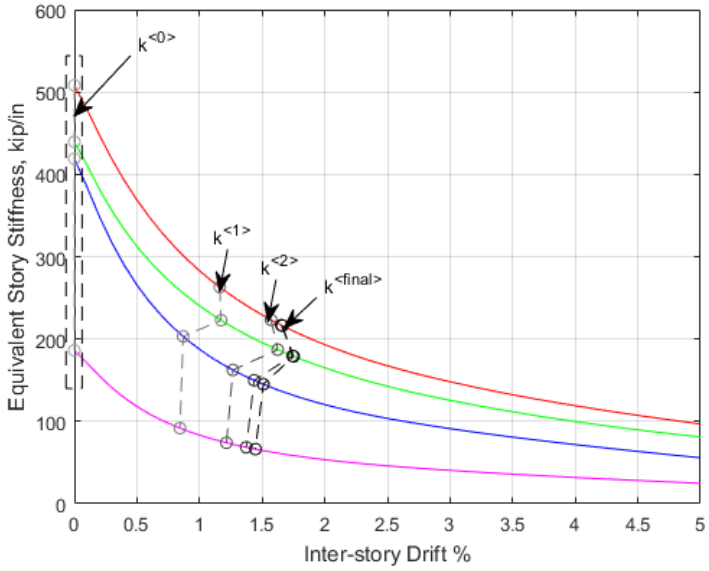

a)

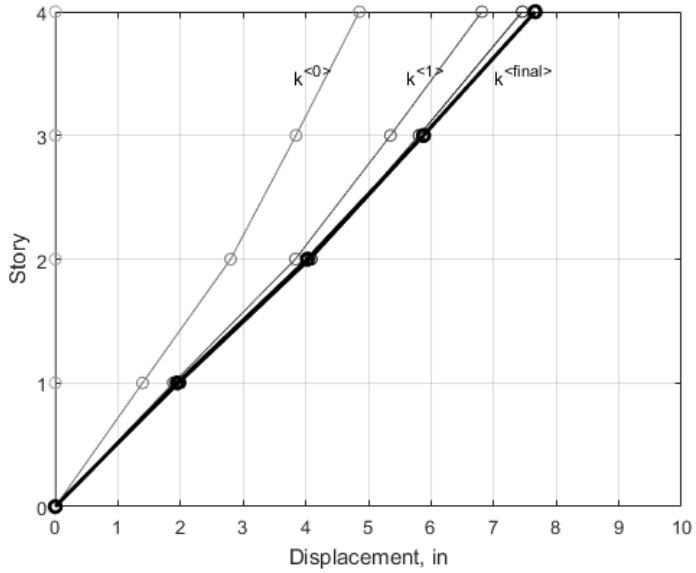

b)

Figure 4-11 DDA iterations (a) along equivalent stiffness curves and (b) as a drift profile

DDA was carried out on each of the six models in Chapter 3 and inter-story drifts at each story after convergence are tabulated in Table 4-9. Drifts normally tend to be

highest in the first story and decrease in the upper stories. However, for V1 (and V2), the drift at the second story is higher than that in the first story. This is likely due to somewhat higher overstrength on the first story compared to other stories. Also, drift at the first story for V3 is very large due to structural as well as non-structural irregularity. But the effect of this is not apparent in V3+NS.

Table 4-9 DDA Inter-story Drifts (in % of story height) for V1, V2 and V3

Story	*Structure Only*			*Full Building*		
	V1	*V2*	*V3*	*V1+NS*	*V2+NS*	*V3+NS*
4	1.49	1.49	0.22	0.18	0.23	0.16
3	1.54	1.54	0.77	0.52	0.63	0.52
2	1.73	1.73	1.50	0.86	1.07	0.92
1	1.62	1.62	2.92	1.02	1.96	1.96

DDA is indeed helpful in assessing a designed building. Few key concepts pertaining to DDA as well as DDD procedure are discussed hereafter using DDA.

4.6.1. Number of modes to consider

Previously it was not mentioned how many modes to consider when obtaining the inter-story drift spectra. The effect of the number of modes considered in DDA on the final drift profile is explored in this section. Number of modes required to be considered in analyses normally depends on the required cumulative effective mass participation factor ($\sum EMPF$). ASCE7-16 Cl. 12.9.1.1 requires that the total modal mass participation in linear dynamic analyses is at least 90% of actual mass. To see the effect of consideration of number of modes on the drift profile, DDA was carried out on V1 building model for

varying number of modes. Figure 4-12 shows four different drift profiles when only one, two, three and four modes are considered.

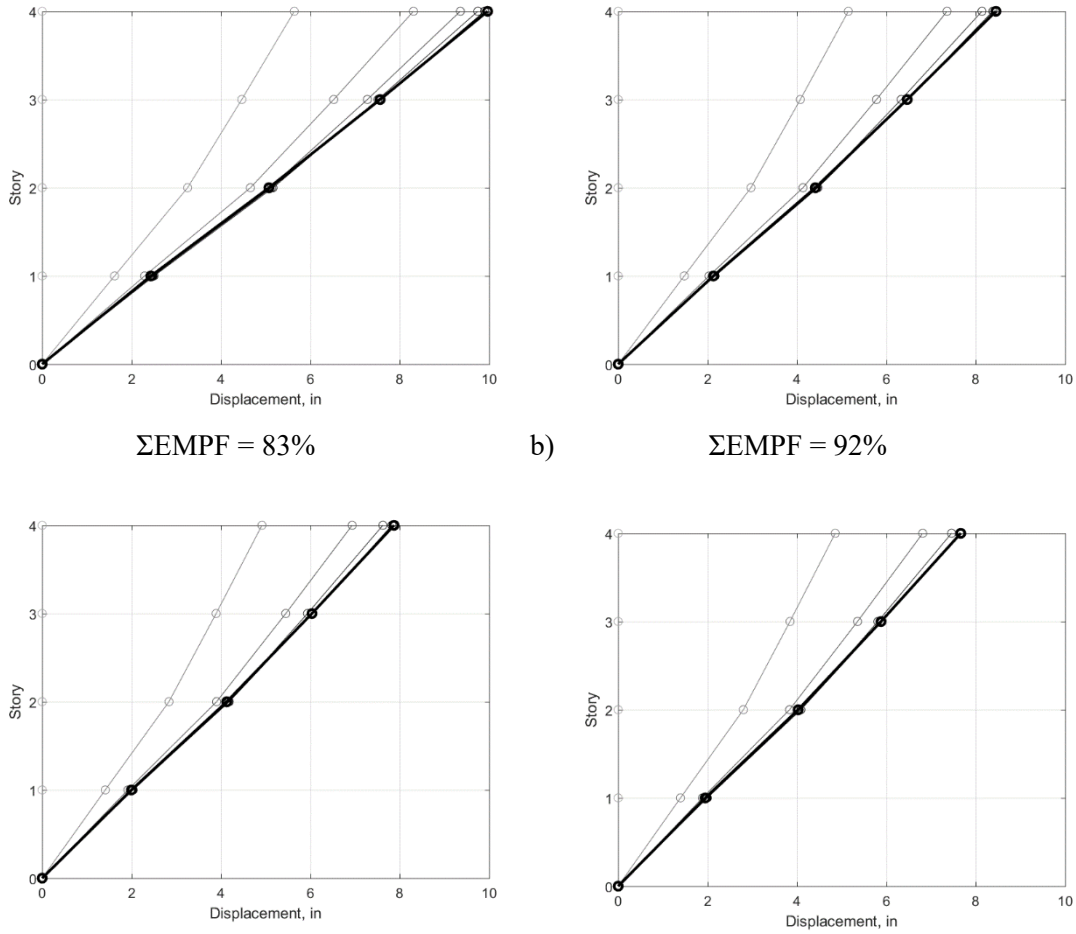

a) ΣEMPF = 83% b) ΣEMPF = 92%

c) ΣEMPF = 98% d) ΣEMPF = 100%

Figure 4-12 DDA Drift Profiles when a) one, b) two, c) three and d) four modes are considered

It can be observed that when two or more modes are considered, the drift profile is essentially the same. Correspondingly, the cumulative EMPF is also greater than 90%. However, when only one mode is considered, the inter-story drifts are cumulatively larger. This could be because of the EMPF term in the spectra line equation that was only introduced in this study. It is understandable that the contribution from the 1st mode would

always be the greatest. The EMPF term in the spectra line equation equals to one when only one mode is considered, however, would be somewhat smaller when higher modes are also taken in account. Hence, the number of modes to be considered depends on if the 90% participation criteria is met.

4.6.2. Inclusion of the EMPF term in the modified spectra line equation

The equation originally provided in Pang & Rosowsky (2009) was as follows:

$$\Delta_j(\bar{T}) = \frac{1}{H_j}\sqrt{\sum_n \left[\gamma_{jn} \times \left(\frac{\bar{T}/\alpha_n}{2\pi}\right)^2 \times S_a(\bar{T}/\alpha_n)\right]^2}$$

The modified equation proposed in this thesis has an additional EMPF term as follows:

$$\Delta_j(\bar{T}) = \frac{1}{H_j}\sqrt{\sum_n \left[\frac{EMPF_n}{\sum EMPF} \times \gamma_{jn} \times \left(\frac{\bar{T}/\alpha_n}{2\pi}\right)^2 \times S_a(\bar{T}/\alpha_n)\right]^2}$$

Using DDA, both of these equations can be tested and verified. Figure 4-13 (a) shows the DDA profile obtained using the original equation and Figure 4-13 (b) shows the DDA profile using the modified equation. It can be clearly observed that the DDA profile using the original equation has an extreme drift in the top story which is not observable in the DDA profile using the modified equation. The drift profiles in reality seldom look like the one on the left and most of the times the soft story is on the first floor only. Figure 4-14 shows the various strength profiles using the original as well as the modified equation. Clearly, without the additional term, DDD procedure requires a higher stiffness on the top story compared to ELF and this is probably the reason behind the extreme drift on the top story. Also, without the additional term, it was speculated that the higher modes are

contributing more to the drift profile than is realistic so to warrant that, the EMPF term was introduced.

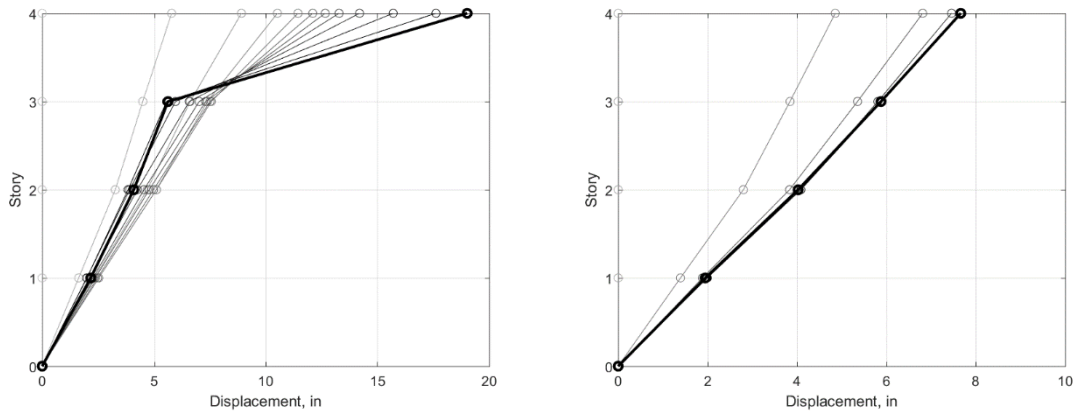

a) b)

Figure 4-13 DDA Drift Profiles using a) the original equation and b) the modified equation

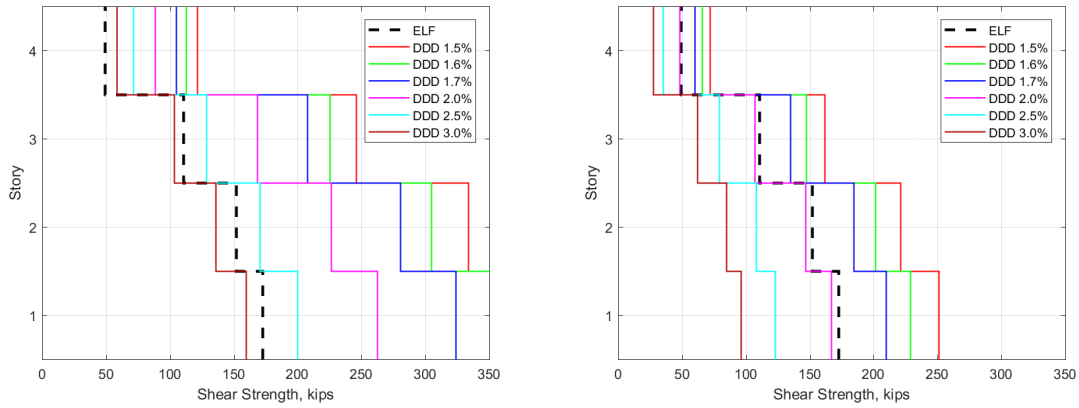

a) b)

Figure 4-14 Strength profiles for different drift limits using a) the original equation and b) the modified equation

Hence, it can be agreed upon that the drift profile in Figure 4-14 a) is unrealistic and inclusion of the EMPF term is justified.

4.6.3. Comparison of DDA drift profile to pushover drift profile at DBE level

Figure 4-15 compares the drift profile during pushover at DBE level against the DDA Drift profile also at DBE level. The drift profile from pushover is taken from the point during pushover when the base shear equals the design base shear ($V_b = C_s W$) or ratio of base shear to total building weight equals the design base shear coefficient (C_s). Since this drift profile is from the linear elastic range, it is required that it be multiplied with the deflection amplification factor of 4 for light-frame construction. Alternatively, an estimate of the drift profile from DDA in the linear, elastic range can be obtained by scaling down the original DDA profile directly or iteratively. After the necessary conversion, it can be observed that the DDA drift profile and pushover drift profile are indeed similar and this helps to validate the DDA procedure.

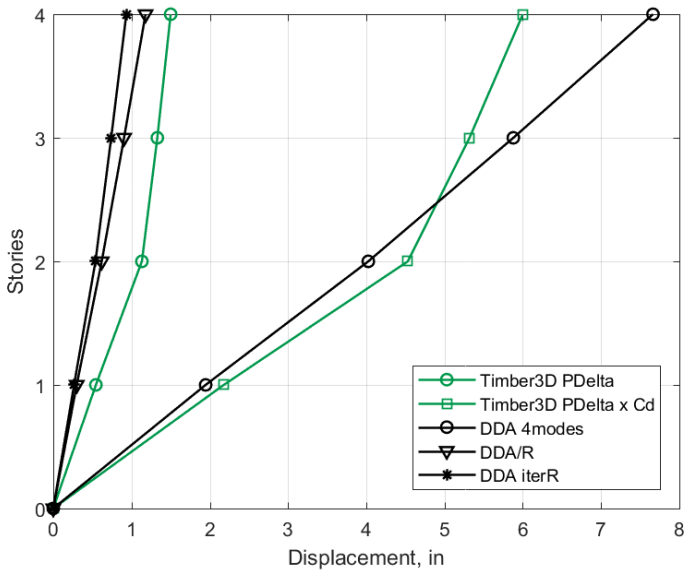

Figure 4-15 Comparing DDA drift profile to non-linear static pushover drift Profile

4.6.4. Comparison of DDA drift profile to median drift profile from IDA

Similarly, DDA drift profile can also be compared to drift profile from non-linear time-history analyses (NLTHA) using ground motions scaled to DBE level (S_{MT} = 1g). The NLTHA drift profiles were obtained by plotting the peak inter-story displacement (relative to ground) for each of the 44 FEMA P695 ground motions. The median for maximum inter-story displacements observed during each of the 44 ground motions were determined and plotted against the DDA drift profile as shown in Figure 4-16. Just to see the difference, the DDA drift profiles considering the first mode only and all the four modes are shown. The DDA drift profile considering all four modes matches the median drift profile from NLTHA relatively well. But also, interestingly, the two DDA profiles encompass the median drift profile showing that DDA does allow the range to include the median drift profile from NLTHA depending on the number of modes it considers.

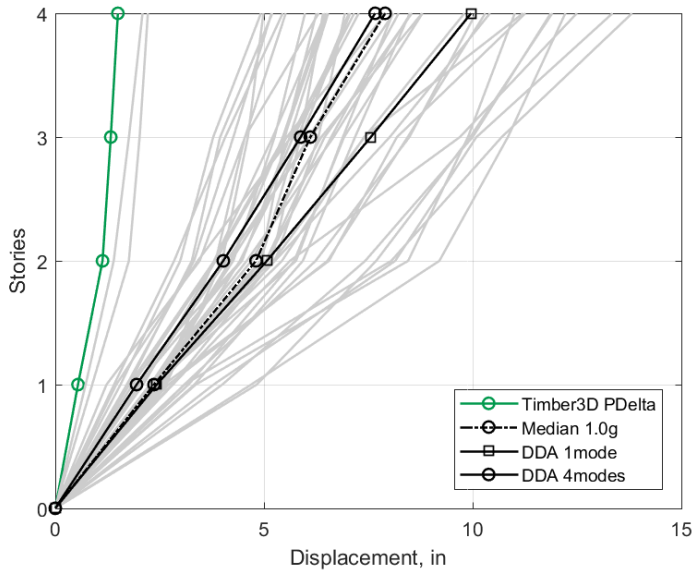

Figure 4-16 Comparing DDA drift profile to NLTHA drift profile(s)

4.6.5. Using DDA to estimate probability of collapse

The drift profile obtained from the DDA is indicative of how the structure will perform at the input seismic hazard level. And if a drift limit were to be associated with such seismic hazard level, DDA can be used to assess if the provided design/building is safe or not.

To further the application of DDA to assess the building performance, DDA may also be used to predict the probability of collapse at MCE_R hazard level. This requires that a distribution be ascertained for the inter-story drift at each story. For illustration purposes, a lognormal distribution was fitted to maximum drift profiles from NLTHA for different seismic levels (drift profiles as the one shown for DBE level in Figure 4-16). The dispersion parameter β (logarithmic standard deviation) for the fitted distribution has been plotted against the seismic intensity level in Figure 4-17. It can be seen that the value of β hovers around 0.35-0.40.

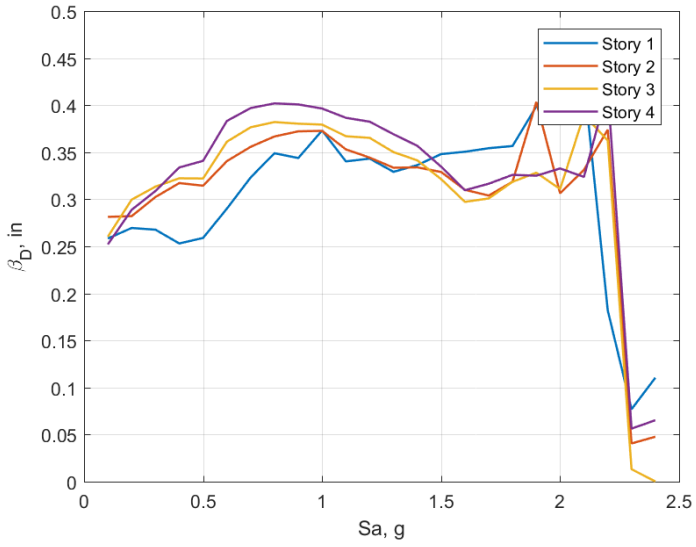

Figure 4-17 Fitted β parameter against seismic intensity level

From Table 4-2, the drift limit (θlim) for Collapse Prevention (CP) performance level is 4% at MCE_R level. The probability that the inter-story drift in a given story from DDA exceeds the design collapse drift limit can be determined as:

$$P_j(\theta > \theta_{lim}|MCE_R) = \Phi\left(\theta_j, \ln(\theta_{lim}), \beta\right)$$

Where θj is the DDA predicted peak inter-story drift for the j-th story.

The system-level probability of failure for the whole building, in terms of collapse occurs in one or more stories, can be determined as:

$$P(\theta > \theta_{lim}|MCE_R) = 1 - \prod_{j=1}^{N}\left(1 - P_j(\theta > \theta_{lim}|MCE_R)\right)$$

From DDA at MCE_R level for V1 building model,

$$\theta_j = \begin{Bmatrix} 2.74 \\ 3.07 \\ 2.89 \\ 2.84 \end{Bmatrix} \begin{matrix} 1 \\ 2 \\ 3 \\ 4 \end{matrix} \text{ hence, } P_j(\theta > \theta_{lim}|MCE_R) = \begin{Bmatrix} 0.14 \\ 0.23 \\ 0.18 \\ 0.16 \end{Bmatrix}$$

And, $P(\theta > \theta_{lim}|MCE_R) = 0.541$ or 54.1%

Clearly, more research is required. This is only an illustration to show the possible extension and application of DDA to determine collapse probability.

5. ADAPTIVE DISPLACEMENT-BASED DESIGN PROCEDURE

The DDD procedure in Pang & Rosowsky (2009), and as was discussed in Chapter 4, gives out a set of optimized stiffness values for each story and leaves the designer to decide on exact values of stiffness to provide without an upper bound limit. The final drift profile of the as-designed building is later verified using the DDA procedure. However, say when the chosen design in a story deviates from the optimized values due to various design constraints (such as building plan requirement, practical wall lengths, limited design options in the shearwall database, etc.), there is no real guidance on how to control and quantify this deviation as well as how to proceed to other stories.

When the true stiffness (and strength) in a story including both structural and non-structural walls is significantly higher than that of the optimized stiffness determined via DDD, it will reduce the drift demand for that particular story and drives the drift demand to other stories resulting in the drifts potentially exceeding the target drift limit. In other words, severe deviation from the optimized stiffness profile obtained from DDD, especially with vertical irregularity, may result in the design failing to meet the target drift limit. Also, the end design could be very different in profile from the optimized design and may not meet the performance levels initially set for the given level of hazard.

To overcome this limitation to the method, this study proposes an adaptive displacement-based design (ADD) procedure. This procedure is an extension of the procedure suggested in Pang & Rosowsky (2009) and Chapter 4. The concept for this procedure stems from the fact that, after target values have been determined, one story is designed at a time. In practice, a light-frame wood building is typically designed from the

bottom. After each story is designed and the shearwalls have been prescribed, the procedure adapts and adjusts the initially determined optimum stiffnesses required for upper stories. If a designer prescribes significantly more shearwalls than required, the proposed ADD procedure will yield a revised stiffness required for the upper stories taking into account the actual as-designed shearwall stiffnesses and strengths in the lower stories.

This allows to tie in the designed and the un-designed stories and continually guide the designer on how to best proceed. It is to be noted that the design does not necessarily need to start from the bottom-story but it is convenient because of how inter-story drift spectra were formulated in Chapter 4. It can be pointed out that this concept of readjusting the target values as the design proceeds is yet to be introduced in the literature, making this thesis the first attempt at addressing the issue.

The subsequent section discusses each step of the design procedure in detail. The following two sections then illustrate this conceptual procedure first with no regard to non-structural elements and then with the consideration of non-structural elements. The section that follows finally presents the results from the nonlinear models for each of these designs and checks if the performance criteria are met.

5.1. ADD Procedure

Conceptually, the various steps involved in this procedure have been elaborated upon below and schematically illustrated in Figure 5-1:

a. The first step is to set up the performance criteria to meet against various seismic hazard levels (for instance, those presented in Chapter 4).

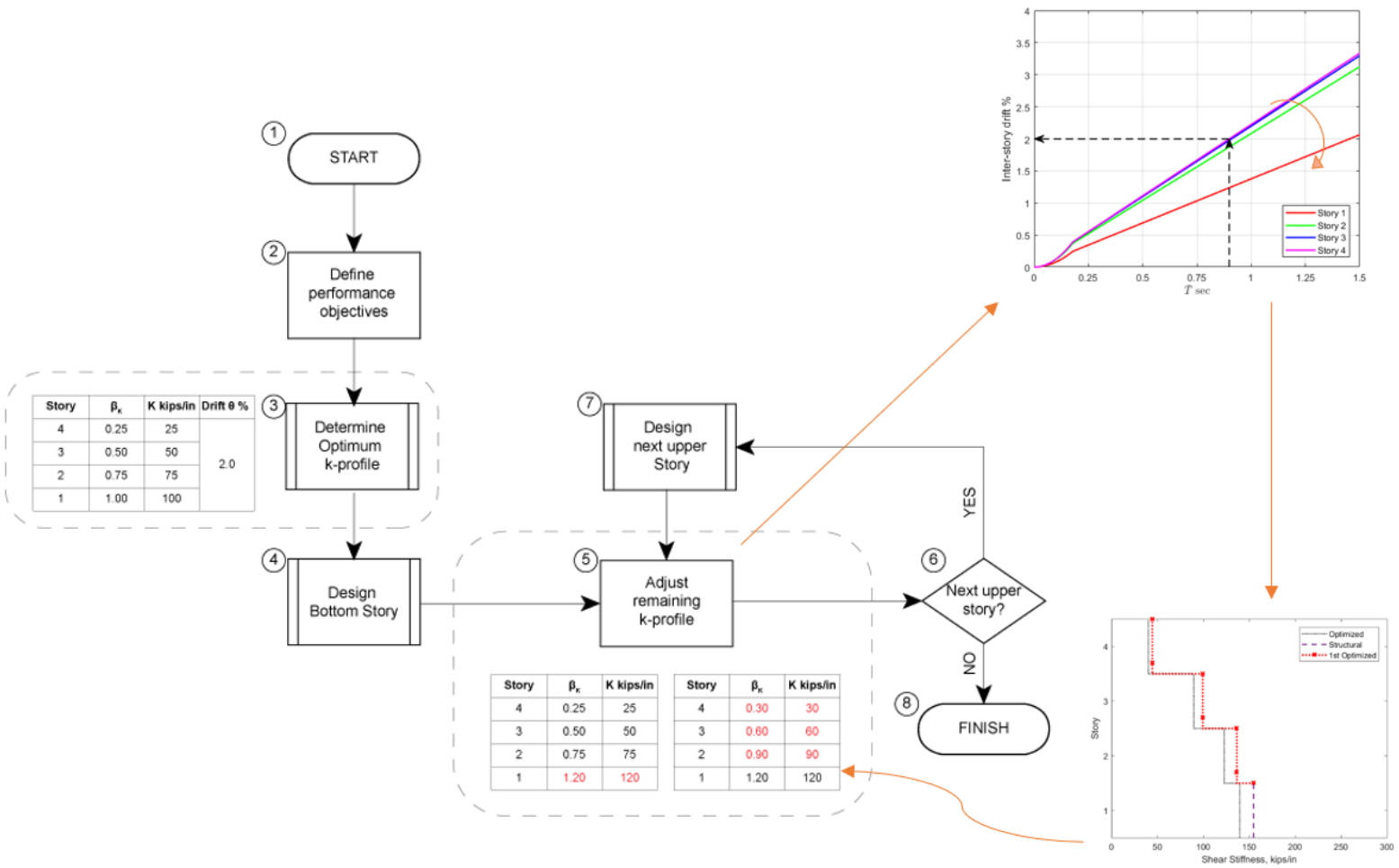

Figure 5-1 Flowchart for ADD procedure without the consideration of NS

b. The next stage in the procedure is the determination of the optimized stiffness profiles for each target performance-seismic hazard level pair (using the approach elaborated in Chapter 4).

c. The subsequent stage would be to design the bottom story and provide for the required minimum stiffness through a combination of shearwalls from the database (in Chapter 4) while adhering to the building plan. It is required that the structural shearwalls provide for at least the required stiffnesses pertaining to performance of structural walls. And if non-structural elements are being considered, the combination of structural and non-structural walls is required to meet each of the required stiffnesses pertaining to performance of non-structural walls.

   Also, the engineer is recommended to design as close as practicably possible to the target stiffness; even though the procedure will adapt to any overstrength, unnecessary overstrength provided in this story requires that other stories also be overdesigned to the similar scale to maintain that the target performance level is achieved.

d. After the bottom story has been designed, the next step is to adjust the required stiffness profile prior to further design depending on the overstrength just provided. This is essentially the step that gives this procedure its namesake. And the key to this adjustment is to realign the target stiffness values for other stories such that the inter-story drift spectra lines re-converge at the target drift limit or less for the provided design in the bottom story. (The adjusted profile has been shown in Figure

5-2 below where the red line that stems from the first story represents the new target profile and this has been further discussed in the design example section).

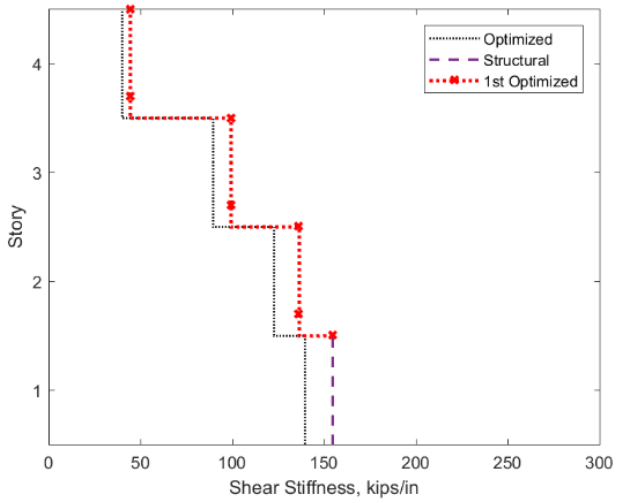

Figure 5-2 Adjusted target profile based on provided design

e. The next stage is to design for the second story based on the revised optimal stiffness profile. The recommendations pointed out in step c apply to this step as well (providing at least for the required stiffness value while being as close as practicably possible). However, if the common practice of providing the same wall lengths in all the floors is being followed, a database consisting of walls with larger nail spacing or thinner structural panel thickness would be desired. And hence, this cannot emphasize enough the requirement of a diverse shearwall database inclusive of multiple nail spacing, structural panel thicknesses etc.

An extension of this step would be to iterate through multiple wall designs depending on the inter-story drift that the design produces, and make sure that the

drift is acceptable while the design is as close as practicably possible to the optimized value.

f. After the design of the second-story, the next step is to readjust the stiffness profile for the remaining stories same as was done in step d. However, since two stories have been designed, it is highly unlikely that all the spectra lines can converge to a single point anymore. Because of this, it is recommended that the engineer pick the least stiff of the two wall designs and converge the spectra lines for the un-designed stories to that and obtain a new set of optimized stiffness values.

g. The succeeding steps would be to repeat steps e and f for each of the upper stories and the design of the final top (or bottom) story concludes the design procedure.

In a nutshell, the ADD procedure leverages the capability of the inter-story drift spectra to gauge the performance of each assigned design at each design step and depending on which the required demand on the successive stories are re-calculated and designed for.

5.2. Design Example Building with no consideration of NS

Herein the V2 building has been designed using the ADD procedure. The reason behind using V2 building is to explore if the ADD procedure can help mitigate the soft-story issue discussed in Chapter 3 when the procedure does consider the contribution from non-structural elements. The design example illustrates a bottom-up approach and does not consider the influence from non-structural elements. The performance criteria set in Chapter 4 has been used (not shown here). The first set of optimized stiffness values from the DDD procedure for a drift limit of 2% are shown in Table 5-1. As in Chapter 3, the shearwalls have been designed at an increment of 4 feet and with the underlying

assumption of a rigid diaphragm. A strength reduction factor of 0.8, decided upon in Chapter 4, has also been used.

Table 5-1 Optimized Stiffness ratios and Stiffness demand for 2% drift limit

Story	*Stiffness ratios*	*Stiffness Demand, Kips/in*	*Strength Equivalent, Kips*
4	0.29	39.99	47.81
3	0.64	89.51	107.0
2	0.88	122.63	146.6
1	1.00	139.28	166.5

Hence, the subsequent subsection only details the design steps. Each design step for a story has been broken down into two sub-steps: the first being the shearwall selection/design and the second being the adjustment of target stiffnesses for upper stories.

Step 1.1: Design Story 1

A suitable combination of exterior and interior walls has to be chosen that meets the stiffness demand at the story without providing too much overstrength. To achieve a comparable overall design to one in Chapter 3, the same design has been used in Story 1. Figure 5-3 shows a schematic illustration of the vertical elevation of the shearwalls along grid line 1-1 and grid line 4-4 and also the shear stiffness profile for this assigned design. Table 5-2 summarizes the optimized stiffness, the target stiffness and the provided stiffness (inclusive of ϕ_k) for Story 1.

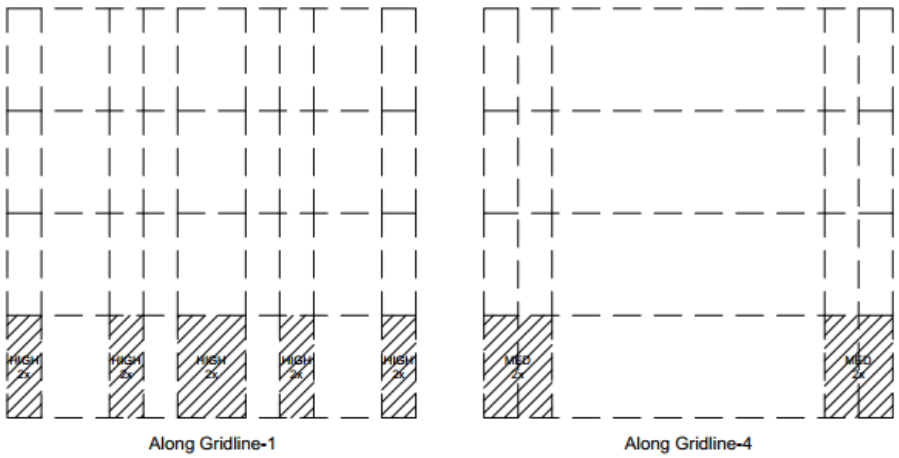

a)

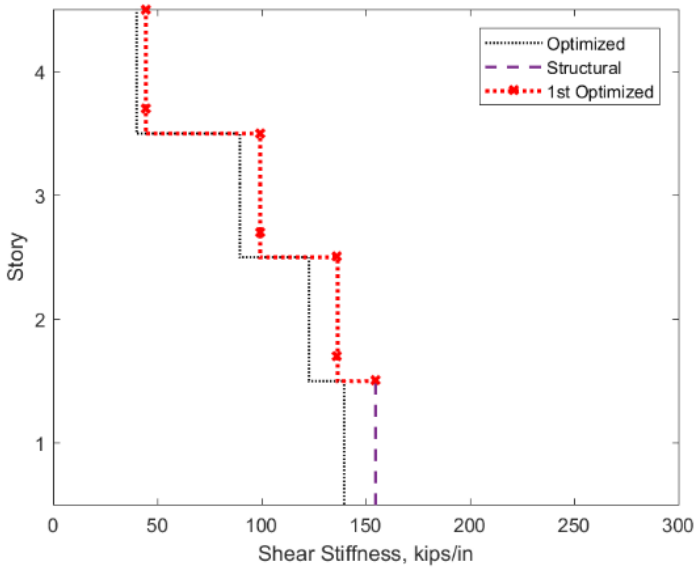

b)

Figure 5-3 Story 1: a) Vertical Elevation of As-designed Shearwalls b) Shear stiffness profile

Table 5-2 Shearwall design summary (for story 1)

Story	*Optimized Stiffness, k_{opt}*	*Target Stiffness, k_{req}*	*Provided Stiffness, $\phi_k k_{prov}$*	*Provided Design**
4	40.40	40.40	-	-
3	89.15	89.15	-	-
2	122.58	122.58	-	-
1	139.30	139.30	154.50	Ext:3 2x12, Int:2 2x08

*: Notation same as was used in Chapter 3

Step 1.2 Adjustment of Target stiffness for upper stories

Figure 5-4 a) and b) show the inter-story drift spectra before and after design. Because of the overstrength assigned, the inter-story drift spectra line for Story 1 drifts away from those of other stories. A similar optimization process as used in Chapter 4 can be used with the only difference being the stiffness ratio for Story 1 is held constant while others are changed until their spectra lines converge to that of Story 1. The adjusted inter-story drift spectra lines are shown in Figure 5-4 c). Table 5-3 tabulates the stiffnesses and drifts observed during this design step. The new optimized shear profile has been shown in Figure 5-3 b).

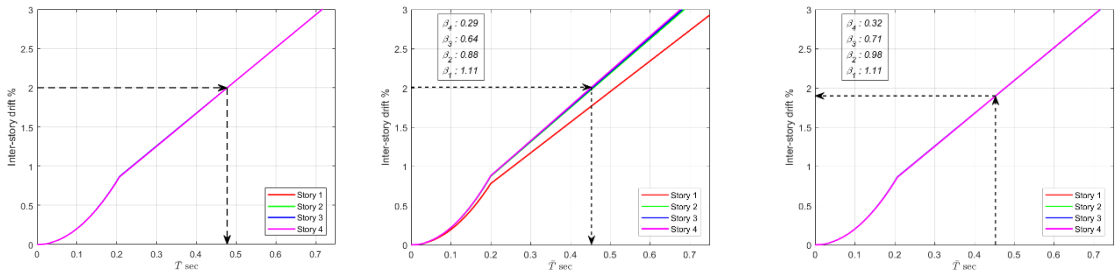

a) b) c)

Figure 5-4 Interstory drift spectra a) before design, b) after design and c) after adjustment

Table 5-3 Summary for design step 1.2

Story	*Before Design*			*After Design*			*After Adjustment*		
	β_k	K_{req}	θ	β_k	K_{prov}	θ	β_k	K_{req}	θ
4	0.29	40.40	2.00	0.29	40.40	2.01	0.32	44.57	1.90
3	0.64	89.15	2.00	0.64	89.15	2.00	0.71	99.18	1.90
2	0.88	122.58	2.00	0.88	122.58	1.98	0.98	136.51	1.90
1	1.00	139.30	2.00	1.11	154.50	1.77	1.11	154.34	1.90

Step 2.1 Design Story 2

Similarly, a suitable combination of exterior and interior walls has to be chosen that meets the stiffness demand on the story 2, however, with a further consideration that the shearwalls on this story can be accommodated atop the shearwalls on story 1 and proper load path is provided. Figure 5-5 shows the vertical elevation and shear stiffness profile of the as-designed shearwalls and Table 5-4 summarizes the stiffness values.

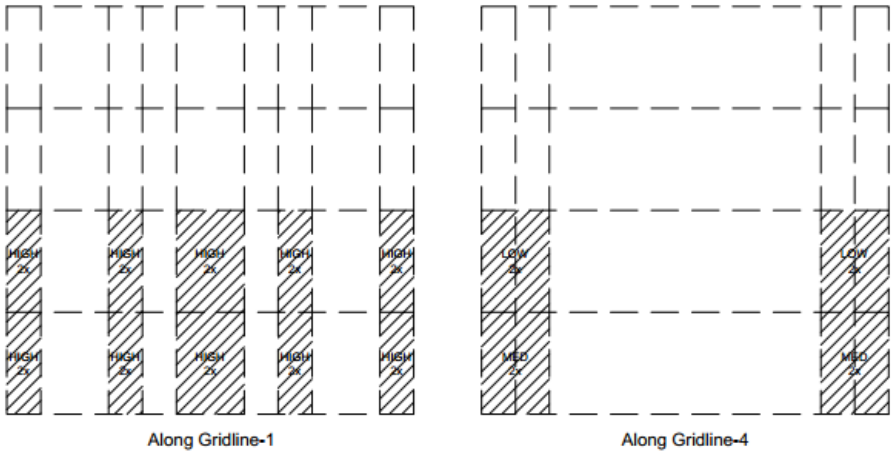

a)

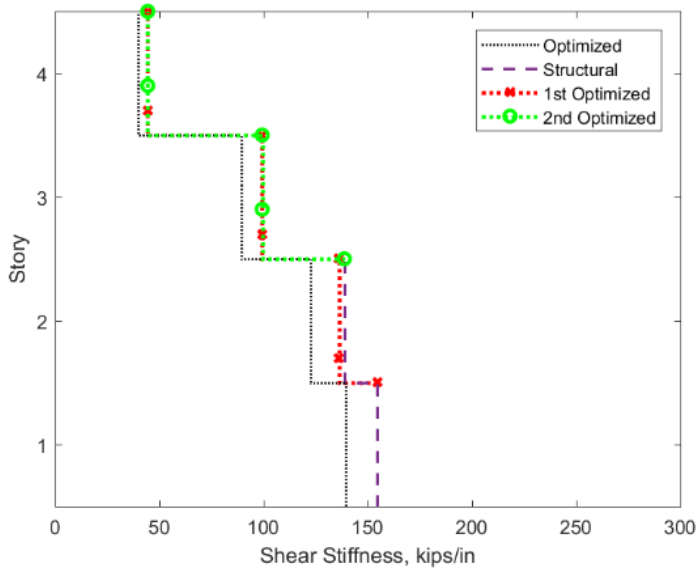

b)

Figure 5-5 Story 2: a) Vertical Elevation of As-designed Shearwalls b) Shear stiffness profile

Table 5-4 Shearwall design summary (for story 2)

Story	*Optimized Stiffness, k_{opt}*	*Target Stiffness, k_{req}*	*Provided Stiffness, $\phi_k k_{prov}$*	*Provided Design*
4	39.99	44.57	-	-
3	89.51	99.18	-	-
2	122.63	136.51	138.80	Ext:3 2x12, Int:1 2x08
1	139.28	154.34	154.34	Ext:3 2x12, Int:2 2x08

An additional step hinted at in the elaborated procedure step was to check for drift the shearwall design produces and depending on if the drift is too small or overstrength too high, iterate through the design process for the story until an acceptable drift and minimal overstrength is achieved. This step has been referred to as checking for a "more appropriate" design. Table 5-5 shows few such iterations that arrive at the assigned design. The iterations are guided by the following relation:

$$K_{req}{}^{<i+1>} = \frac{\theta^{<i>}}{\theta_{target}} \times K_{prov}{}^{<i>}$$ where $<i>$ is the iteration number

And $\theta^{<i>}$ and θ_{target} are the drift observed and target drift respectively.

Table 5-5 Iterations to obtain a "more appropriate" design

Iteration no.	*Optimized/Adjusted Target, K_{req}*	*Provided, K_{prov}*	*Story drift, θ*
1	139.3	154.4	1.69
2	$\frac{1.69}{2.00} \times 154.4 = 130.6$	138.8	1.87
3	$\frac{1.87}{2.00} \times 138.8 = 129.7$	138.8	1.87

Step 2.2: Adjustment of Target Stiffness for upper stories

Figure 5-6 show the inter-story drift spectra before design, after design and after adjusting target for other stories. It can be pointed out that the spectra lines do not converge just as well as they did even after target adjustment. This is because of the little overstrength in the design in story 2. But since the drifts in all of the stories are within the drift limit, the design is acceptable. Table 5-6 summarizes this design step.

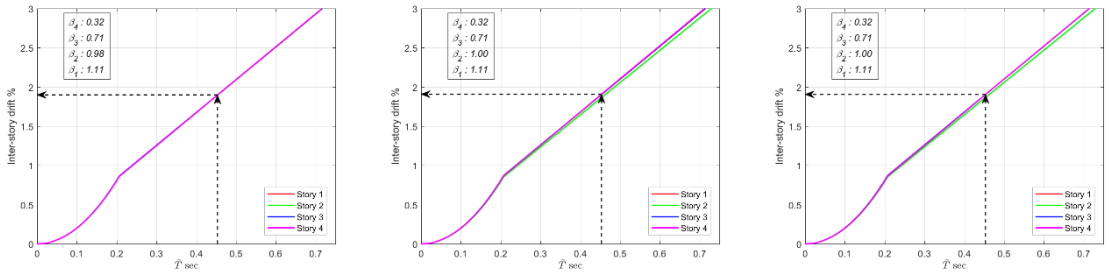

a) b) c)

Figure 5-6 Interstory drift spectra a) before design, b) after design and c) after adjustment

Table 5-6 Summary for design step 2.2

Story	*Before Design*			*After Design*			*After Adjustment*		
	β_k	K_{req}	θ	β_k	K_{prov}	θ	β_k	K_{req}	θ
4	0.32	44.57	1.90	0.32	44.57	2.01	0.32	44.57	1.90
3	0.71	99.18	1.90	0.71	99.18	2.00	0.71	99.18	1.90
2	0.98	136.51	1.90	0.98	138.80	1.98	1.00	138.80	1.90
1	1.11	154.34	1.90	1.11	154.34	1.77	1.11	154.34	1.90

Step 3 and 4: Design Story 3 and 4

Stories 3 and 4 can be designed in the same way as story 2.

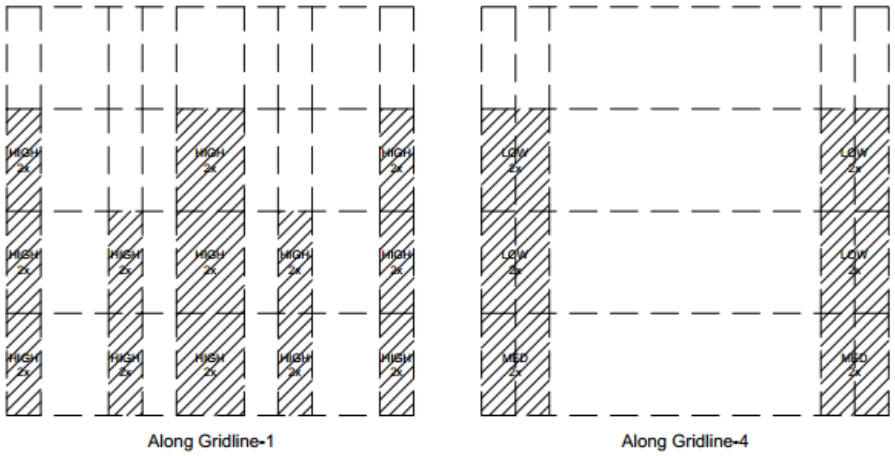

a)

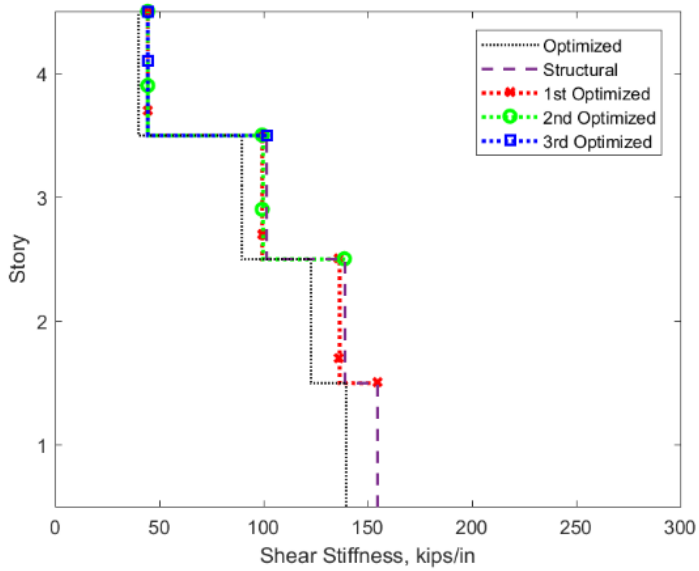

b)

Figure 5-7 Story 3: a) Vertical Elevation of As-designed Shearwalls b) Shear stiffness profile

Table 5-7 Shearwall design summary (for story 3)

Story	*Optimized Stiffness, k_{opt}*	*Target Stiffness, k_{req}*	*Provided Stiffness, $\phi_k k_{prov}$*	*Provided Design*
4	39.99	44.57	-	-
3	89.51	99.18	101.50	Ext:3 2x08, Int:1 2x08
2	122.63	138.80	138.80	Ext:3 2x12, Int:1 2x08
1	139.28	154.34	154.34	Ext:3 2x12, Int:2 2x08

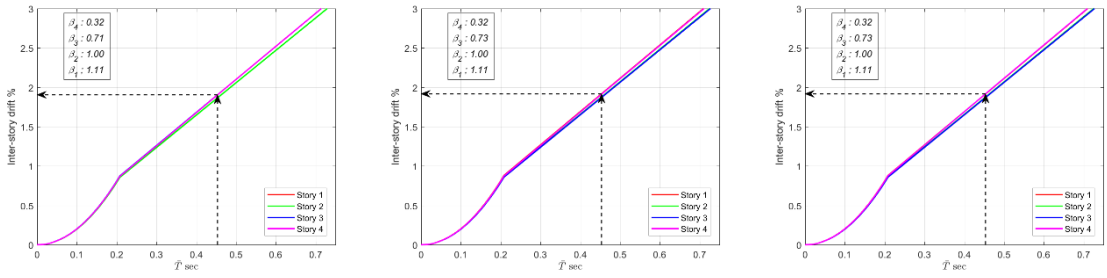

a) b) c)

Figure 5-8 Interstory drift spectra a) before design, b) after design and c) after adjustment

Table 5-8 Summary for design step 3.2

Story	*Before Design*			*After Design*			*After Adjustment*		
	β_k	**K_{req}**	**θ**	**β_k**	**K_{prov}**	**θ**	**β_k**	**K_{req}**	**θ**
4	0.32	44.57	1.90	0.32	44.57	2.01	0.32	44.57	1.90
3	0.71	99.18	1.90	0.71	101.50	2.00	0.73	101.50	1.90
2	1.00	138.80	1.90	1.00	138.80	1.98	1.00	138.80	1.90
1	1.11	154.34	1.90	1.11	154.34	1.77	1.11	154.34	1.90

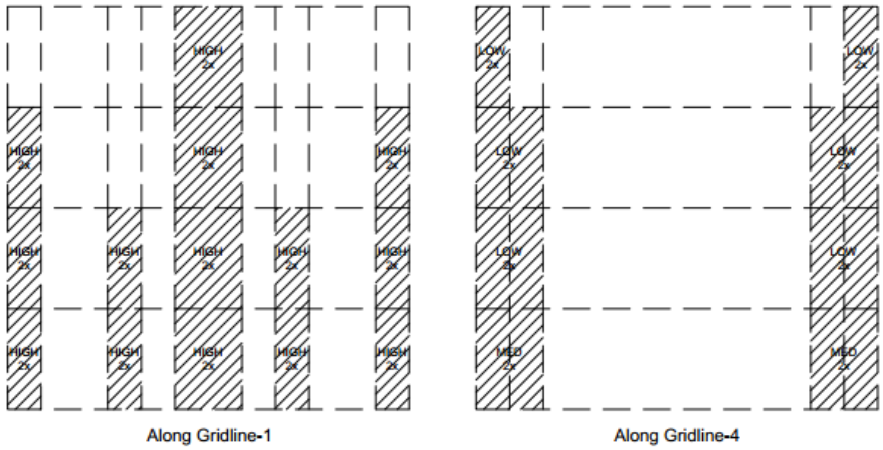

a)

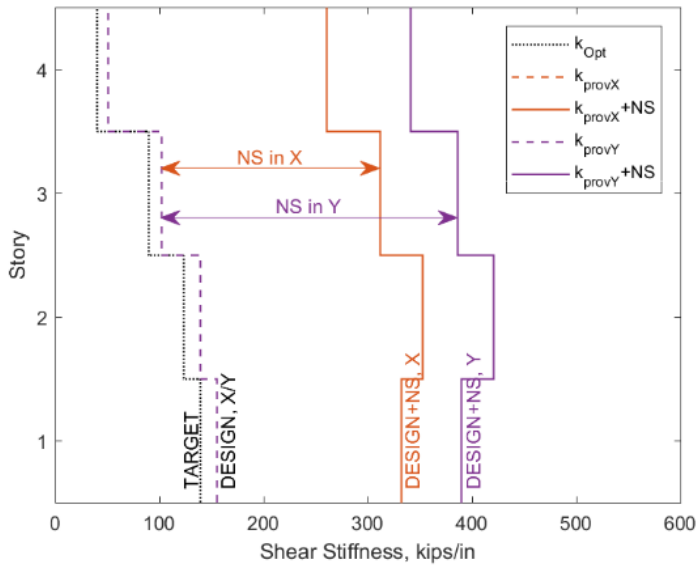

b)

Figure 5-9 Story 4: a) Vertical Elevation of As-designed Shearwalls b) Shear stiffness profile

Table 5-9 Shearwall design summary (for story 4)

Story	*Optimized Stiffness, k_{opt}*	*Target Stiffness, k_{req}*	*Provided Stiffness, $\phi_k k_{prov}$*	*Provided Design**
4	39.99	44.57	50.80	Ext:3 2x04, Int:1 2x04
3	89.51	101.50	101.50	Ext:3 2x08, Int:1 2x08
2	122.63	138.80	138.80	Ext:3 2x12, Int:1 2x08
1	139.28	154.34	154.34	Ext:3 2x12, Int:2 2x08

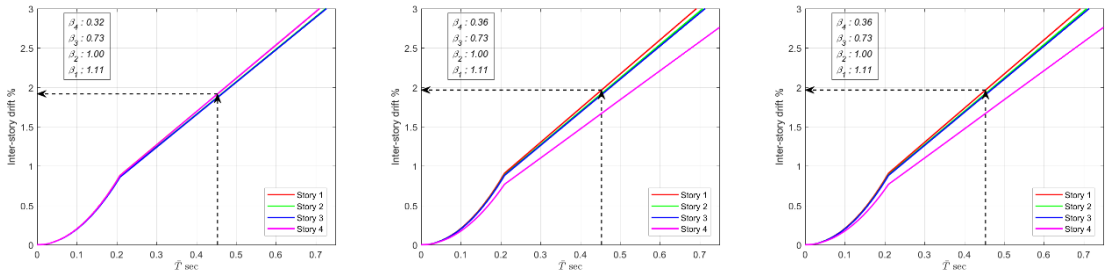

a) b) c)

Figure 5-10 Interstory drift spectra a) before design, b) after design and c) after adjustment

Table 5-10 Summary for design step 4.2

Story	*Before Design*			*After Design*			*After Adjustment*		
	β_k	**K_{req}**	**θ**	**β_k**	**K_{prov}**	**θ**	**β_k**	**K_{req}**	**θ**
4	0.32	44.57	1.90	0.32	50.80	1.67	0.36	50.80	1.67
3	0.73	101.50	1.90	0.73	101.50	1.90	0.73	101.50	1.90
2	1.00	138.80	1.90	1.00	138.80	1.92	1.00	138.80	1.92
1	1.11	154.34	1.90	1.11	154.34	1.97	1.11	154.34	1.97

It is clear from the Table 5-10 that the provided design using ADD procedure meets the 2% drift limit at the DBE level. Also shown in the Figure 5-9 is the combined shear profile along X- and Y-direction of the building.

5.3. Design Example Building with consideration of NS

The ADD procedure discussed in the previous section could be tweaked a bit so that it allows for the consideration of non-structural elements in design. The procedure remains almost the same with the only exception that during the shearwall design/selection step, interstory drift spectra for seismic hazard levels from the performance criteria for non-structural elements are also plotted and the stiffness requirements and the drift limits are checked for. This additional step has been included in the flowchart and shown in Figure 5-12.

But first, to see if the V2 building from the previous section (just as it is) meets the non-structural performance criteria, an inter-story drift spectra plot for the full building for each hazard level can be drawn. Figure 5-11 a) and b) show the spectra lines for 50%/50yr and 20%/50yr hazard levels respectively. It can be seen that the full building clearly does not meet the associated 0.5% and 1% drift limits and is slightly above them. This is likely due to the persisting soft-story defect in the full building seen in Figure 5-9 and also the fact that this building was never designed for these limits. It may be noted that $\bar{T}$ is different. This is because of the difference in the story stiffness at 0.5% and 1.0% drifts. Hence, the design is to be revised if the non-structural performance criteria is to be met.

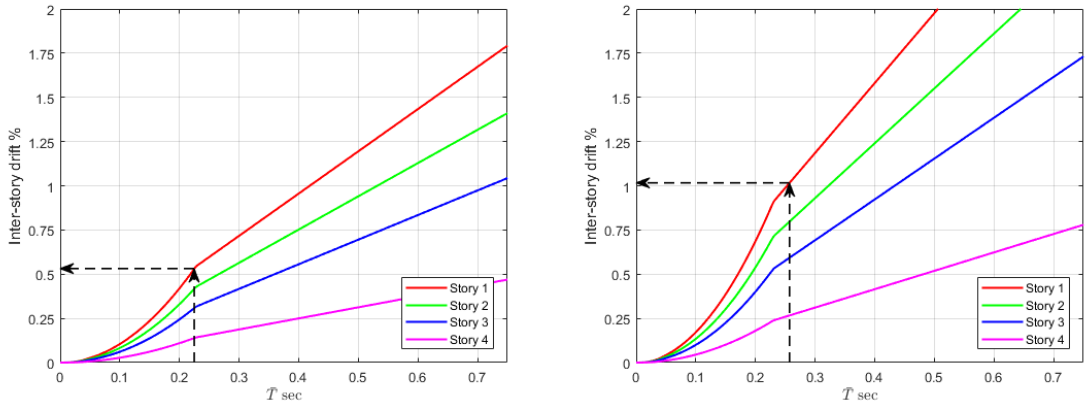

a) To be checked against 0.5% drift *b) To be checked against 1.0% drift*

Figure 5-11 Interstory drift spectra plots for (a) 50%/50yr and (b) 20%/50yr hazard levels

The reader might also be quick to think that an easy fix to this could be to eliminate the irregularity by compensating with additional structural shearwalls in the first story. To see if this works, the design at first story from previous section was changed such that the combined profile looks more stepped as shown in Figure 5-13. Inter-story drift spectra plot for this alternative design are shown in Figure 5-14. This alternative design just about meets each of the non-structural performance criteria.

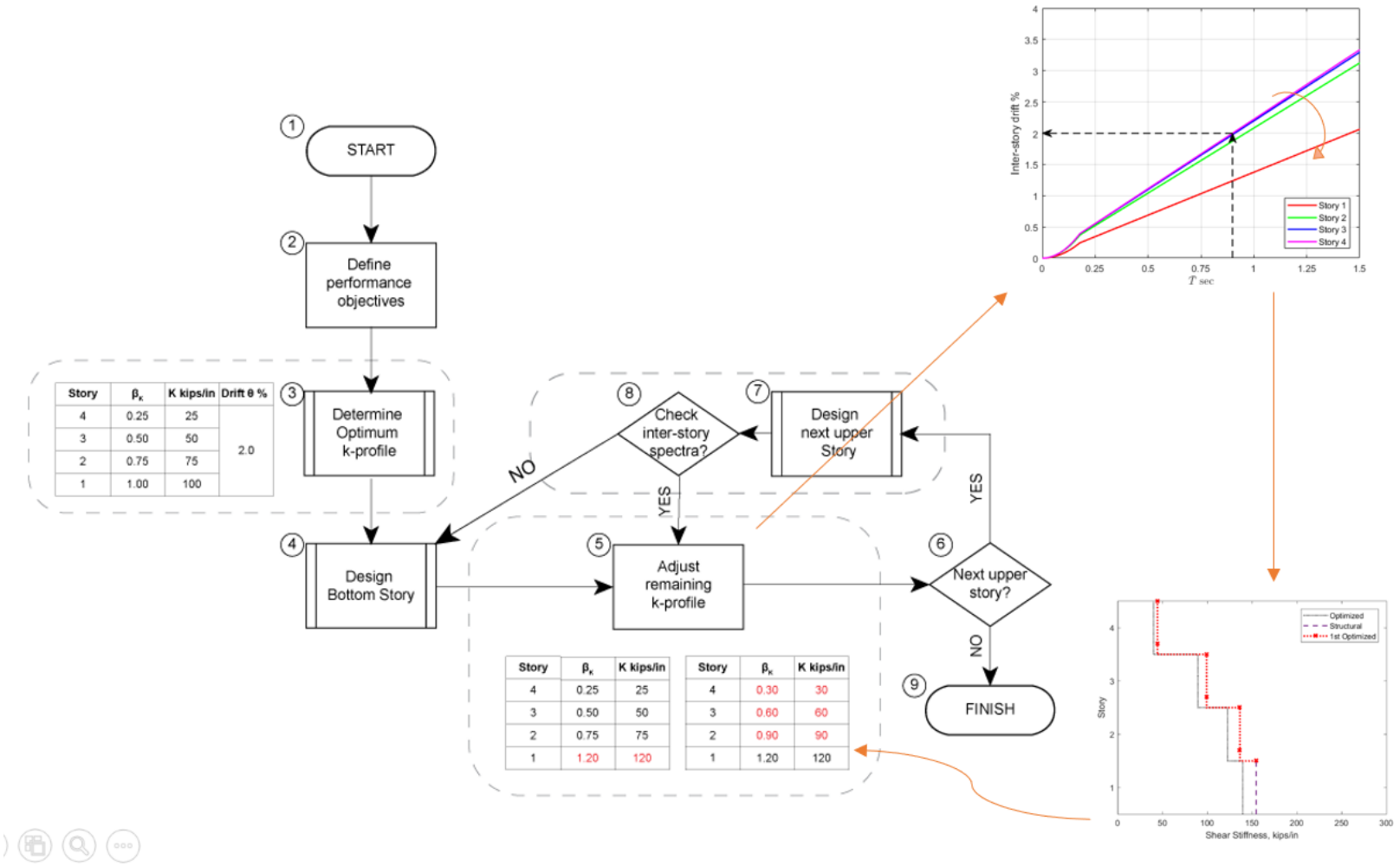

Figure 5-12 Flowchart for ADD procedure with the consideration of non-structural elements

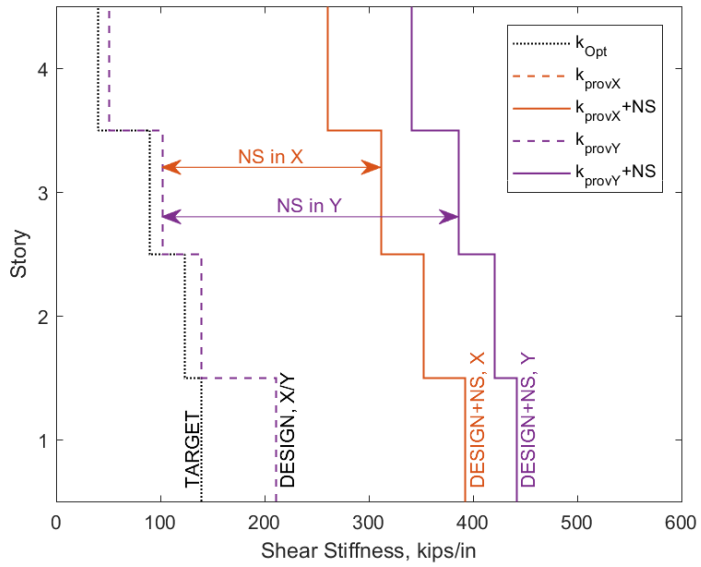

Figure 5-13 Alternative Stiffness profile and design

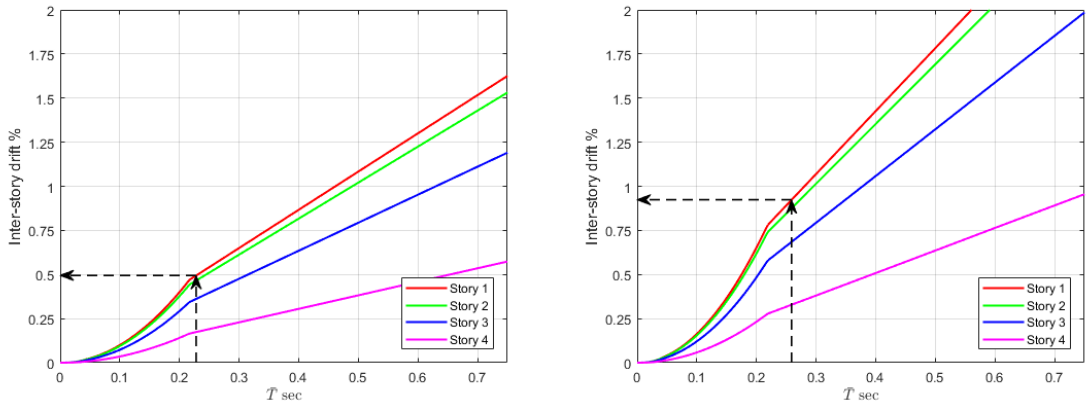

a) To be checked against 0.5% drift *b) To be checked against 1% drift*

Figure 5-14 Inter-story drift spectra plots for alternative design for (a) 50%/50yr and 20%/50yr hazard levels

However, it is also required to check if this new building still meets the structural performance criteria. Interstory drift spectra for the building structure only are shown in Figure 5-15. It can be observed that because of the high overstrength provided in the first story, the drifts in the other stories (highest being in the 2nd story) have significantly

increased but the building does meet the performance criteria. Hence, this approach is indeed viable. However, providing just as much additional shearwalls in only one story may not always be possible, so, if ADD procedure can achieve the performance criteria by providing lesser walls but distributing the additional walls among all the stories, it could be a better option.

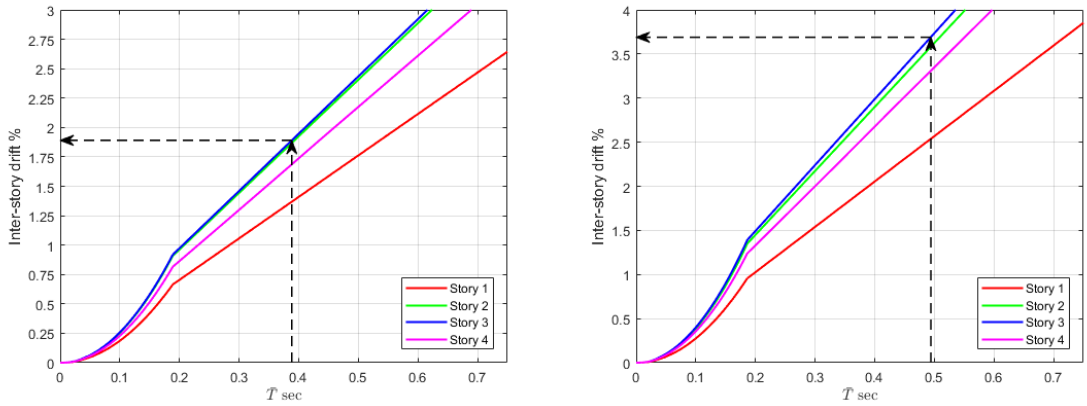

a) To be checked against 2% drift *b) To be checked against 4% drift*

Figure 5-15 Inter-story drift spectra plots for alternative design for (a) DBE and (b) MCE level

An alternative approach could also be to design for the combined structure first using ADD procedure, deduct the contribution of the non-structural elements and then check for the building structure only (stiffness and drifts). However, it is required that the contribution from structural walls is at least equal to the optimized target profile from DDD procedure. NS elements are a function of building plan, an engineer cannot be certain that this floor plan would be retained throughout the life of the building. Also, there could be a case where the NS elements only surpass the strength of the structural walls (possibly on the top story). Hence, if minimal stiffness is provided for a building like V2, the design

essentially becomes same as the building designed simply using DDD procedure (or even ELF procedure) and the soft-story defect is not really resolved. Therefore, it is best if non-structural elements are considered secondary and only checked for alongside or after structural shearwall design.

Hence, if non-structural elements are to be considered, the ADD procedure for the building structure is performed with the only new addition that inter-story drift spectra for the full building is plotted and checked if the nonstructural performance criteria are met. Because of the inclusion of the non-structural performance criteria, the design procedure becomes bit of a hit-and-trial procedure since the ADD procedure in itself cannot encompass the performance of non-structural inclusive full building. Which means, if during the design process, say after design of Story-3, if structural performance criteria is met but not the non-structural performance criteria for any combination of walls, the only alternative might have to be to revise the walls for either or all of the lower stories. Hence, for brevity, only the final designs that met all of the performance criteria are only shown. Figure 5-16 shows the wall profiles along gridline 1-1 and 4-4 and Figure 5-17 shows the shear stiffness profile for the design. Table 5-11 tabulates the optimum profiles, provided designs, provided stiffness profile and drifts developed for each hazard level.

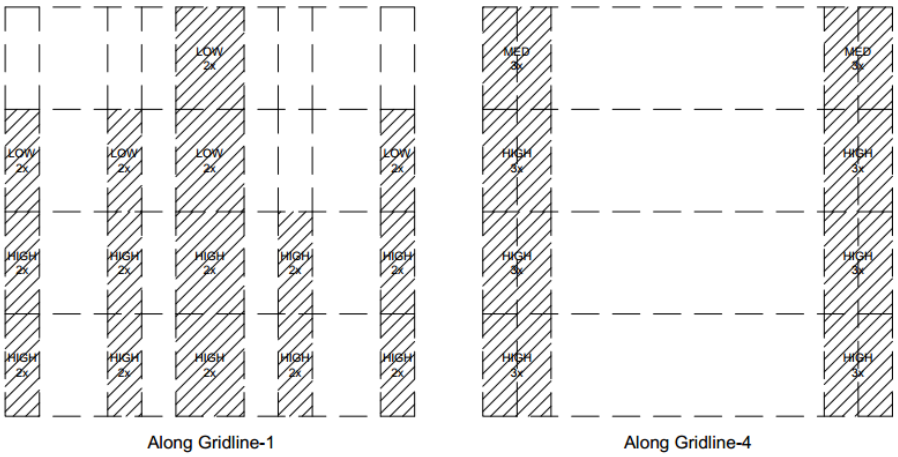

Figure 5-16 Vertical Shearwall Profile

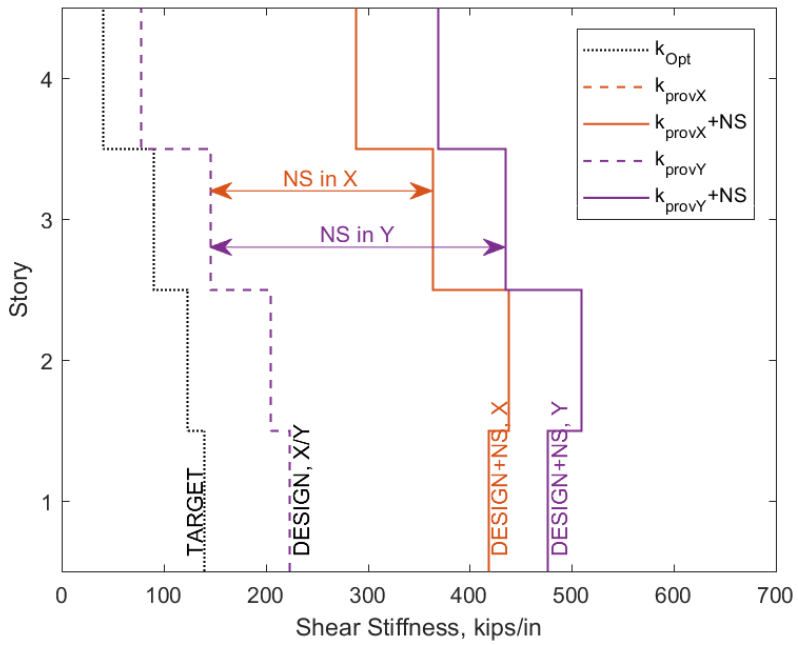

Figure 5-17 Shear stiffness profile

Table 5-11 Design Example Summary for ADD with consideration of non-structural elements

Story	*Optimized Stiffness, k_{opt}*	*Provided Stiffness, $\phi_k k_{prov}$*	*Provided Design**	*Drifts (in %) for hazard levels*			
				50%/50yr	*20%/50yr*	*10%/50yr*	*2%/50yr*
4	39.99	64.18	Ext:1 2x04, Int:2 3x08	0.16	0.32	1.31	2.66
3	89.51	111.75	Ext:1 2x10, Int:3 3x08	0.31	0.64	1.61	3.16
2	122.63	138.75	Ext:3 2x10, Int:3 3x08	0.39	0.78	1.58	2.93
1	139.28	154.54	Ext:3 2x12, Int:3 3x08	0.48	0.96	1.65	3.06

To attain each of the performance criteria, double sheathing only was found not sufficient. Hence, a mid-ply construction as shown in Figure 5-18 with an OSB in the middle and one on either of the outer faces is intended to be used. It has been assumed that such a construction provides three times the strength of a single sheathing.

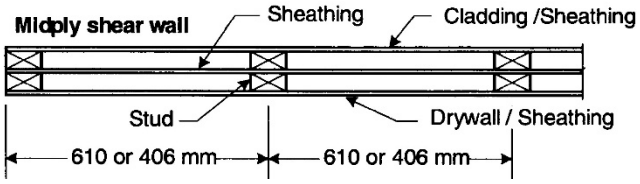

Figure 5-18 Mid-ply construction

Figure 5-19 shows the inter-story drift spectra for the final design at each of the hazard levels.

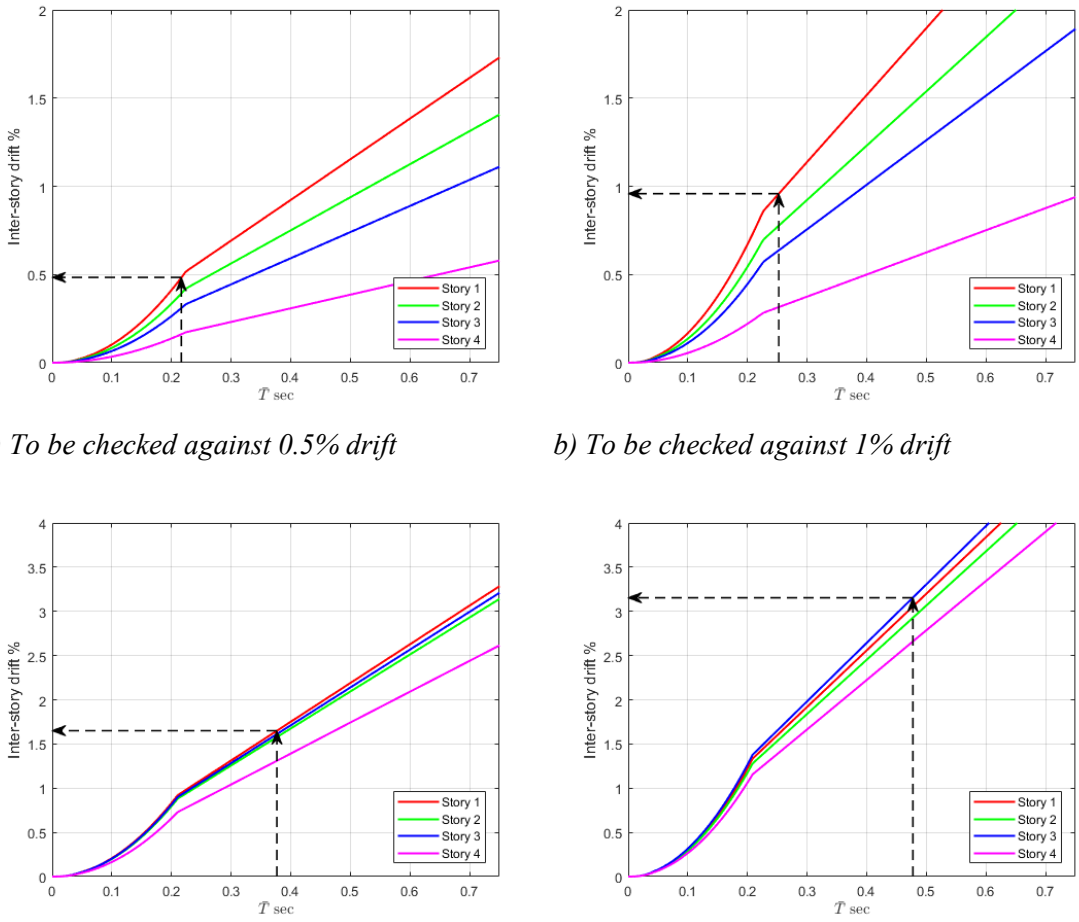

a) To be checked against 0.5% drift

b) To be checked against 1% drift

c) To be checked against 2% drift

d) To be checked against 4% drift

Figure 5-19 Inter-story spectra plots for Final Design for (a) 50%/50yr, (b) 20%/50yr, (c) 10%/50yr and (d) 2%/50yr hazard levels

5.4. Performance Evaluation and Comparison with FBD

To differentiate between the ADD designs without and with the consideration of non-structural elements, they have been named as ADD1 and ADD2. Each of these variants of V2 building can be compared with the original ELF-designed building from Chapter 3, which has been simply referred to as ELF. Inclusion of V2 in their name was not found essential since these are all a variant of V2, just with different structural design. Figure

5-20 shows the stiffness profile of the buildings at the design drift of 2%. It may be noted that each of these designs retains the soft-story in profile. There is a slight change in profile between ELF and ADD1 building due to different structural design causing different amount of complementary non-structural elements.

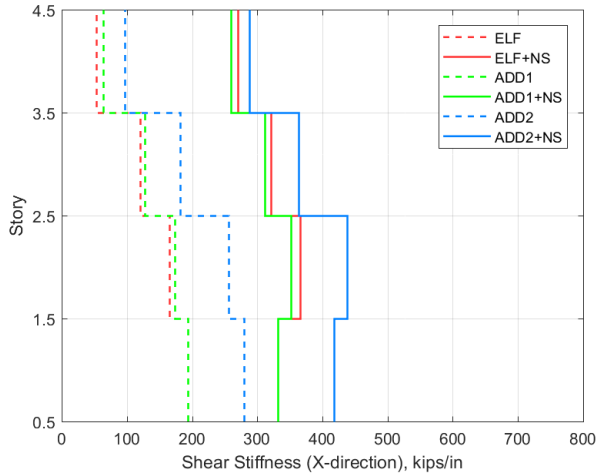

a)

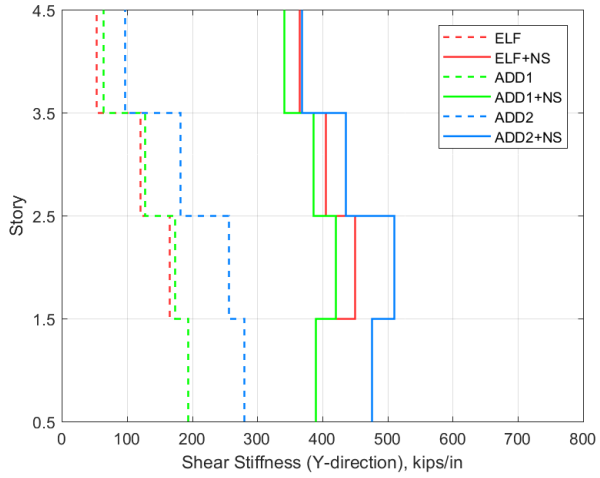

b)

Figure 5-20 Stiffness profiles for variants of V2 at the design drift of 2% along (a) X-direction and (b) Y-direction

5.4.1. Modal analyses

Modal analyses were conducted on each of the models and it was observed that these buildings also show visually similar mode shapes as in Figure 3-20 in Chapter 3 (i.e. the first two modes are largely translational in each of the horizontal direction while the third is torsional) and hence, are not shown here. The time periods for these set of buildings are tabulated and compared against those designed using ELF in Table 5-12.

Table 5-12 First three periods (in seconds) for V2 with and without NS

Mode	*Structure Only*			*Full Building*		
	ELF	**ADD1**	**ADD2**	**ELF+NS**	**ADD1+NS**	**ADD2 +NS**
1	0.71	0.81	0.67	0.57	0.57	0.56
2	0.68	0.79	0.65	0.51	0.53	0.50
3	0.57	0.50	0.48	0.46	0.48	0.48

5.4.2. IDAs

Three-dimensional IDAs were also conducted on each of the models. Figure 5-21 shows the fragility curves and Table 5-13 tabulates the relevant IDA parameters for V2 building designed using ELF against ADD procedure.

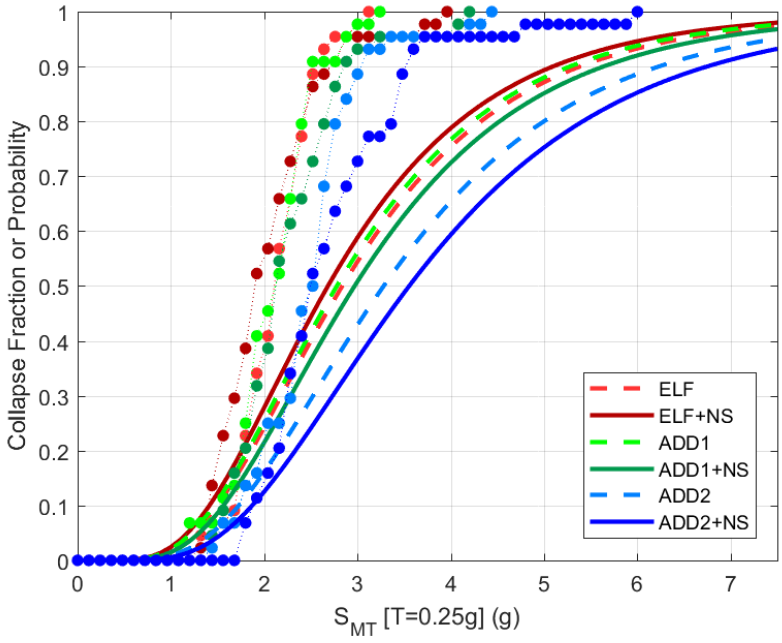

Figure 5-21 Fragility curves for V2 designed using ELF and ADD procedure

Table 5-13 IDA parameters for V2 designed using ELF and ADD procedure

Parameters	*ELF*	*ADD1*	*ADD2*	*ELF +NS*	*ADD1 +NS*	*ADD2 +NS*
S_{CT} *(g)*	2.84	2.78	3.28	2.68	2.97	3.55
CMR	1.42	1.39	1.64	1.34	1.49	1.78
ACMR	1.89	1.85	2.19	1.79	1.98	2.37
P(COL|MCE)	10.1%	10.9%	5.9%	12.2%	8.6%	4.2%

It can be seen that the ELF building and the ADD1 building have similar collapse performance while the ADD2 has much better performance. This is clearly because the ADD2 has higher strength among the three variants. Also, performance degradation after the addition of non-structural elements in the ELF building has been reversed in ADD1 as well as ADD2 building even though each of these buildings as seen in Figure 5-20 still

retain the soft story. Apparently, performance in the case of ADD1 improved because of the slight decrease in the irregularity between 1st and 2nd story. On the other hand, ADD2 has higher overstrength and was also designed for structural as well as non-structural performance, hence so.

The performance of these buildings can be best assessed by checking the actual displacement that occurred at various hazard levels against their associated drift limits. Table 5-14 shows the survival rate for building ADD1 against each of the performance criteria and Figure 5-22 shows the performance curves for the same. From the table as well as the plot, it can be checked that the building structure only and the full building both meet the DBE and MCE level requirements. In fact, the full building also achieves the desirable 80% probability of non-exceedance at DBE level. On the other hand, the full building does not meet either of the 0.5% and 1.0% limit by some margin clearly because it was not designed and checked for it. Also, the full building does indeed perform better than the structure only.

Table 5-14 Probabilities of non-exceedance in % for ADD1

		Full Building				Structure Only	
Drift Limits		***0.5%***	***1.0%***	***2.0%***	***4.0%***	***2.0%***	***4.0%***
P_{NE} (in %)		***50***	***50***	***50***	***50***	***50***	***50***
Hazard Levels	***50%/50yr***	43	93	100	100	100	100
	20%/50yr	5	43	100	100	86	100
	10%/50yr	2	25	89	100	73	93
	2%/50yr	0	5	23	73	9	61

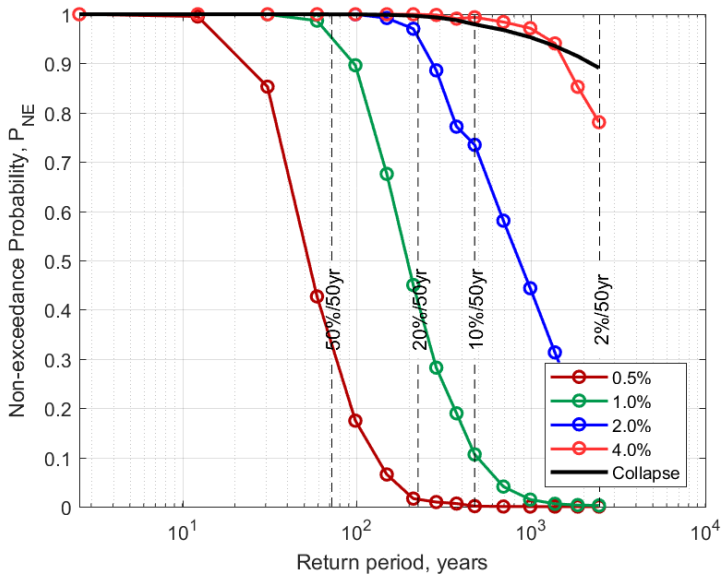

a)

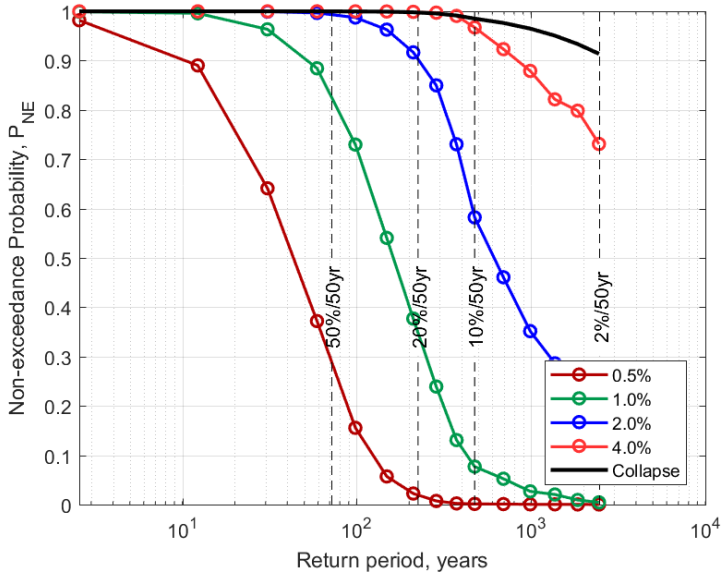

b)

Figure 5-22 Performance curves for ADD1

Table 5-15 and Figure 5-23 show the survival rates for building ADD2 and performance curves. ADD2 meets all of the set performance criteria for full building and structural

performance criteria for building structure only. And also achieves the 80% probability of non-exceedance at DBE as well as MCE level. But it may be noted that survival rates are slight greater for structure only compared to the full building. This is likely due to the building irregularity and is same as was observed in ELF-designed V2 building.

Table 5-15 Probabilities of non-exceedance in % for ADD2

		Full Building				Structure Only	
Drift Limits		***0.5%***	***1.0%***	***2.0%***	***4.0%***	***2.0%***	***4.0%***
P_{NE} (in %)		***50***	***50***	***50***	***50***	***50***	***50***
Hazard Levels	***50%/50yr***	59	98	100	100	100	100
	20%/50yr	9	66	98	100	100	100
	10%/50yr	5	25	86	100	89	100
	2%/50yr	0	5	46	80	18	89

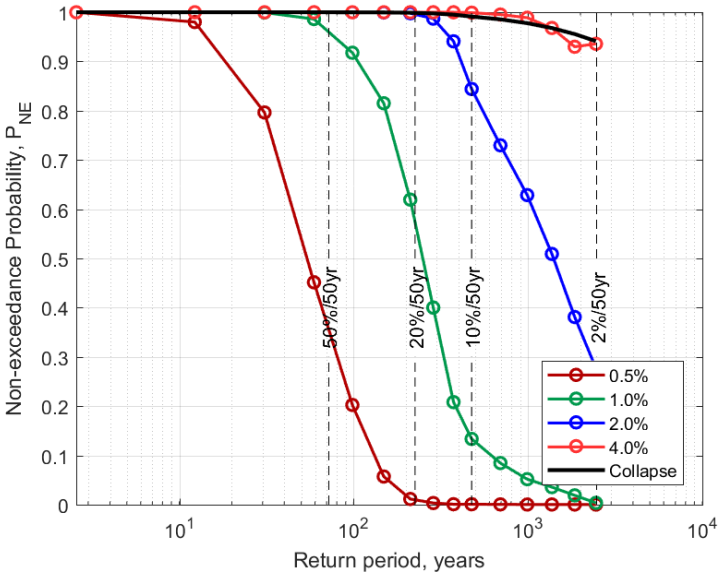

a)

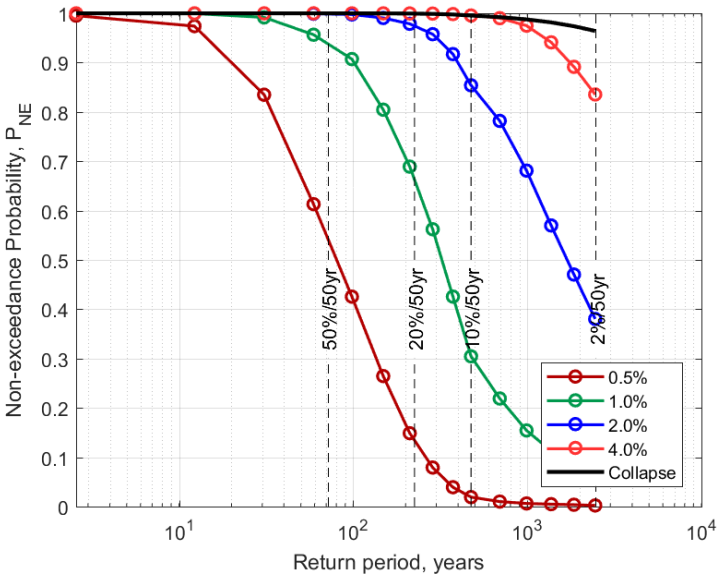

b)

Figure 5-23 Performance curves for ADD2

6. COMPARISON STUDY BETWEEN 2D AND 3D SEISMIC ANALYSES

Each ground motion consists of two components, one in each horizontal orthogonal direction. A building model in 3D space can be subjected to a ground motion pair with each component in each of its horizontal (X- and Y-) directions simultaneously. On the other hand, a two-dimensional model of the same building can only be subjected to a component of the ground motion pair at a time. It can be agreed upon that, since a 3D model is subjected to two ground motions simultaneously and a 2D model is subjected to only a ground motion at a time, the 3D models tend to collapse more than their 2D counterparts for the same intensity of ground motion. Given that the same building is being analyzed, there has to be a correlation between the collapse performance in 2D and 3D. To add another dimension to this problem, what if the building were designed such that its strengths in the two directions are different? The same 3D model can be used and analyzed but with the components swapped. However, if it were a 2D model, representative 2D models for each direction are to be built and analyzed separately. The two 2D models cannot influence each other anymore and the performance in each case is completely independent of the other. The uneven strength in the two directions is almost always the case in practical use, hence, the collapse performance of the two 2D models is bound to be very different as well. Hence, this raises two questions: first how the 2D and 3D performance can be correlated and second, does the correlation apply to buildings with different strengths in the two directions?

Figure 6-1 shows a three-dimensional 1-story Timber3D model with each accompanying circle representing a set of analyses that can be run on the model and uses the 22 ground motion pairs from FEMA P695 (2009). In the case of 2D analyses, each of the 44 ground motions is applied one at a time in a direction and repeated for the other direction, making up 44 analyses for each direction. In the case of 3D analyses, a ground motion pair is applied simultaneously on the model making up 22 analyses and then the components swapped to make up the other 22 analyses, totaling up 44 analyses.

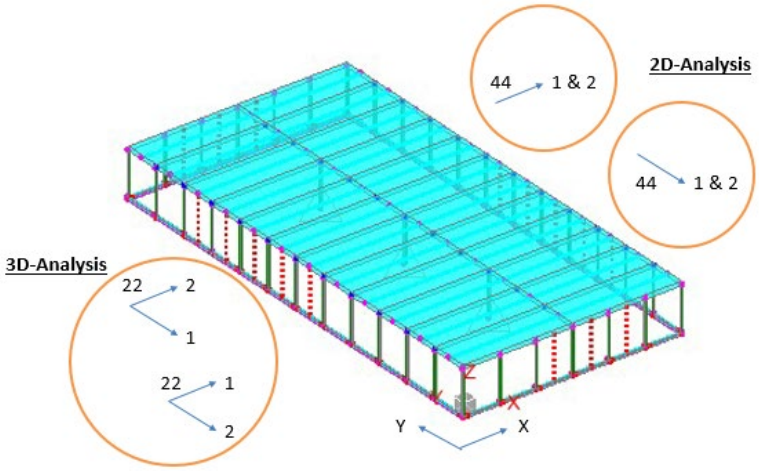

Figure 6-1 2D and 3D analyses

FEMA P-695 study answers the first question on how the 2D and 3D models are relatable. It suggests that the median collapse intensity from 3D analyses is on average 20% less than the median collapse intensity from 2D analyses given that all the other possible parameters stay the same i.e. mathematically, it can be written as

$$S_{CT,2D} = 1.2 \times S_{CT,3D}$$

From the expression, however, it is not clear which 2D direction it refers to if it is viewed in the light of buildings with different strengths in the two directions. This chapter compares the results from each of the 2D directions against those from the 3D model and tries to verify the applicability of the factor. It also suggests an alternative approach wherein results from the two 2D analyses set are combined to obtain the performance parameters and see if using this approach extends the applicability of the 3D factor in any way. The models are largely single-story in addition to a few four-story models. And finally, even though 2D models are simpler to build and analyze, do they truly represent the building performance since the buildings are built 3D? This will also be discussed at the end of the chapter.

6.1. Building Models used in the Study

This study uses its own set of building models independent of those in the preceding chapters. These models were also built in Timber3D. Timber3D, even though being a 3D analysis program, can do one-dimensional nonlinear time history analysis if only one component of each ground motion pair were to be imposed on the building at a time. This limits the displacements largely in the direction of the ground motion other than that in the vertical direction and hence, can replicate 2D analysis done in OpenSees or any other 2D structural analysis software.

This set of models were adapted from the COM1B building originally developed in the ATC116 Developing Solutions to the Short-period Building Performance Paradox Study for Wood Light-frame Buildings (ATC, 2017). This study retains the dimensions and weight of the building from the original study, however, uses a different shearwall

backbone (i.e. OSB-High introduced in Chapter 3) from the one assigned in the original building. Hence to avoid confusion, a new naming convention was developed.

Figure 6-2 Naming convention for a 1-story building

Here, B1St signifies a 1-story building while the first suffix 100 or so represents the capacity-to-demand ratio in X-direction and the second 100 or so in the Y-direction that the building has been designed for; the demand here being the story shear according to the Equivalent Lateral Force method as defined in ASCE 7-16. With the demand being the same for all the models in the set, all the models scale the same backbone to achieve the different capacities accordingly. Table 6-1 and Table 6-2 enlist all the 1-story models used with same design in two directions and those with different designs in two directions.

Table 6-1 1-story Models with Same Designs in Two Directions

Model name	*C/D in X-direction*	*C/D in Y-direction*
B1St-050050	0.50	0.50
B1St-100100	1.00	1.00
B1St-110110	1.10	1.10
B1St-120120	1.20	1.20
B1St-200200	2.00	2.00

Table 6-2 1-story Models with Different Designs in Two Directions

Model name	*C/D in X-direction*	*C/D in Y-direction*
B1St-100125	1.00	1.25
B1St-100150	1.00	1.50
B1St-100175	1.00	1.75
B1St-100200	1.00	2.00
B1St-050200	0.50	2.00

Additionally, this study explores the performance of four-story models as well and checks if the reasoning developed for single-story models is also applicable to multi-story buildings. However, there is also vertical strength distribution associated with multi-story buildings. Hence, the scope was only limited to equal strength models. The four-story buildings were developed as an extension of the 1-story buildings with same story heights and total seismic weight. Table 6-3 shows the story weights, story heights and the calculations of the lateral shear forces on each story and Table 6-4 enlists all the four-story models used.

Table 6-3 Equivalent Shear Demand Calculation in Four-story models

Story i	$\beta_{m,i}$	m_i *kips/g*	h_i *in*		C_{vxi}	*Cumulative* C_{vxi}	V_{xi} *kips*
(1)	**(2)**	**(3)**	**(4)**	**(5) = (2)*(4)**	**(6)**	**(7)**	**(8)**
4	0.5	25.5	480	237.7	0.25	0.25	6.9
3	1.00	51.5	360	360.0	0.38	0.62	17.3
2	1.00	51.5	240	240.0	0.25	0.87	24.2
1	1.00	51.5	120	120.0	0.13	1.00	27.7
		180.0		**957.7**			

Table 6-4 Four-story Models with same design in both directions but varying vertical strength distribution

Story	*B4St-C100*	*B4St-ELF*	*B4St-125*	*B4St-153*	*B4St-300*	*B4St-600*
4	1.00	0.25	x 1.25	x 1.53	x 3.00	x 6.00
3	1.00	0.62	x 1.25	x 1.53	x 3.00	x 6.00
2	1.00	0.87	x 1.25	x 1.53	x 3.00	x 6.00
1	1.00	1.00	x 1.00	x 1.00	x 1.00	x 1.00

Here, the naming convention has been altered because we are only looking at 'equal strengths in both directions' cases. The overstrength factors in the two directions were dropped, instead a suffix representative of the irregularity of the building was used. The values are in terms of base shear of the building. The '-C100' building has a constant strength on all of the floors while the '-ELF' building has the strengths exactly equal to ELF demand. The remaining four cases are variants of the '-ELF' building with added overstrength of 25%, 53%, 200% and 500% on the upper floors. The added overstrength could be because of the structural contribution only or a combination of structural and non-structural contribution. Also, the last two models were built and analyzed only to see how bad can the performance of a soft-story building really be and are by no means practical.

6.2. Comparing 2D and 3D analyses in Timber3D

6.2.1. Single-story models

6.2.1.1. Same Design in Two directions

The similarity (or difference) between the results from 2D and 3D analyses of the same models can be observed in the IDA curves as well as the fragility curves from the

IDA. Since the designs in the X- and Y-directions are exactly the same, these curves for the 2D models would also be the same in both directions. The combined 88 case even though shown on the plots for 2D models holds little significance here as it would be the same as the original 44 for these set of models. And finally, the scaled results are shown for 3D models to better compare against the 2D models as well as verify its use.

Figure 6-3 and Figure 6-4 show the IDA curves for the model B1St-100100. The IDA curves for X- and Y-directions as well the combined 88 case are the same and hence, overlap. Also, it can be seen that the median collapse intensity for the 3D model with the 1.2 factor and that for the 2D model without any adjustments are about the same. This supports the use of 1.2 factor. However, it should be noted that the spread of IDA curves for 2D models is larger than that of the scaled IDA curves of the 3D model. This possibly means the 1.2 factor works only for the median and not for extreme collapse intensities.

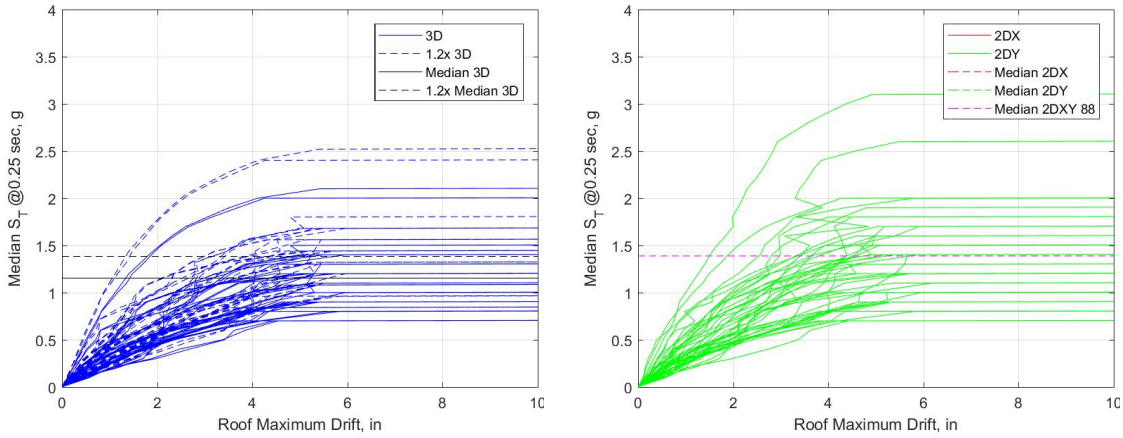

(a) (b)

Figure 6-3 IDA Curves for B1St-100100 from (a) 3D analysis and (b) 2D analysis

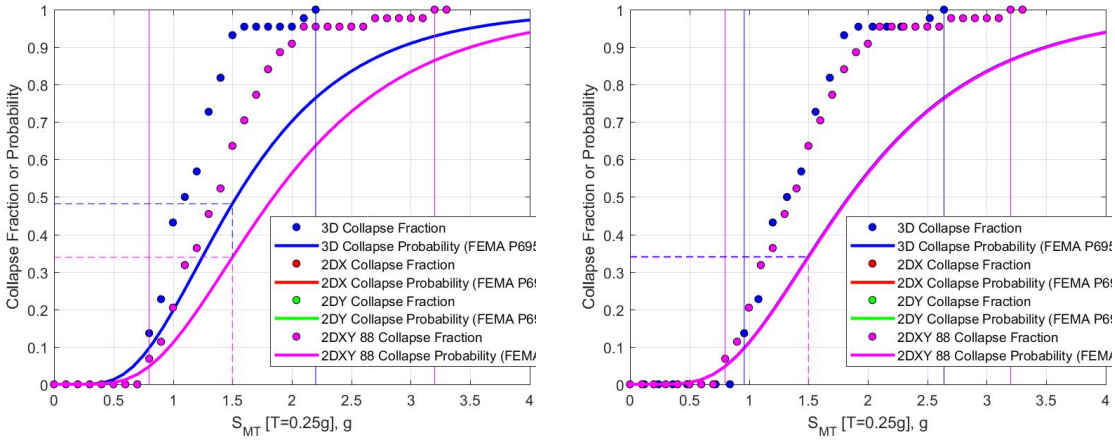

(a) (b)

Figure 6-4 Fragility Curves for B1St-100100 (a) without and (b) with 1.2 factor

Figure 6-5, Figure 6-6, Figure 6-7 and Figure 6-8 show the IDA curves and the fragility curves for B1St-050050 and B1St-200200. The median collapse intensities for the 2D and the 3D model are similar albeit not as close as for B1St-100100. Also, it can be noted that the spread of collapse intensities is much smaller for the 3D model of B1St-050050 than its 2D counterpart, which suggests that the difference of the spread of the IDA curves increases drastically with the decrease in the provided strength of the walls. However, same cannot be said for the increase in the provided strength.

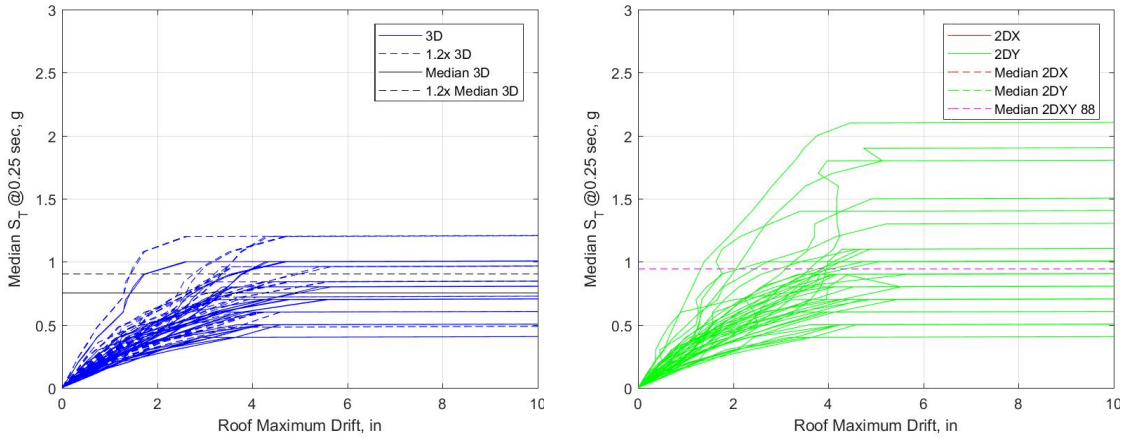

(a) (b)

Figure 6-5 IDA Curves for B1St-050050 from (a) 3D analysis and (b) 2D analysis

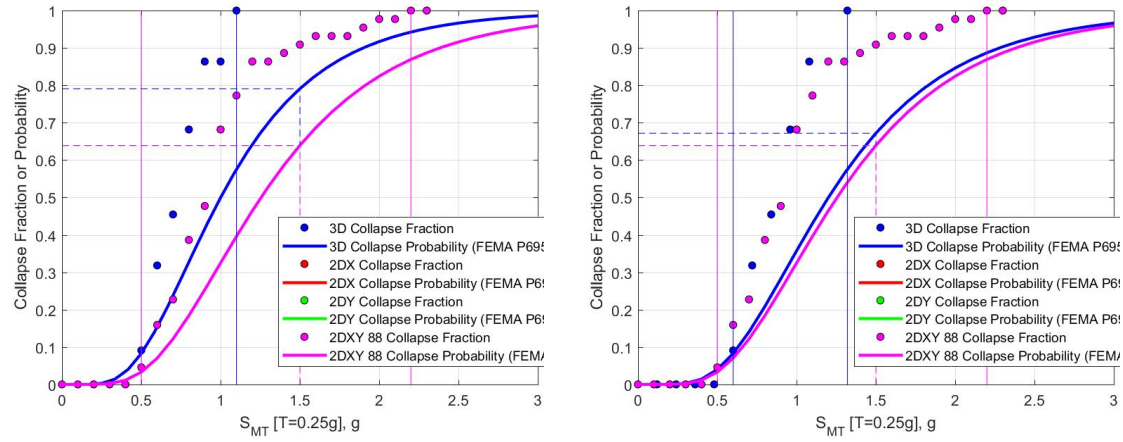

(a) (b)

Figure 6-6 Fragility Curves for B1St-050050 (a) without and (b) with 1.2 factor

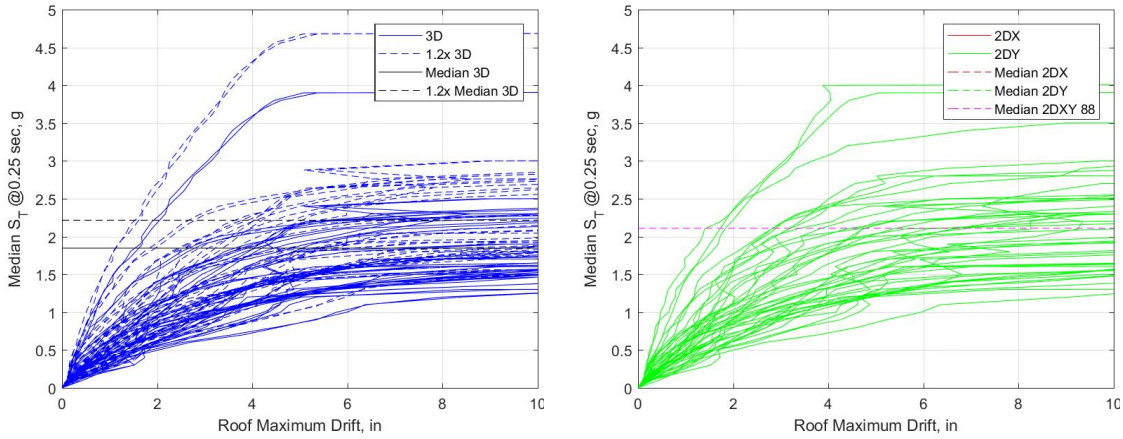

(a) (b)

Figure 6-7 IDA Curves for B1St-200200 from (a) 3D analysis and (b) 2D analysis

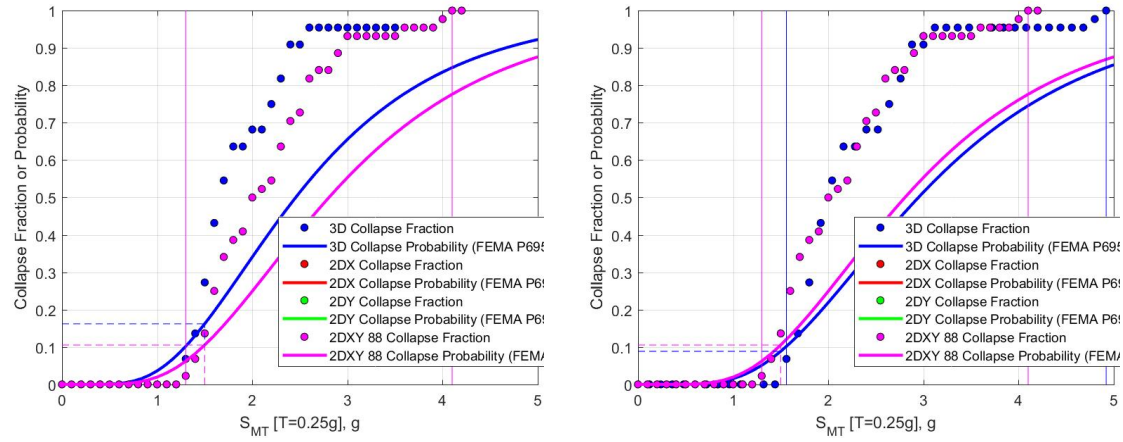

(a) (b)

Figure 6-8 Fragility Curves for B1St-200200 (a) without and (b) with 1.2 factor

Table 6-5 and Table 6-6 show the results from the IDA of this set of models. The 1.2 factor has been used to calculate the performance indicators for all of the 3D analyses cases. It can be observed that performance indicators like ACMR and P(COL|MCE) are very close to each other and hence, it can be agreed upon that the 1.2 factor does work for models with same designs in both directions. The similarity can be further seen from Figure

6-9 where the results from 2D and 3D analysis are juxtaposed onto one another. However, it is to be noted that the similarity decreases as the capacity provided differs away from the required demand.

Table 6-5 Results from 2D analysis

Parameter	*B1St-050050*	*B1St-100100*	*B1St-110110*	*B1St-120120*	*B1St-200200*
S_{CT}	1.26	1.85	1.97	2.07	2.81
CMR	0.63	0.93	0.99	1.04	1.41
ACMR	0.84	1.23	1.31	1.38	1.87
P(COL|MCE)	58.6%	29.0%	24.7%	21.6%	8.2%

Table 6-6 Results from 3D analysis with 1.2 factor

Parameter	*B1St-050050*	*B1St-100100*	*B1St-110110*	*B1St-120120*	*B1St-200200*
S_{CT}	1.20	1.84	1.96	2.07	2.95
CMR	0.60	0.92	0.98	1.04	1.48
ACMR	0.80	1.23	1.31	1.38	1.96
P(COL|MCE)	62.1%	29.2%	24.9%	21.6%	6.8%

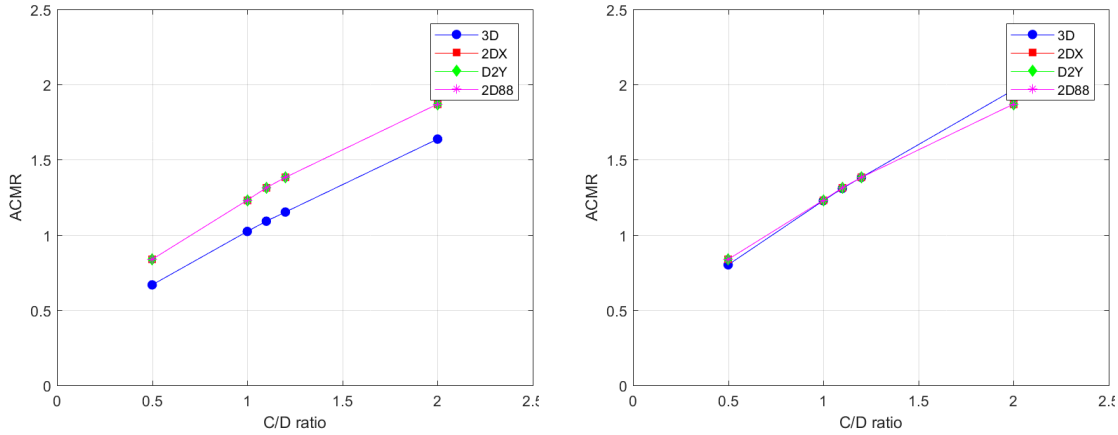

(a) (b)

Figure 6-9 Variation of ACMR with C/D ratio (a) without and (b) with 1.2 factor

6.2.1.2. Different Design in Two directions

Similar plots are shown for this set of models as well. However, this set encompasses the problematic models as earlier discussed because of the unequal design strength in the two directions. Also, it is to be noted that since the results from two 2D models are now different, the hybrid approach of combining 88 cases can be of use.

Figure 6-10, Figure 6-11 and Figure 6-12 show the IDA curves for B1St-100150, B1St-100200 and B1St-050200. It can be seen in Figure 6-10 and Figure 6-11 that the scaled median collapse intensity for the 3D model is not similar to the median collapse intensity of either the X- or Y- directions at all but rather similar to the combined 88 case. Also, in Figure 6-12, the median collapse intensities are not just as close but still similar enough. This possibly means that the 1.2 factor applied on the 3D models is much more comparable and accurate when the results from both of the directions are combined. In addition, it can also be noted that the spread of the IDA curves for the 2D models is much

larger for the stronger Y-direction than the X-direction and that of the scaled 3D models lies somewhere in between the two and hence, the factor does not indeed work for the extreme collapse intensities.

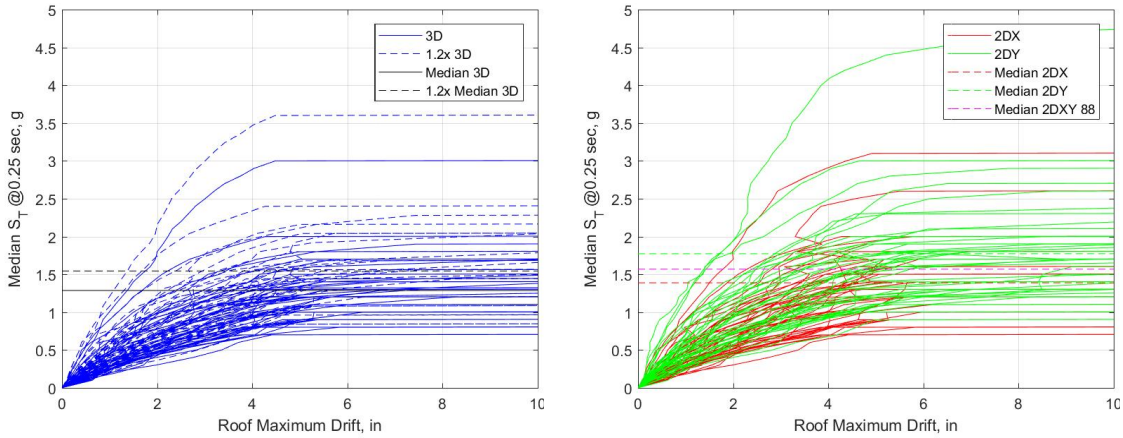

(a) (b)

Figure 6-10 IDA Curves for B1St-100150 from (a) 3D analysis and (b) 2D analysis

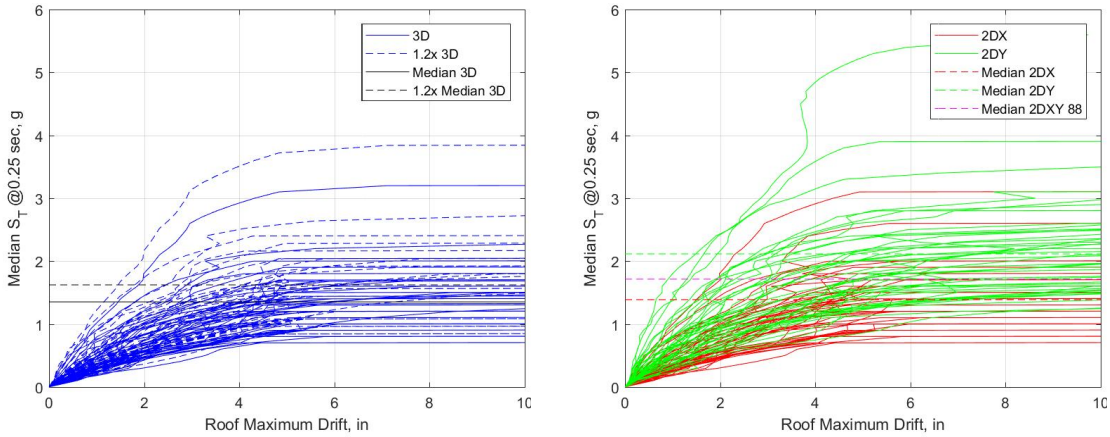

(a) (b)

Figure 6-11 IDA Curves for B1St-100200 from (a) 3D analysis and (b) 2D analysis

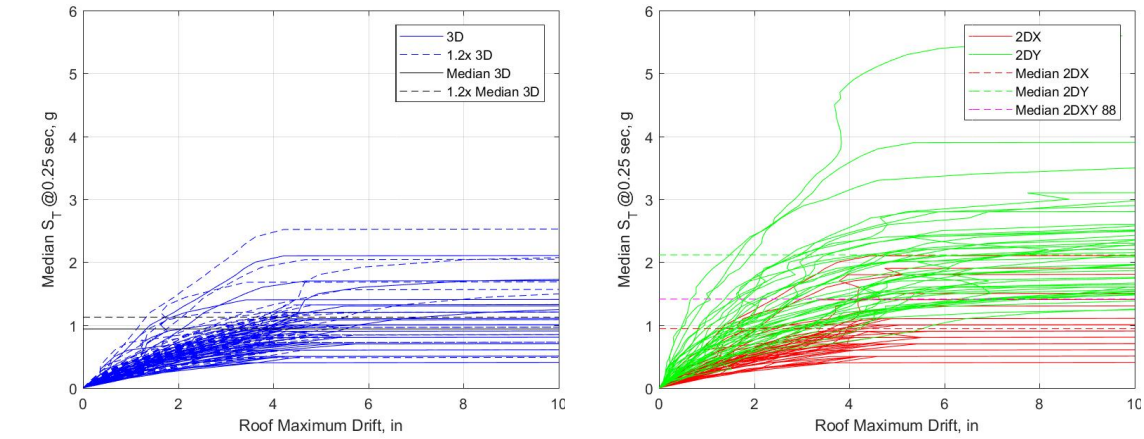

(a) (b)

Figure 6-12 IDA Curves for B1St-050200 from (a) 3D analysis and (b) 2D analysis

Table 6-7 and Table 6-8 show the results from the IDA of this set of models. For the 2D models, only the results from the 2D model along Y-direction have been used to calculate the performance indicators. The results for B1St-100100 have been included for better comparison. It can be observed that performance indicators like ACMR and P(COL|MCE) are similar when the designs are similar in strength in the two directions. However, as the difference between the strengths in two directions increases, so does the difference in their performance and hence, it can be agreed upon that the 1.2 factor cannot be used to correlate 2D and 3D analyses results when with different designs in the two directions and if only one 2D model/direction (in this case Y-) is considered. The difference can be further seen in Figure 6-13 where the results from 2D and 3D analysis are juxtaposed onto one another. The ACMR values for the 3D multiplied by the 1.2 factor only works for same design in both directions and not for different designs.

Table 6-7 Results from 2D analysis of design along Y-direction

Parameter	*B1St-100100*	*B1St-100125*	*B1St-100150*	*B1St-100175*	*B1St-100200*
S_{CT}	1.85	2.10	2.36	2.59	2.81
CMR	0.93	1.05	1.18	1.30	1.41
ACMR	1.23	1.40	1.57	1.73	1.88
P(COL|MCE)	29.0%	20.8%	14.8%	10.9%	8.1%

Table 6-8 Results from 3D analysis with 1.2 factor

Parameter	*B1St-100100*	*B1St-100125*	*B1St-100150*	*B1St-100175*	*B1St-100200*
S_{CT}	1.84	1.96	2.05	2.13	2.16
CMR	0.92	0.98	1.03	1.07	1.08
ACMR	1.23	1.31	1.37	1.42	1.44
P(COL|MCE)	29.2%	25.1%	22.2%	20.2%	19.3%

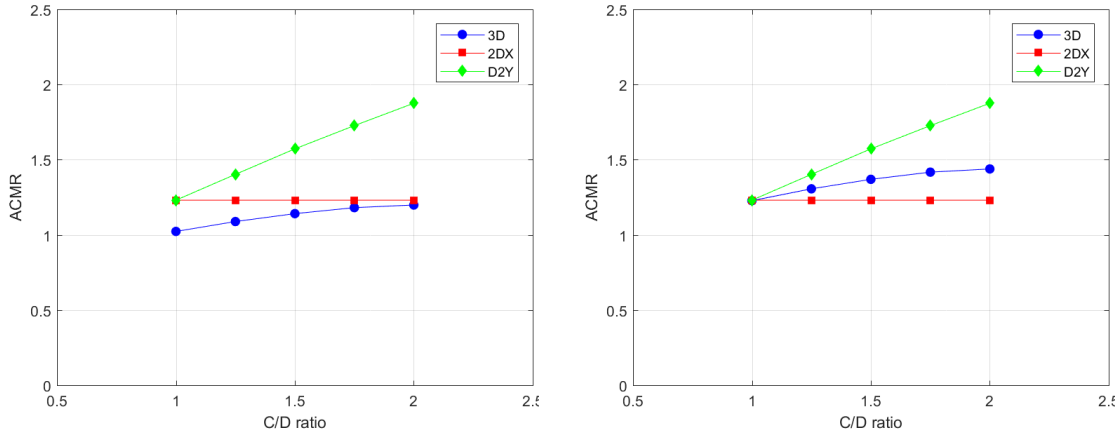

(a) (b)

Figure 6-13 Variation of ACMR with C/D ratio (a) without and (b) with 1.2 factor

Table 6-9 shows again the results from the IDA of the 2D models but the performance indicators have been calculated using all 88 cases from both directions. It can be observed that the performance indicators are comparably much similar to the scaled 3D analyses results. Hence, this warrants the possibility that if results from both models/directions are combined, the 1.2 factor can be better used to correlate the 2D and 3D analyses results. Same observation can also be made in Figure 6-14.

Table 6-9 Results from 2D analyses encompassing all 88 ground motion cases

Parameter	*B1St-100100*	*B1St-100125*	*B1St-100150*	*B1St-100175*	*B1St-100200*
S_{CT}	1.85	1.97	2.09	2.19	2.27
CMR	0.93	0.99	1.05	1.10	1.14
ACMR	1.23	1.31	1.39	1.46	1.51
P(COL|MCE)	33.7%	29.3%	25.5%	22.5%	20.4%

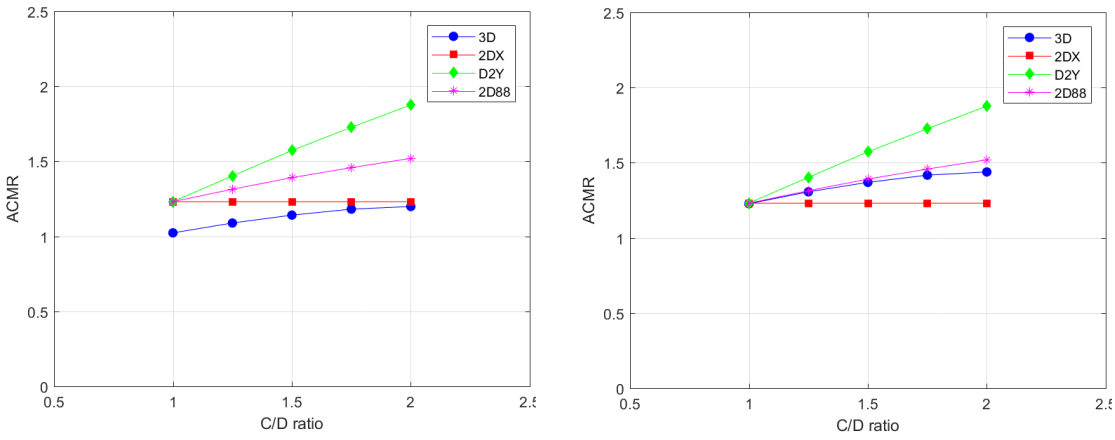

(a) (b)

Figure 6-14 Variation of ACMR with C/D ratio (a) without and (b) with 1.2 factor

Figure 6-15, Figure 6-16 and Figure 6-17 show the fragility curves for models B1St-100150, B1St-100200 and B1St-050200. It can be observed that the 1.2 works better with the combined 88 case rather than the individual cases.

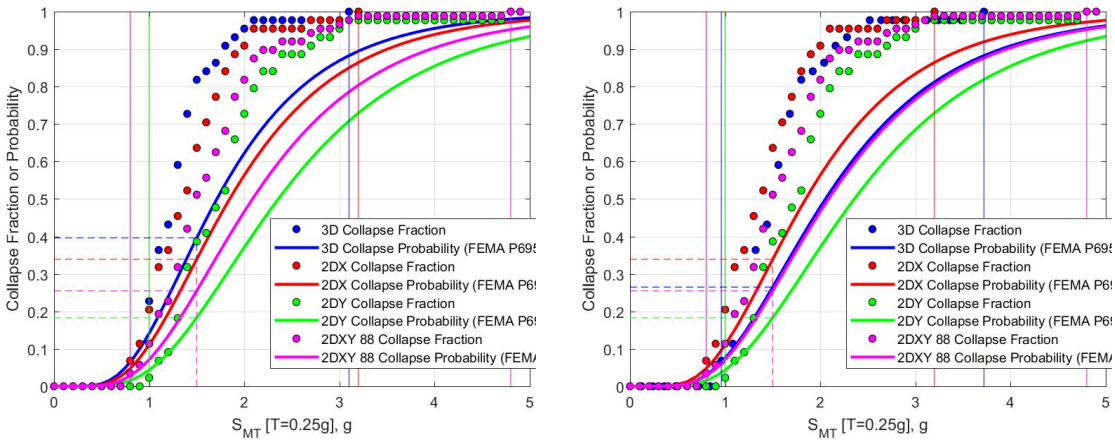

(a) (b)

Figure 6-15 Fragility curves for B1St-200200 (a) without and (b) with 1.2 factor

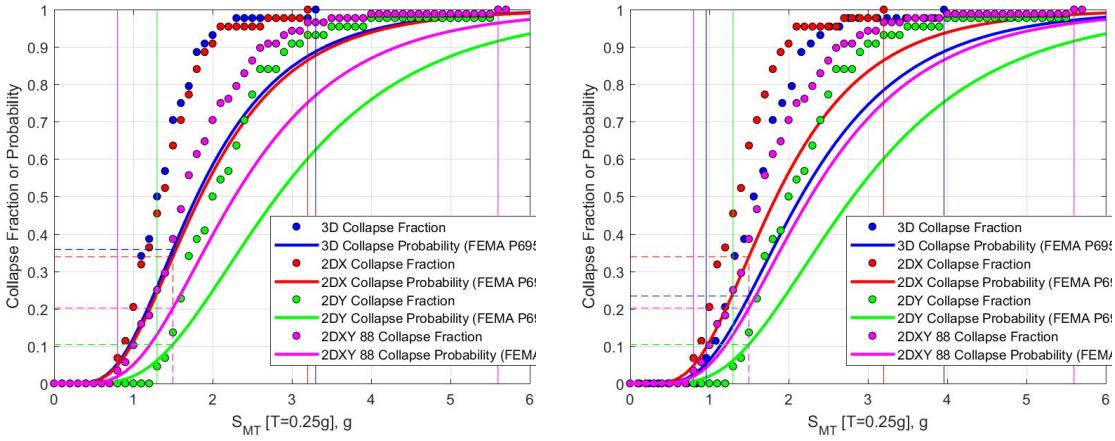

(a) (b)

Figure 6-16 Fragility curves for B1St-200200 (a) without and (b) with 1.2 factor

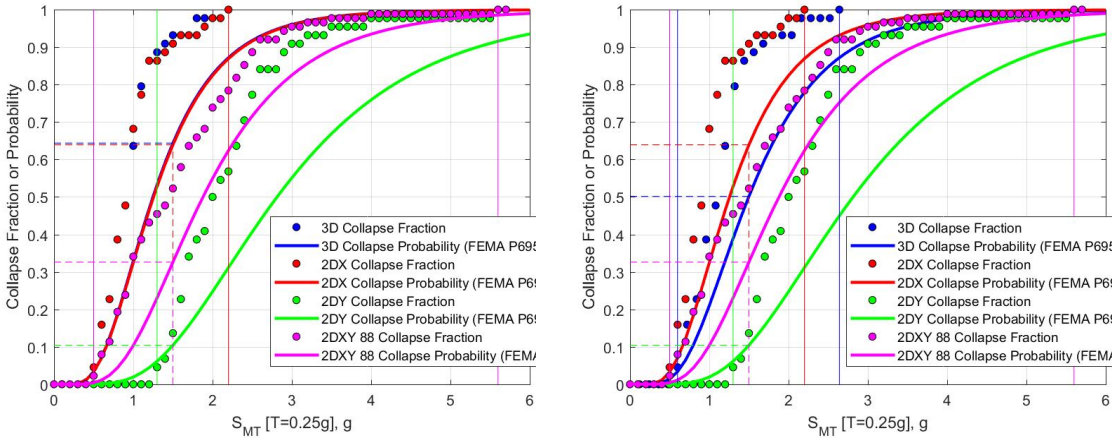

(a) (b)

Figure 6-17 Fragility curves for B1St-200200 (a) without and (b) with 1.2 factor

6.2.2. Four-story models

IDAs were carried out on each of the four-story models and results are shown and discussed herein. Figure 6-18 and Figure 6-19 show the IDA curves and the fragility curves for B4St-ELF model and it can be seen that the 3D factor is indeed applicable here as well. Since these models are 'equal strengths in both directions' cases, the combined 88 case holds little significance again. And finally, Table 6-10 tabulates the performance indicators for all of the four-story models in the set and it can be drawn upon that the 3D factor does apply to four-story models as well even when varying vertical strength distributions are used.

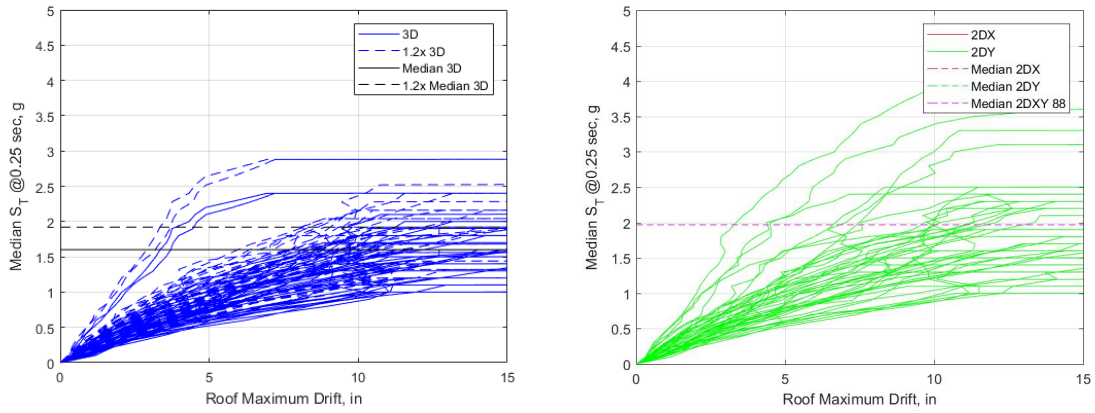

a) b)

Figure 6-18 IDA curves for B4St-ELF from (a) 3D analyses and (b) 2D analyses

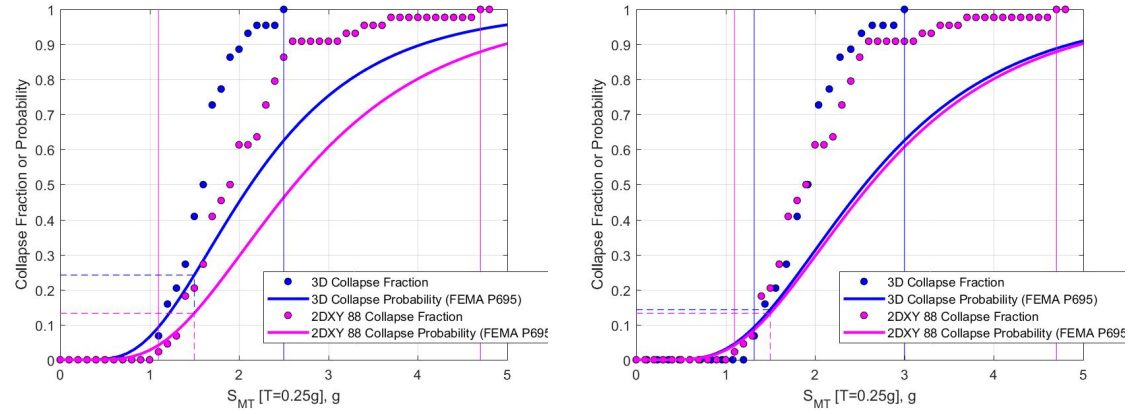

a) b)

Figure 6-19 Fragility curves for B4St-ELF (a) without and (b) with 3D factor

Table 6-10 Results from 2D analyses encompassing all 88 cases for four-story models

Parameter	*B4St-C100*	*B4St-ELF*	*B4St-125*	*B4St-153*	*B4St-300*	*B4St-600*
S_{CT}	2.21	2.62	2.30	2.12	1.92	1.90
CMR	1.11	1.31	1.15	1.06	0.96	0.95
ACMR	1.47	1.75	1.53	1.41	1.28	1.27
P(COL|MCE)	21.9%	13.2%	19.6%	24.4%	31.1%	31.8%

Table 6-11 Results from 3D analyses

Parameter	*B4St-C100*	*B4St-ELF*	*B4St-125*	*B4St-153*	*B4St-300*	*B4St-600*
S_{CT}	2.16	2.56	2.19	2.04	1.92	1.91
CMR	1.08	1.28	1.10	1.02	0.96	0.96
ACMR	1.44	1.71	1.46	1.36	1.28	1.27
P(COL|MCE)	23.3%	14.3%	22.5%	26.9%	31.1%	31.4%

The ACMR values for four-story models have been plotted in Figure 6-20. In addition to applicability of the 3D factor for four-story models, it can be observed that the ACMR for ELF model is higher than that of C100 model meaning added strength does not necessarily translate to better performance and also, ACMR decreases as the irregularity increases and tends to plateau for highly extreme cases suggesting that regardless of how extreme the soft-story is, there is minimum performance that the building can provide.

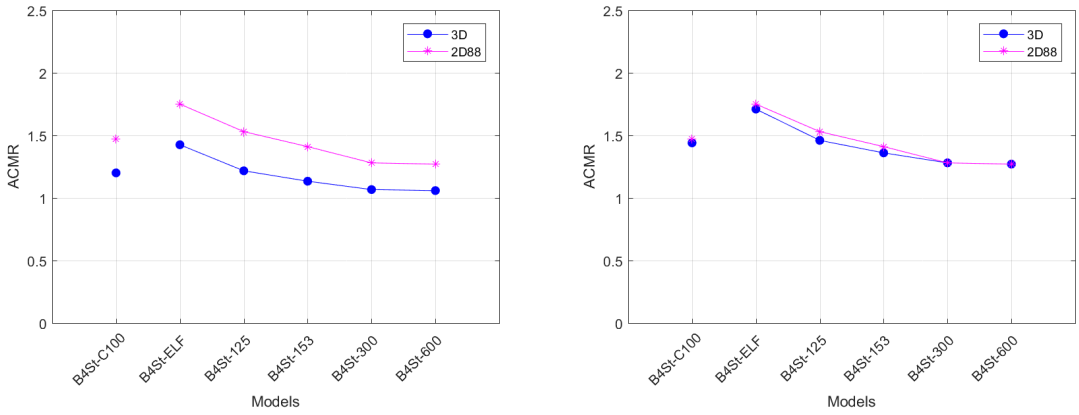

a) b)

Figure 6-20 Variation of ACMR among the four-story models (a) without and (b) with 3D factor

6.3. A Case for the 3D analyses

Throughout this chapter, the results from the 3D and 2D analyses were compared and it was found that the 1.2 3D factor suggested in FEMA P695 does indeed work but with an added stipulation that all 88 ground motion cases, in case of 2D analyses, are required to be combined so that they can be better correlated to 3D cases. By and large, it can be agreed upon that 2D analyses are required to be performed in each principal direction and then combined to get the true results. In retrospect, all of the analyses done in this chapter as well as the preceding ones, the 3D results were converted to their 2D equivalents using the now verified 3D factor as suggested in FEMA P695 thinking that this is the true performance. But structures are seldom 2D and neither are seismic excitations, then is the progression of calculation to convert the 3D results into 2D correct? Admittedly, the 2D equivalent results are convenient because 2D models can be checked for manually and are simple to build and analyze. But shouldn't the performance of a building not be

gauged in the true sense of how it would be built i.e. in 3D? The author believes that the correlation between the 2D and 3D analyses discussed in the preceding sections is correct but it should be used to convert the 2D results into their 3D equivalents rather than the other way around.

7. CONCLUSIONS AND RECOMMENDATIONS

7.1. Conclusions and Findings

This thesis primarily investigated a common defect known as “soft-story” in light-frame wood buildings and developed a new design methodology to address this deficiency. The defect was first investigated through the use of the Equivalent Lateral Force (ELF) procedure in the current U.S. building codes to design a light-frame wood building and then the building was redesigned using an Adaptive Displacement-based Design (ADD) procedure. The seismic performances of the buildings designed using ELF and ADD were quantified in terms of probability of collapse at the Risk Targeted Maximum Considered Earthquake (MCE_R) following the FEMA P-695 procedure [FEMA, 2009]. Additionally, the buildings designed via the ADD procedure were evaluated in regards to performance objectives namely, immediate occupancy, damage control, life safety, and collapse prevention for various seismic hazard levels. Moreover, as part of the FEMA P-695 procedure, both 2D and 3D numerical models may be used to perform time-history analyses and to evaluate the MCE_R collapse probability. A comparison study was also carried out to investigate the differences in MCE_R collapse probabilities obtained using 2D and 3D analyses.

The key conclusive remarks and findings are listed as follows:

a) Non-structural (NS) elements such as partition walls sheathed with gypsum wallboards contribute significantly to lateral strength in light-frame wood buildings. A soft-story deficiency may occur when drastic differences in floor

plans between stories exist. In the current design procedure, the vertical distribution of lateral strength contribution from structural walls is proportioned based on seismic demand. On the other hand, the contribution of lateral strength from non-structural walls is governed by the number of partition walls in each story. Consequently, significant vertical irregularities in terms of strength and stiffness may occur in buildings with open floor plan in the first-story and multi-unit floor plans in the stories above.

b) Numerical models representing various vertical strength and stiffness irregularities as the results of the current ELF design procedure were created. The analyses revealed that the inclusion of a soft-story does lead to worse performance (i.e. increased MCE_R collapse probability). While non-structural elements contribute to lateral strength, if the contribution results in severe vertical irregularity (as in Model V2), the addition of NS elements could actually be detrimental. Moreover, if a building were designed with unnecessary overstrength on the upper stories (as in Model V3), the seismic performance only further exacerbates.

c) An adaptive displacement-based design (ADD) procedure, which gives optimal vertical strength (or stiffness profile) based on the user-specified target displacement profile in a building was developed. ADD yields a similar normalized strength profile to that of ELF when equal peak inter-story displacements are specified in all stories. Even though the profiles are similar,

ADD has a clear advantage because it allows designers to specify a target displacement for a given seismic hazard level, which the ELF method does not.

d) To facilitate the evaluation of the new ADD procedure, a set of basic performance objectives for light-frame construction were decided upon based on the NEESWood Benchmark test results [Christovasilis, Filiatrault, Wanitkorkul, 2009] as well as the results from the prior numerical simulations. The drift limits of 0.5%, 1.0%, and 2.0% were found appropriate for the performance levels of Immediate Occupancy, Damage Control, and Life Safety. And a drift limit of 4.0% was found suitable as a proxy to collapse based on numerical simulations of the as-designed buildings.

e) Using inter-story drift spectra, the ADD procedure was used to design a multi-story building with an open floor plan in the first story and avoid potential soft-story deficiency in the designed building. The procedure was carried out first without any consideration of non-structural elements and then revised to consider the non-structural elements. Each of these designs was then assessed using the FEMA P-695 procedure and also checked for if the previously set performance objectives were achieved. After the redesign using the ADD procedure, the previously "soft-story" building performed better (i.e. reduced MCE_R collapse probability) on the inclusion of non-structural elements while also meeting all of the set performance objectives.

f) Comparison between the Incremental Dynamic Analyses (IDA) using 2D and 3D building models revealed that the 1.2 3D factor recommended in FEMA

P695 is appropriate given that for 2D seismic performance, results from both directions are combined and then only compared against their 3D counterpart. And finally, in the author's opinion, the 3D results are the more realistic of the two and the 2D results should be converted to their 3D equivalents and not the other way around.

g) The ground motions that make up a biaxial ground motion pair do not necessarily need to be of equal intensities. Because of this, the IDA for 2D building models presented a higher CoV in terms of observed collapse intensities than their 3D counterparts while the medians were about the same.

7.2. Recommendations for Future Study

Recommendations for future works are listed below:

a) This study was largely limited to one example building with the same mass and floor plans used in all of the models. Even though the building was representative of multi-unit apartments or office buildings, building-to-building uncertainty was not considered in this study. A future work could be to extend and use the displacement-based procedure used in this study to explore and design buildings with different relative mass ratios and functional use.

b) A threshold for capacity-to-demand (C/D) ratio for upper stories were observed in this study, beyond which the degradation of seismic performance was observed (i.e. MCE_R collapse probability increases) with increasing C/D ratios in the upper stories when compared to C/D ratio in the first story. A future study

could be carried out to accurately quantify the C/D threshold in terms of relative stiffness between stories.

c) Connection details differentiate structural walls from non-structural walls. Even though the thesis focused on the effect of non-structural elements on the seismic performance, no potential connection details were brought up during design. A good addition could have been to mention some of those pertinent connection details.

d) The DDA procedure was developed for design purposes. The DDA procedure may be modified and adapted to estimate vertical displacement profiles for various seismic hazard levels, similar to pushover analysis. It is recommended that a future study be conducted to modify DDA for "analytical pushover analysis".

e) The comparison study between 2D and 3D analyses only looked into the four-story models with the same design in both directions. It is recommended that a future study be carried out to validate the 1.2 3D factor for multi-story buildings with different designs in the two directions as well.

f) And in addition to the 1.2 3D factor, another factor accounting for the spread of the IDA curves (i.e. the variability of the collapse intensities between various earthquakes) might as well be developed.

8. Works Cited

AP Photo/Chuck Jackson. (2014, January 17). *The Northridge Earthquake: 20 Years Ago Today*. Retrieved from theatlantic.com: https://www.theatlantic.com/photo/2014/01/the-northridge-earthquake-20-years-ago-today/100664/

ASCE. (2016). *Minimum Design Loads for Buildings and Other Structures (ASCE/SEI 7-16).* Reston, VA.

ASCE. (2017). *Seismic Evaluation and Retrofit of Exsting Building (ASCE/SEI 41-17).* Reston, VA.

ATC. (2017). *Developing Solutions to the Short-period Building Performance Paradox Study for Wood Light-frame Buildings, ATC-116.* Redwood City, CA.

AWC. (2015). *National Design Specification for Wood Construction, 2015 Edition, American Wood Council.* Leesburg, Virginia.

AWC. (2015). *Special Design Provisions for Wind and Seismic, 2015 Edition, AF&PA American Wood Council.* Washington D.C.

Chopra, A. (2001). *Dynamics of Structures: Theory and Applications to Earthquake Engineering* (Second ed.). Prentice Hall Inc.

Christovasilis, I. P., Filiatrault, A., & Wanitkorkul, A. (2009). *NEESWood Seismic Testing of a Full-scale Two-story Light-frame Wood Building:NEESWood Benchmark Test.*

Continuing Eduation Center. (2019, January). *Introduction to Light-frame Structural Systems.* Retrieved from https://engineeringcenter.bnpmedia.com

Ekotrope. (2020, September 28). *Prescriptive vs. Performance Building Codes*. Retrieved from Ekotrope: https://www.ekotrope.com/blog/prescriptive-vs-performance-building-energy-codes

FEMA. (2000). *Prestandard and Commentary for the Seismic Rehabilitation of Buildings (FEMA356).* Washington D.C.

FEMA. (2009). *Quantification of Building Seismic Performance Factors, FEMA P-695, prepared by the Applied Technolgy Council for the Federal Emergency Management Agency.* Washigton, D.C.

FEMA. (2012). *FEMA P-807 Seismic Evaluation and Retrofit of Multi-Unit Wood-frame Buildings with Weak First Stories.* Washington, D.C.

Filiatrault, A., & Folz, B. (2002). Performance-based seismic design of wood framed buildings. *J. Struct. Eng. 128*, 39-47.

Filiatrault, A., Christovasilis, I., Wanitkorkul, A., & Folz, B. (2006). Displacement-based design of light-frame wood buildings. *Proceedings of the 9th World Conference on Timber Engineering.* Portland, OR.

Folz, B., & Filiatrault, A. (2001). Cyclic Analysis of Wood Shearwalls. *Journal of Structural Engineering*, 433-441.

Folz, B., & Filiatrault, A. (2001). *SAWS - Version 1.0, A Computer Program for the Seismic Analysis of Woodframe Structures.* UCSD, Department of Structural Engineering, La Jolla, CA.

Ghehnavieh, E. Z. (2017). Seismic Analysis of Light-frame Wood Building with a Soft-Story Deficiency. *All Dissertations*. Retrieved from https://tigerprints.clemson.edu/all_dissertations/2025

Lam, D. F. (2004). Recent research and Developement in Timber Engineering in North America. *Internationales Holzbau-Forum 2004.*

Line, P., Hohbach, D., & Waltz, N. (2019). In-Plane Racking Strength Tests of Wood-frame Wood Structural Panel Shearwalls with 2-inch Panel Edge Nail Spacing and Representative Multi-Story Details. *SEAOC Convention Proceedings.*

Line, P., Waltz, N., & Skaggs, T. (2008). Seismic Equivalence Parameters for Engineered Woodframe Wood Structural Panel Shearwalls. *Wood Design Focus*.

Loss, C., Tannert, T., & Tesfamariam, S. (2018). State-of-the-art review of displacement-based seismic design of timber buildings. *Construction and Building Materials*, 481-497.

Pang, W., & Rosowsky, D. V. (2009). Direct Displacement Procedure for Performance-based Seismic Design of Mid-rise Wood-framed Structures. *Earthquake Spectra, 25*(3), 583-605.

Pang, W., & Shirazi, S. M. (2012). Corotational model for Cyclic analysis of Light-frame Wood Shearwalls and Diaphragms. *Journal of Structural Engineering*, 1303-1317.

Pang, W., Rosowsky, D. V., Pei, S., & van de Lindt, J. W. (2010). Simplified Direct Displacement Design of Six-story Woodframe Building and Pretest Seismic Performance Assessment. *J. Struct. Eng*, 813-825.

Pang, W., Ziaei, E., & Filiatrault, A. (2012). A 3D Model for Collapse Analysis of Soft-story Light-frame Wood Buildings. *World Conference on Timber Engineering.* Auckland, New Zealand.

PEER Center. (n.d.). Retrieved from PEER Ground Motion Database: https://ngawest2.berkeley.edu/

Priestley, M. (1998). Displacement-based approaches to rational limit states design of new structures. *Proceedings of the 11th European Conference on Earthquake Engineering.* Paris, France.

Stewart, W. G. (1987). *The Seismic Design of Plywood-sheathed Shearwalls.* Christchurch, New Zealand: University of Canterbury.

Todd, D., Carino, N., R.M., C., Lew, H., Taylor, A., & Walton, W. (1994). *1994 Northridge Earthquake Performance of Structures, Lifelines and Fire Protection Systems.* Gaithersburg, MD 20899: NIST Building and Fire Research Laboratory.

Vamvatsikos, D., & Cornell, A. (2002). Incremental Dynamic Analysis. *Earthquake Eng. Struct. Dyn., 31*(3), 491-514.

9. APPENDICES

Appendix A: Seismic Weight Calculation

$L := 100\ ft$ $B := 48\ ft$ *Length and Width of the Building*

$h := 10\ ft$ *Typical Story Height*

$w_{DL\_floor} := 40\ psf$ $w_{LL\_floor} := 50\ psf$ *Dead Load and Live Load on the floor except roof*

$w_{wall} := 16\ psf$ *Self-weight of the wall*

$w_{DL\_roof} := 27\ psf$ $w_{LL\_roof} := 20\ psf$ *Dead Load and Live Load on the roof*

Total Loads on each Story other than roof

$W_{DL\_floor} := w_{DL\_floor} \cdot (L \cdot B) + w_{wall} \cdot (2 \cdot (L + B) \cdot h)$ *Total Floor Load due to Dead Load*

$W_{DL\_floor} = 239.36\ kip$

$W_{LL\_floor} := w_{LL\_floor} \cdot (L \cdot B) = 240\ kip$ *Total Floor Load due to Live Load*

Total Load on the roof

$W_{DL\_roof} := w_{DL\_roof} \cdot (L \cdot B) + 0.5 \cdot w_{wall} \cdot 2 \cdot (L + B) \cdot h$ *Total Roof Load due to Dead Load*

$W_{DL\_roof} = 153.28\ kip$

$W_{LL\_roof} := w_{LL\_roof} \cdot (L \cdot B) = 96\ kip$ *Total Roof Load due to Live Load*

Load Combination

$W_{floor} := 1.05 \cdot W_{DL\_floor} + 0.25 \cdot W_{LL\_floor} = 311.328\ kip$ *Combined Load on each floor except roof*

$W_{roof} := 1.05 \cdot W_{DL\_roof} + 0.25 \cdot W_{LL\_roof} = 184.944\ kip$ *Combined Load on the roof*

Toal Building Weight

$W_{total} := 3 \cdot W_{floor} + W_{roof} = 1118.928\ kip$

$\frac{W_{roof}}{W_{floor}} = 0.594$

Appendix B: Sample Diaphragm Design Calculations

Diaphragm dimension: $W := 24\ ft$ $L := 44\ ft$

Uniform Loads on diaphragm: $w_{uT} := \frac{70}{100}\ \frac{kip}{ft}$ $w_{uL} := \frac{70}{48}\ \frac{kip}{ft}$

a) Diaphragm unit shear

Along transverse direction,

$$R_T := w_{uT} \cdot \left(\frac{L}{2} + \frac{12}{2}\ ft\right) = 19.6\ kip$$

$$v_{uT} := \frac{R_T}{2 \cdot W} = 408.333\ \frac{lbf}{ft}$$

Along longitudinal direction,

$$R_L := w_{uL} \cdot \left(\frac{W}{2} + \frac{W}{2}\right) = 35\ kip$$

$$v_{uL} := \frac{R_L}{2 \cdot L + 12\ ft} = 350\ \frac{lbf}{ft}$$

b) Check diaphragm aspect ratio *[SDPWS 2008 Table 4.2.4]*

$\frac{L}{W} = 1.833$ < 3 OK for Wood structural panel, unblocked

< 4 OK for Wood structural panel, blocked

c) Unit Shear Capacity

$\phi_D := 0.80$ *Diaphragm shear resistance factor* *[SDPWS 4.2.3]*

Required minimum unit shear capacities

$$v_{nT\_req} := \frac{v_{uT}}{\phi_D} = 510.417\ plf \qquad v_{nL\_req} := \frac{v_{uL}}{\phi_D} = 437.5\ plf$$

Transverse Load Case: ***Case 1 (load parallel to joist, staggered and load perpendicular to continuous panel edges***

Use 15/32" STR I, nominal 2x members, blocked with 10d nails @ 4" spacing.

$v_{nT} := 850\ plf$ > $v_{nT\_req} = 510.417\ plf$ *[SDPWS 4.2C]*

Longitudinal Load Case: ***Case 3 (load perpendicular to joist, staggered and load parallel to continuous panel edges***

Use 15/32" STR I, nominal 2x members, blocked with 10d nails @ 4" spacing.

$v_{nL} := 850\ plf$ > $v_{nL\_req} = 437.5\ plf$ *[SDPWS 4.2C]*

Nailing Requirements

> 10d common nails, blocked diaphragm
> 10d @ 4" o.c. at edges
> 10d @ 4" o.c. for field nails

d) Maximum adjusted chord force

$M_u := \frac{w_{uT} \cdot L^2}{8} = 169.4$ ***kip·ft***

$T_u := \frac{M_u}{W} = 7.058$ ***kip***

$C_u := T_u = 7.058$ ***kip***

Design for Tension/Compression

Reference Design values for Nominal 2x6 Select Structural DF-L

$F_t := 575$ ***psi*** $E := 1400$ ***ksi*** $b := 1.5$ ***in***

$F_c := 1350$ ***psi*** $E_{min} := 580$ ***ksi*** $d := 5.5$ ***in***

Adjustement factors

$C_M := 1.0$ $C_i := 1.0$ $C_T := 1.0$ $\lambda := 1.0$

$C_t := 1.0$ $C_{Ft} := 1.3$ $C_{Fc} := 1.1$ $C_P := 1.0$

Check for Tension

$F'_t := 0.8 \cdot \lambda \cdot (2.7 \cdot F_t) \cdot C_M \cdot C_t \cdot C_{Ft} \cdot C_i = 1.615$ ***ksi***

$T'_n := F'_t \cdot (b \cdot d) = 13.32$ ***kip***

Check for Compression

$F'_c := 0.9 \cdot \lambda \cdot (2.4 \cdot F_t) \cdot C_M \cdot C_t \cdot C_{Ft} \cdot C_i \cdot C_P = 1.615$ ***ksi***

$C'_n := F'_c \cdot (b \cdot d) = 13.32$ ***kip***

Use 2x6 DF-L as chord members.

e) Diaphragm Deflection

$W = 24$ ***ft*** $A := b \cdot d = 8.25$ ***in***^{2} $v := v_{uT} = 408.333$ ***plf***

$L = 44$ ***ft*** $E = 1400$ ***ksi*** $G_a := 15$ $\frac{\textbf{kip}}{\textbf{in}}$

Flexural Deflection

$\Delta_b := \frac{5 \cdot v \cdot L^3}{8 \cdot E \cdot A \cdot W} = 0.941$ ***in*** $\Delta_{shear} := \frac{0.25 \cdot v \cdot L}{1000 \cdot G_a} = 0$ ***in*** $\Delta_{splice} := 0$ ***in***

$\Delta := \Delta_b + \Delta_{shear} + \Delta_{splice} = 0.941$ ***in*** *<< 2x Shear wall drift (2x1in) [ASCE 12.3.1.3]*

Diaphragm can be assumed as rigid.

Appendix C: Sample Shearwall Design Calculations

Design Data: $C_s := 0.154$ *Seismic base shear coefficient*

$S_{DS} := 1.0$ *Design short-period spectral accelearation*

Uniform seismic loads on diaphragm $w_u := \frac{172.25}{100} \frac{kip}{ft}$

a) Design Shear wall along Line 1

Check aspect ratio of each wall segment

$B_1 := 4\ ft$ $H := 10\ ft$

$\frac{H}{B_1} = 2.5$ < 3.5 OK if blocked

< 2.0 OK if unblocked

Reaction from diaphragm atop shear wall 1

$R_{u1} := (w_u \cdot 100\ ft) \cdot \left(\frac{24\ ft}{80\ ft}\right) = 51.675\ kip$

Seismic shear for wall 1

$V_{u1} := R_{u1} = 51.675\ kip$

Unit shear for wall segment

$v_{u1} := \frac{V_{u1}}{24\ ft} = 2153.125\ plf$

$\phi_D := 0.8$

$v_{n1\_req} := \frac{v_{u1}}{\phi_D} = 2691.406$ **plf**

Use *2x 15/32" Sheathing panels*
10d @ 2" o.c. at edges
10d @ 12" o.c. for field nails

$v_{n1} := 2 \cdot 1740$ **plf** > $v_{n1\_req} = 2691.406$ **plf** *OK*

b) Tension and Compression chords for a 4 ft wall segment

Tension force $T_{uh} := \left(\frac{R_{u1}}{6 \cdot B_1}\right) \cdot 10$ **ft** $= 21.531$ **kip**

Compression force $C_{uh} := T_{uh} = 21.531$ **kip**

Each of these forces represents the seismic force i.e. $\rho \cdot Q_E = T_{uh}$

Uniform dead load on the wall $DL_{wall} := 16$ **psf**

Dead load on either the compression or the tension chord

$D := DL_{wall} \cdot 10 \cdot \text{ft} \cdot \frac{4 \cdot \text{ft}}{2} = 0.32$ **kip**

Load Combinations

$C_u := 1.2 \cdot D + C_{uh} + 0.2 \cdot S_{DS} \cdot D = 21.979$ **kip**

$T_u := 0.9 \cdot D - T_{uh} - 0.2 \cdot S_{DS} \cdot D = -21.307$ **kip**

Try two 2x8 No. 2 DFL and 1" diameter bolts for hold-downs.

$b := 1.5$ **in** $d := 7.25$ **in** $D_{bolt} := 1.0$ **in**

Reference Design values *[NDS Suppl Table 4A]*

$F_t := 575$ **psi** $E_{min} := 580$ **ksi**

$F_c := 1350$ **psi** $E := 1600$ **ksi**

Check tension chord

$C_M := 1.0$ *Wet-service factor*

$C_t := 1.0$ *Temperature factor*

$C_i := 1.0$ *Incising factor*

$\lambda := 1.0$ *Time-effect factor for seismic combination*

$\phi_t := 0.80$ *Resistance factor for tension*

$K_{Ft} := 2.70$ *Format conversion factor*

$C_{F\_t} := 1.3$ *Size factor*

$F'_t := \lambda \cdot \phi_t \cdot \langle K_{Ft} \cdot F_t \rangle \cdot C_M \cdot C_t \cdot C_{F\_t} \cdot C_i = 1614.6$ **psi**

$A_n := 2 \cdot \langle b \cdot \langle d - D_{bolt} \rangle \rangle = 18.75$ **in**^{2} *Net member area*

$T'_n := F'_t \cdot A_n = 30.274$ **kip** > $T_u = -21.307$ **kip** *OK*

Check compression chord

$\phi_c := 0.90$

$K_{Fc} := 2.40$

$C_{F\_c} := 1.1$

Column Stability factor

$L_{ex} := 10$ **ft** $L_{ey} := 0$ **ft** (fully braced by sheathing)

Check Slenderness ratio

$\frac{L_{ex}}{d} = 16.552$ < 60 $\frac{L_{ey}}{b} = 0$

Adjusted Emin

$\phi_s := 0.85$ *Resistance factor for Stability*

$K_{FE} := 1.76$

$C_T := 1.0$ *Buckling stiffness factor* *[NDS 4.4.2]*

$E'_{min} := \phi_s \cdot \langle K_{FE} \cdot E_{min} \rangle \cdot C_M \cdot C_t \cdot C_i \cdot C_T = 867.68$ **ksi**

Nominal Euler critical buckling stress

$$F_{cE} := \frac{0.822 \cdot E'_{min}}{\left(\frac{L_{ex}}{d}\right)^2} = 2603.424 \text{ psi}$$

$F_{c\_star} := \lambda \cdot \phi_c \cdot \langle K_{Fc} \cdot F_c \rangle \cdot C_M \cdot C_t \cdot C_i \cdot C_{F\_c} = 3207.6$ **psi**

$\alpha_c := \frac{F_{cE}}{F_{c\_star}} = 0.812$

$c := 0.8$

$$C_P := \left(\frac{1+\alpha_c}{2\cdot c}\right) - \sqrt{\left(\frac{1+\alpha_c}{2\cdot c}\right)^2 - \frac{\alpha_c}{c}} = 0.615$$

$F'_c := F_{c\_star} \cdot C_P = 1972.916$ **psi**

$C'_n := F'_c \cdot A_n = 36.992$ **kip** > $C_u = 21.979$ **kip** OK

Use double 2x8 at each end of the wall segments.

c) Select Hold-down

$T_u = -21.307$ **kip** *LRFD Tension force*

$\frac{T_u}{K_{Ft}} = -7.892$ **kip** *Convert to ASD tension force*

Use $T_{HD\_ASD} := 9.920$ **kip** ***Simpson Strong tie HD9B DF with 3.5" member thickness (double 2x6)***
(from manufacturer catalog)

Check Shear wall deflection

Deflection due to Bending of End Post

Due to bending of end post

$v := v_{u1} = 2153.125$ **plf**

$E := 1400$ **ksi** *Average modulus of elasticity for No 2 DF-L*

$b_{sw} := B_1 = 4$ **ft** *Shear wall length*

$A := 2 \cdot (b \cdot d) = 21.75$ **in**^{2} *End post cross sectional area*

$$\Delta_b := \frac{8 \cdot \frac{v}{\text{plf}} \cdot \left(\frac{H}{\text{ft}}\right)^3}{\frac{E}{\text{psi}} \cdot \frac{A}{\text{in}^2} \cdot \frac{b_{sw}}{\text{ft}}} \cdot \text{in} = 0.141 \text{ in}$$

Due to vertical slip in hold-down

$\Delta_a := 0.178$ **in** *(from manufacturer catalog)*

$$\Delta_{hd} := \frac{\frac{H}{\text{ft}} \cdot \Delta_a}{\frac{b_{sw}}{\text{ft}}} = 0.445 \text{ in}$$

Due to panel nail slip and panel shear deformation

$G_a := 48\ \frac{kip}{ft}$ *15/32" Sheathing OSB panels* *[NDS SDPWS Table 4.3A]*
10d@ 2" o.c. at edges
10d@ 12" o.c. for the field nails

$$\Delta_{vn} := \frac{\frac{v}{plf} \cdot \frac{H}{ft}}{1000 \cdot \frac{G_a}{klf}} \cdot in = 0.449\ in$$

Total deflection

$\Delta := \Delta_b + \Delta_{hd} + \Delta_{vn} = 1.035\ in$ $<$ $0.025 \cdot H = 3\ in$ *OK*

ASCE7-16 Table 12.12-1 Allowable Story Drift

Appendix D: Design CAD Drawings (Floor plans)

V2-ELF Design Drawings

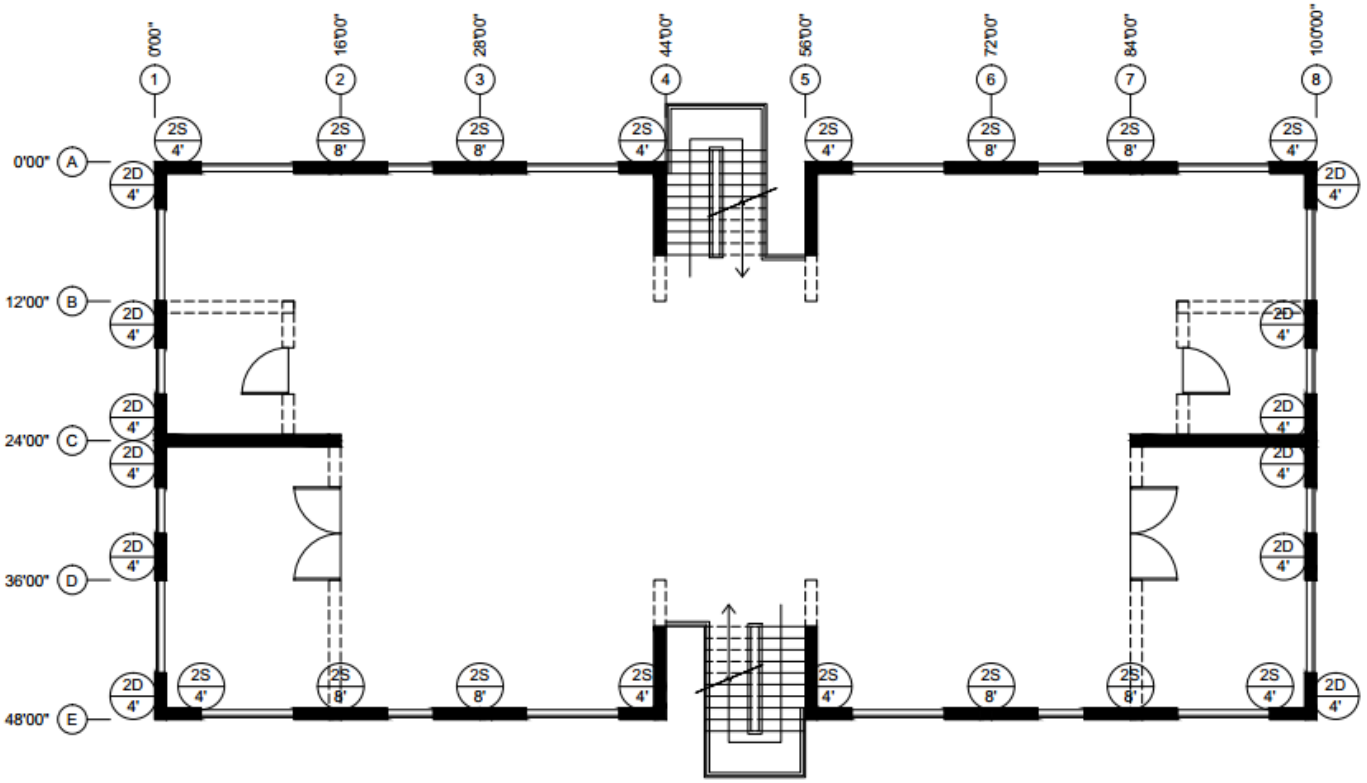

V2-ELF Floor 1

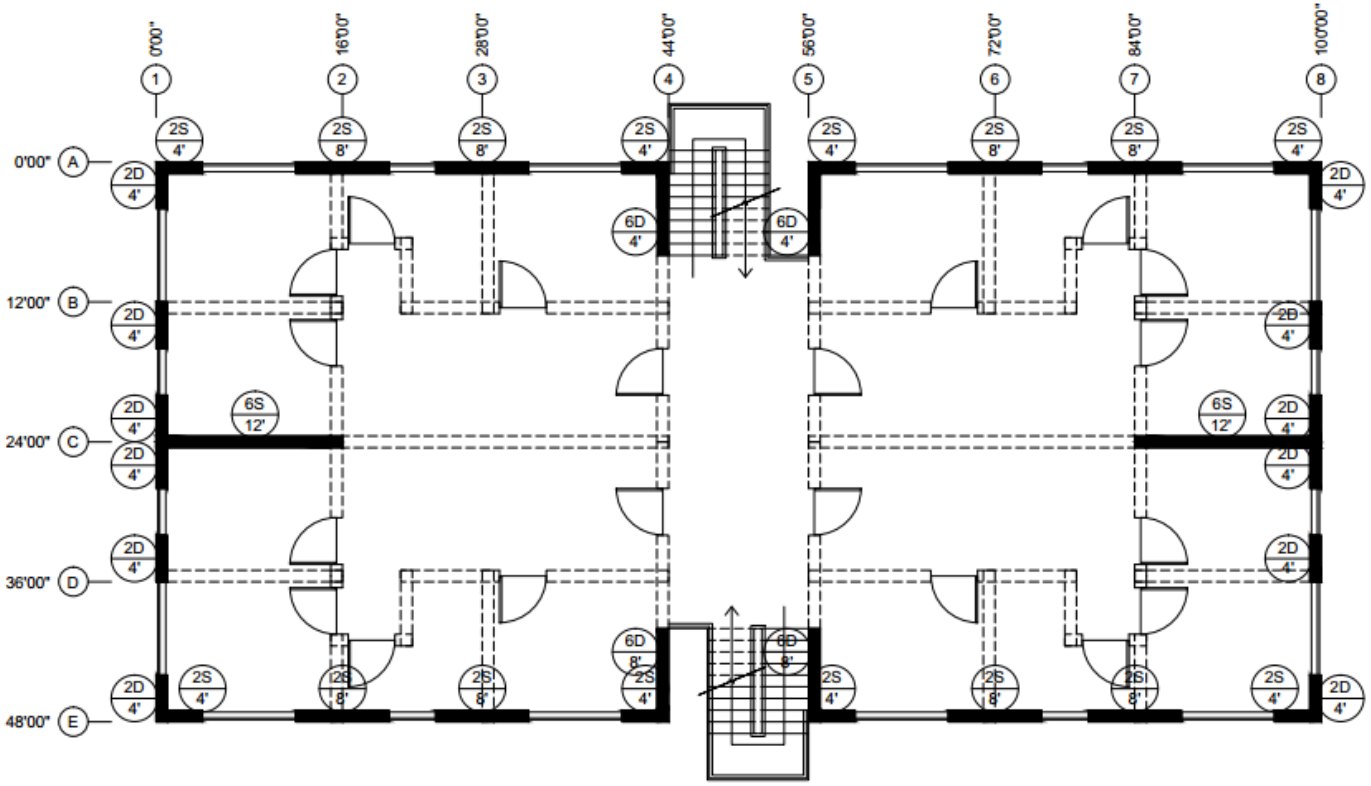

V2-ELF Floor 2

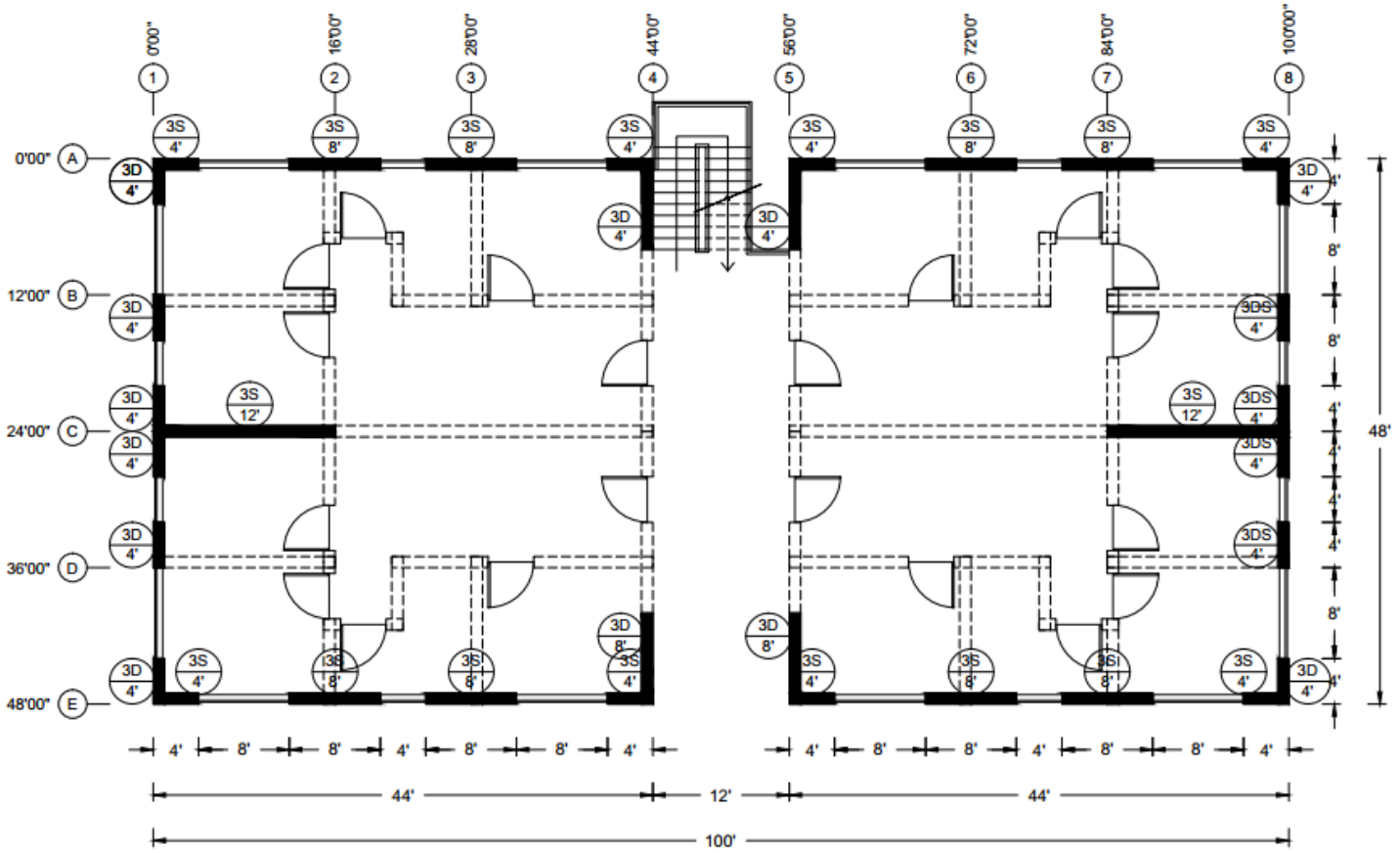

V2-ELF Floor 3

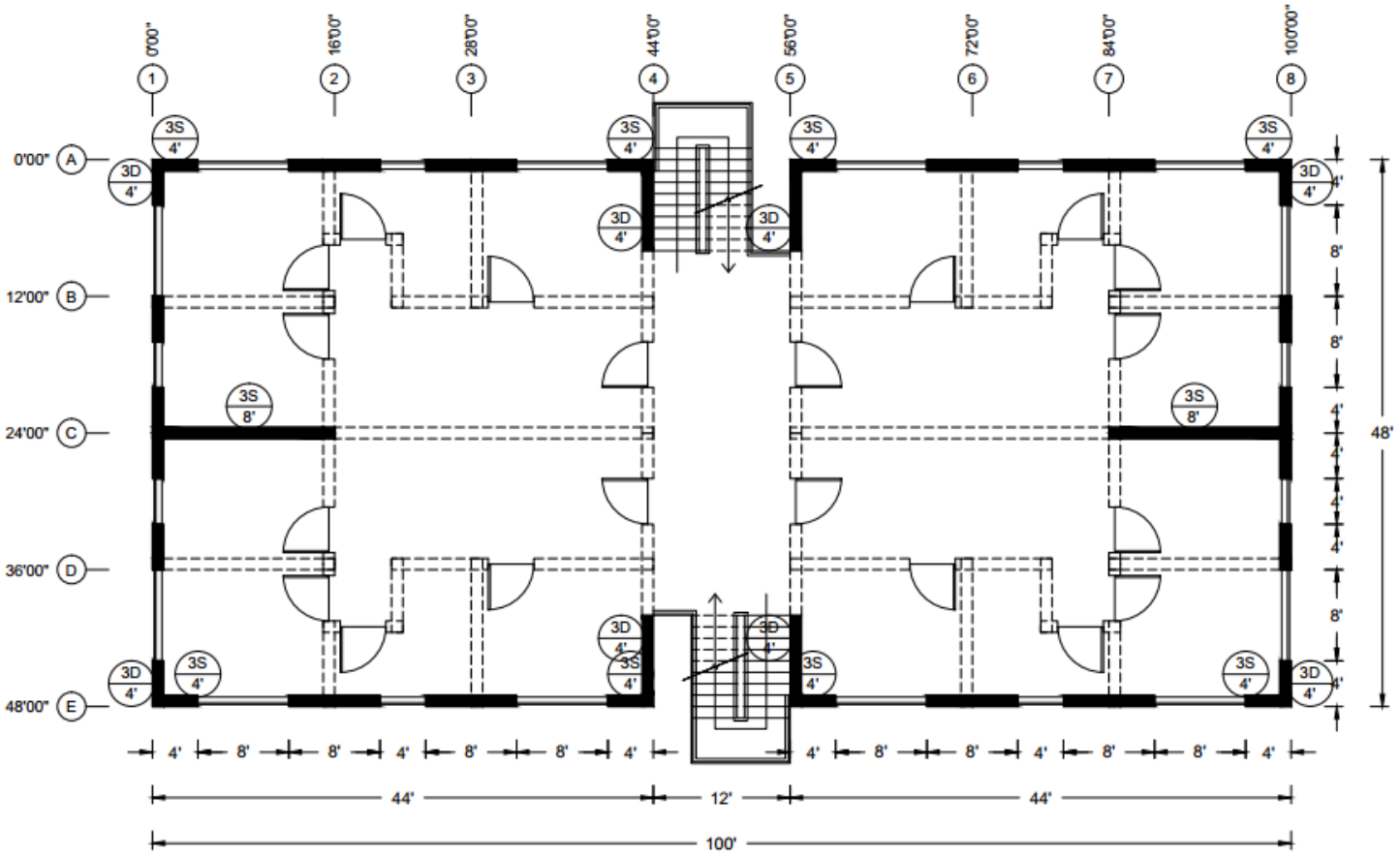

V2-ELF Floor 4

V2-ADD1

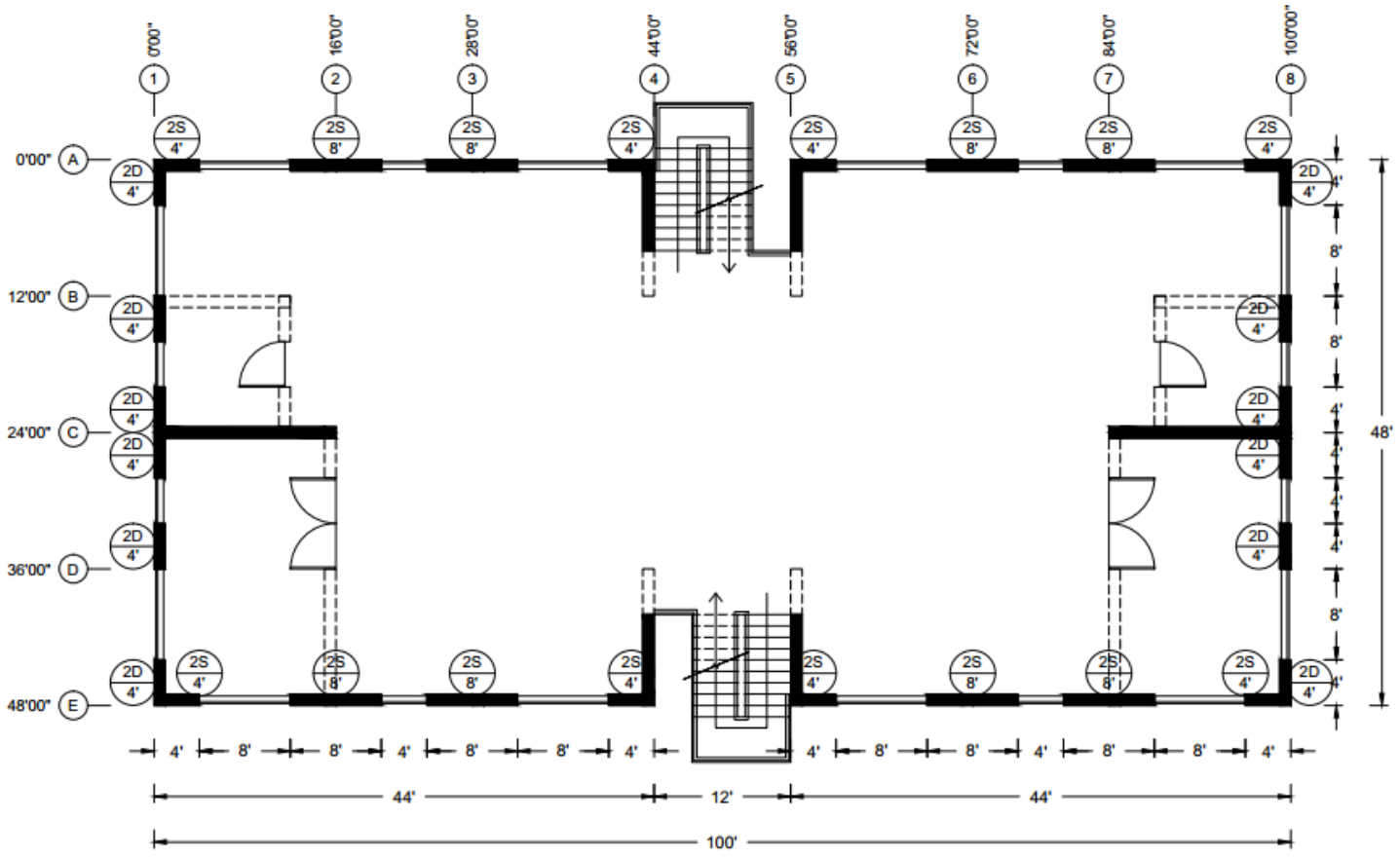

V2-ADD1 Floor 1

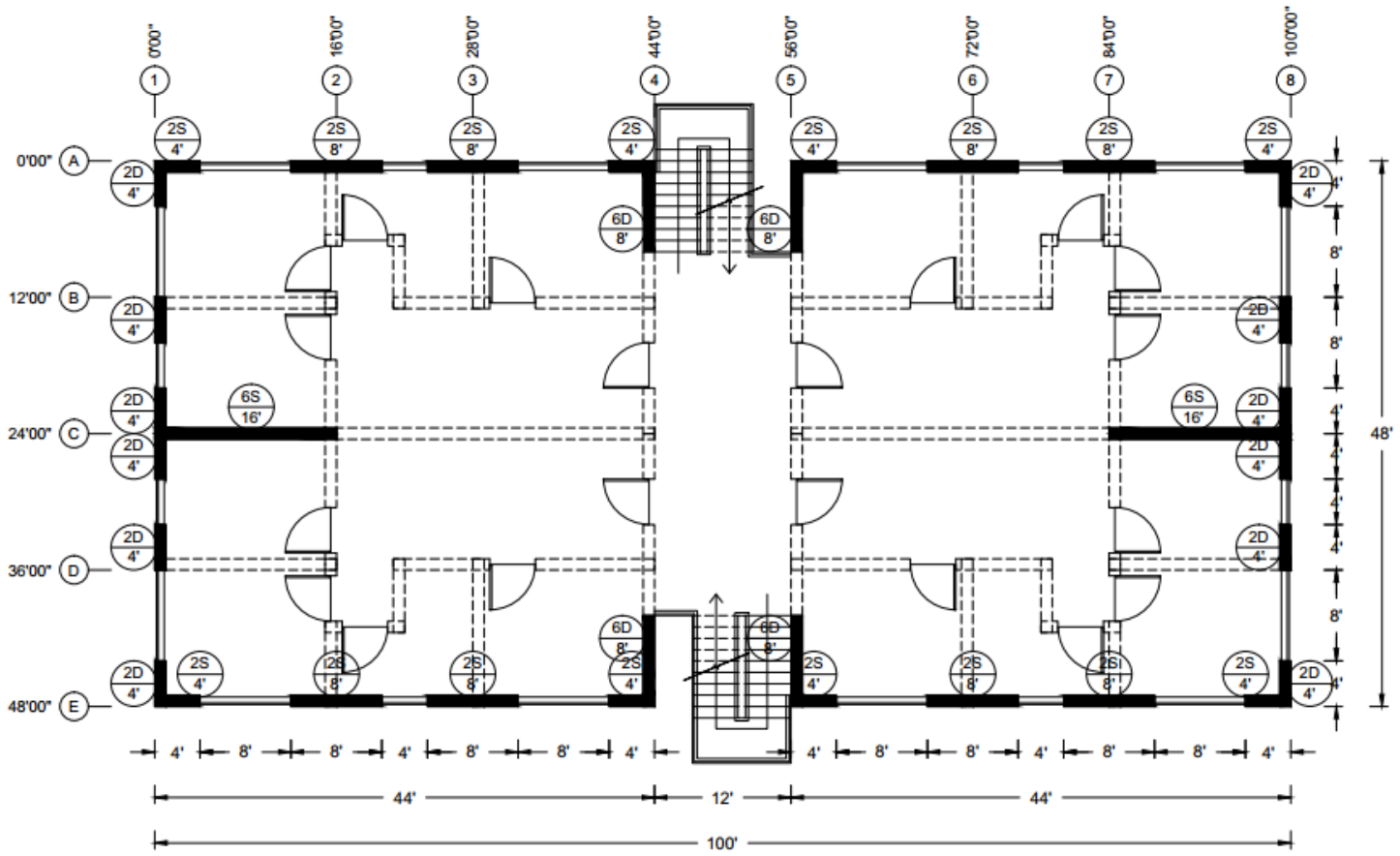

V2-ADD1 Floor 2

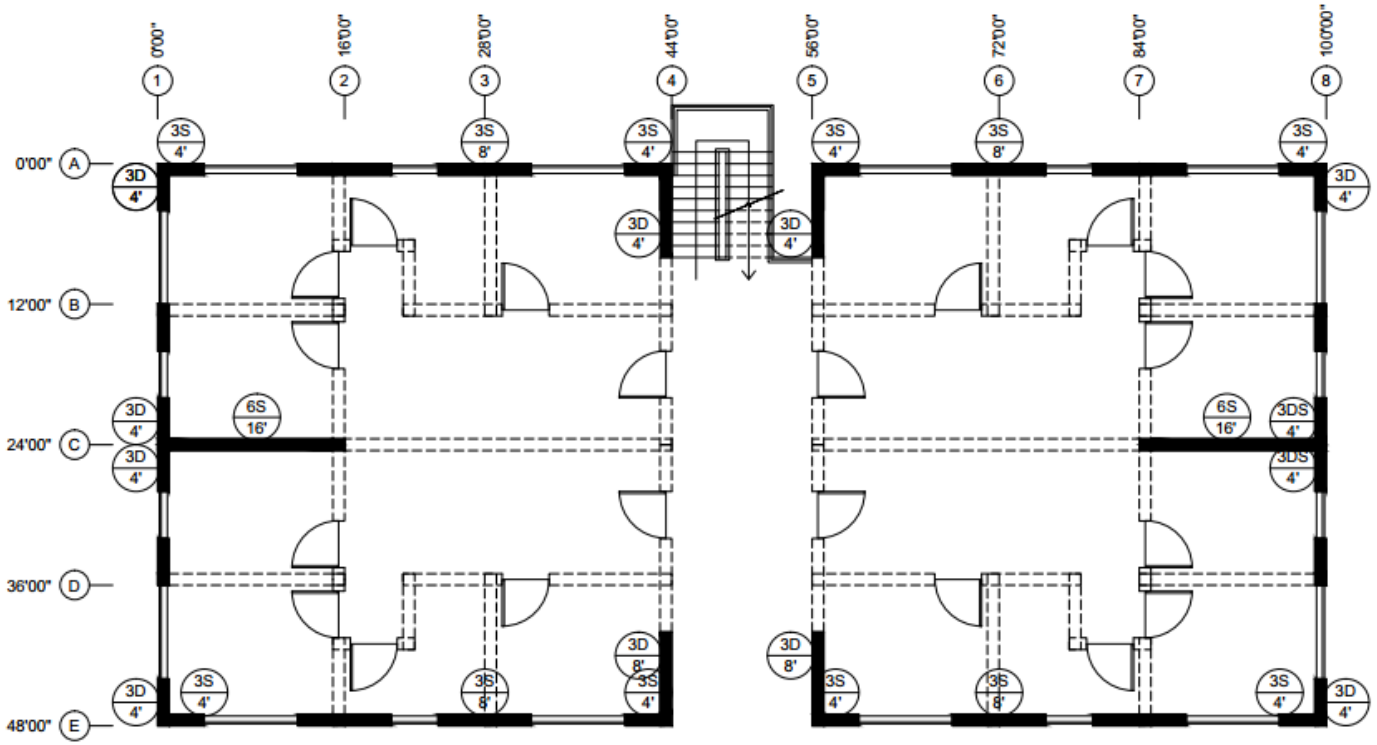

V2-ADD1 Floor 3

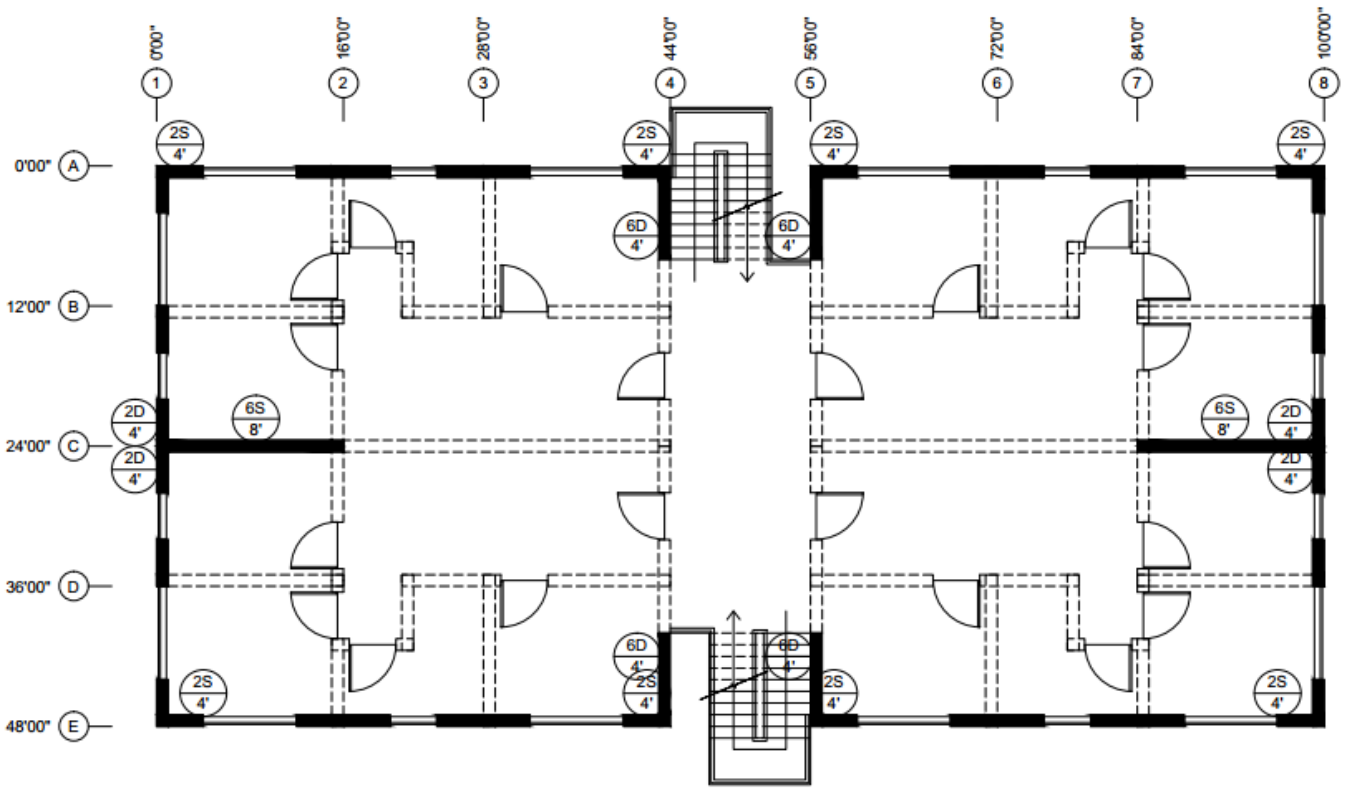

V2-ADD1 Floor 4

V2-ADD2

Floor 1

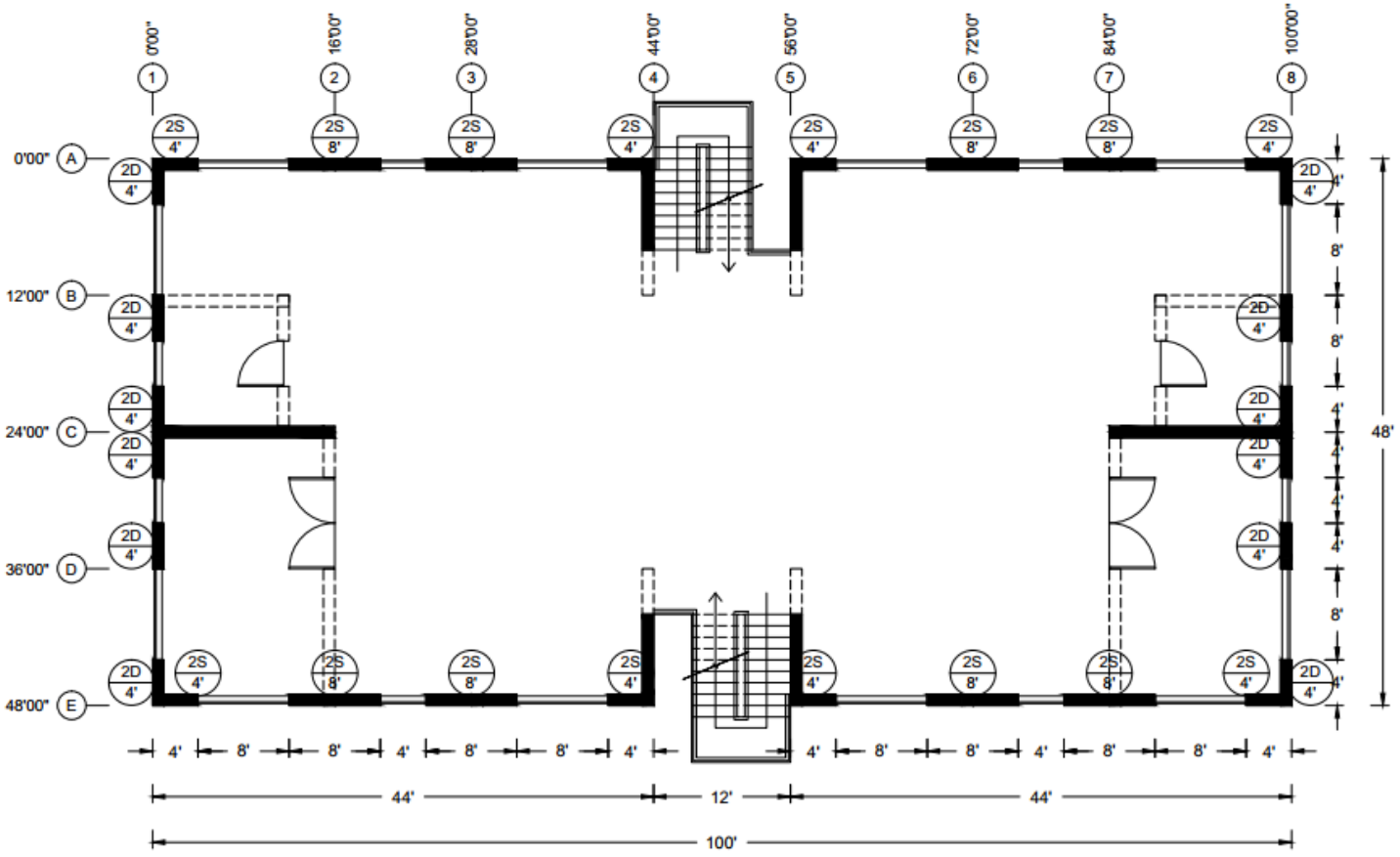

V2-ADD2 Floor 1

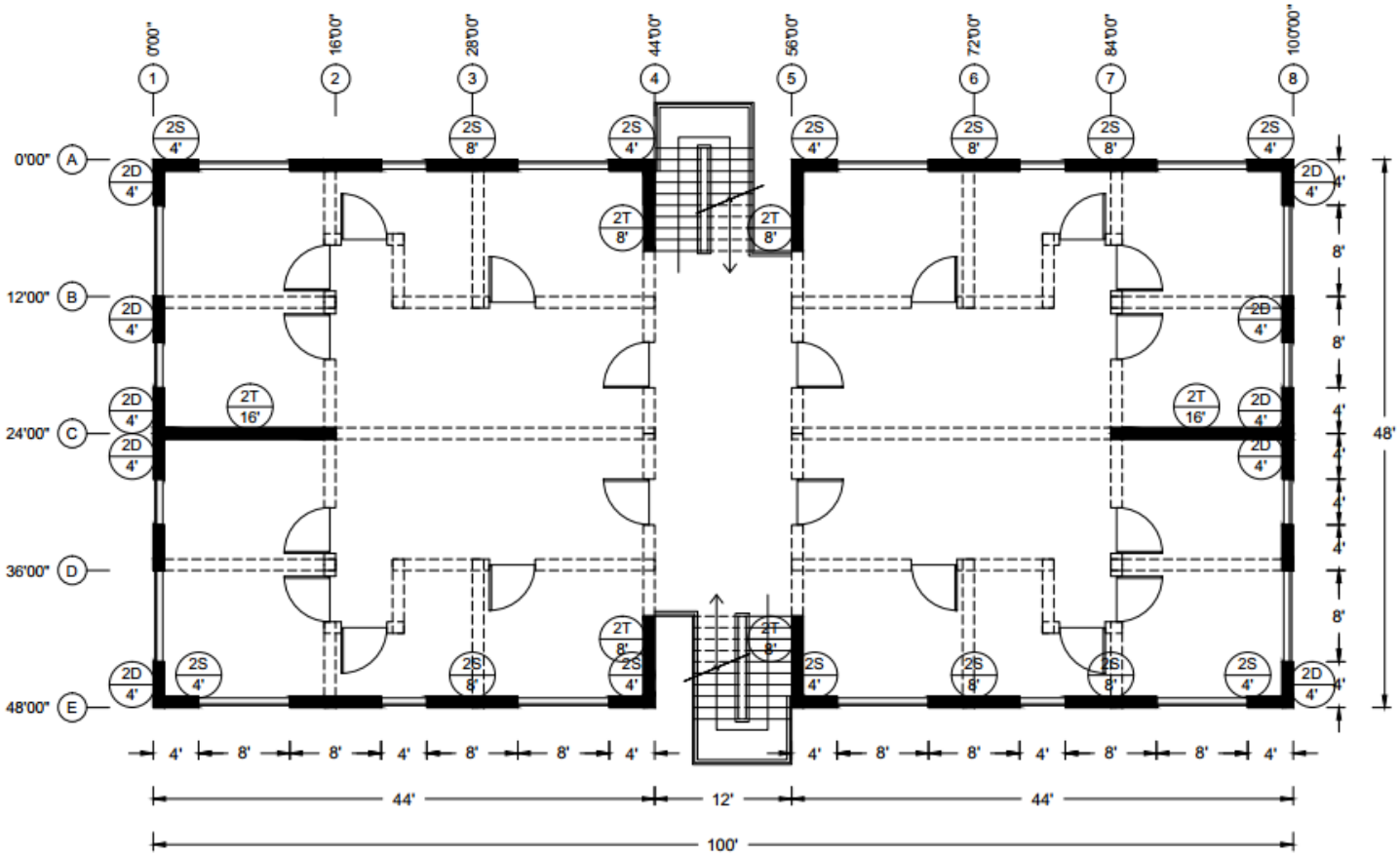

V2-ADD2 Floor 2

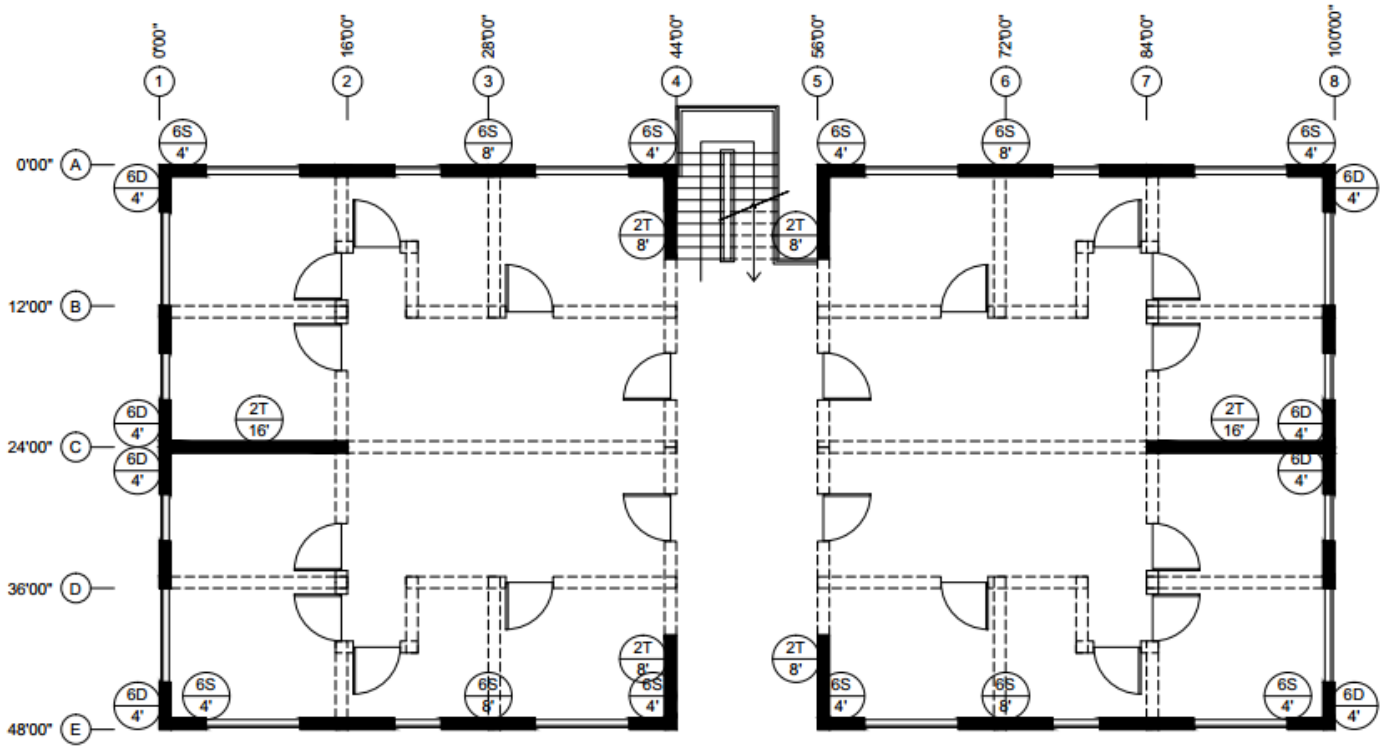

V2-ADD2 Floor 3

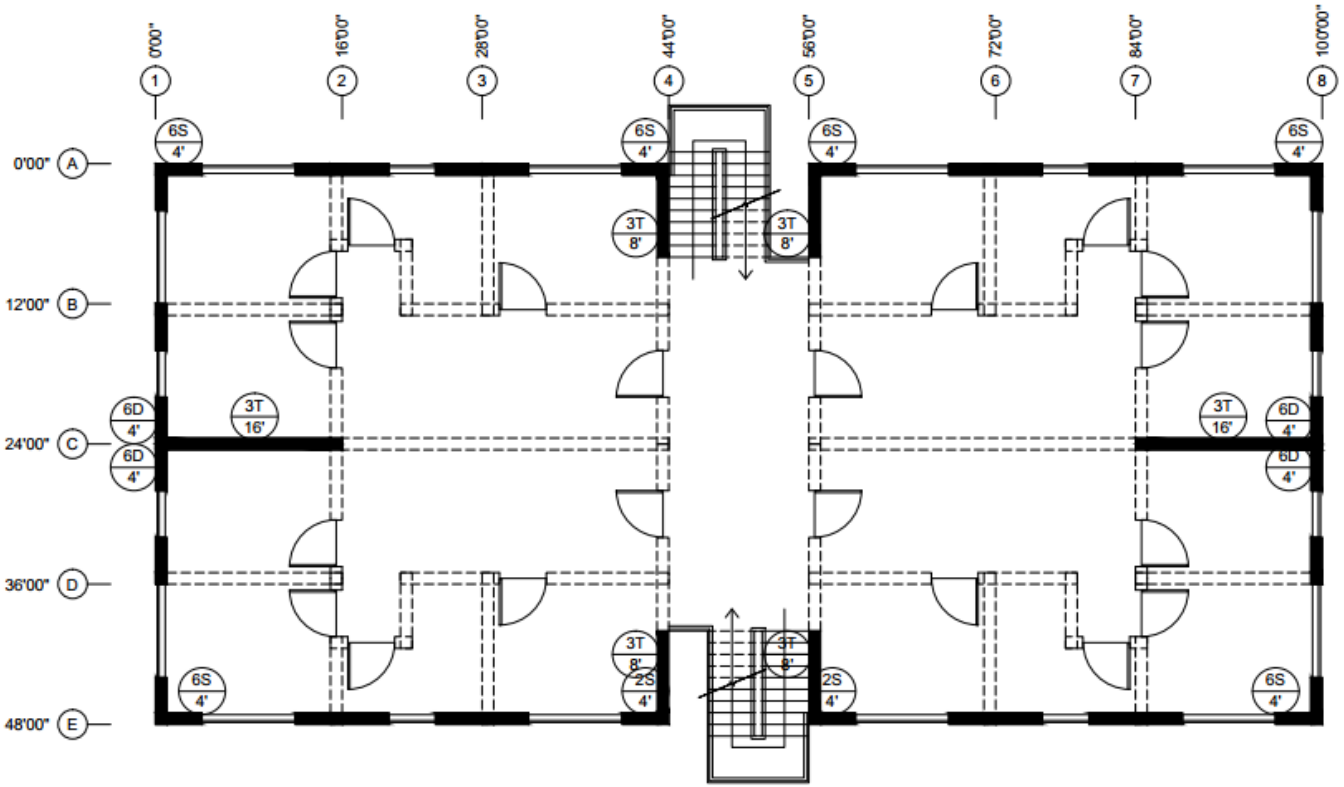

V2-ADD2 Floor 4